

Dissolution behaviour of HLW glasses under OPERA repository conditions

OPERA-PU-IBR511A

Radioactive substances and ionising radiation are used in medicine, industry, agriculture, research, education and electricity production. This generates radioactive waste. In the Netherlands, this waste is collected, treated and stored by COVRA (Centrale Organisatie Voor Radioactief Afval). After interim storage for a period of at least 100 years radioactive waste is intended for disposal. There is a world-wide scientific and technical consensus that geological disposal represents the safest long-term option for radioactive waste.

Geological disposal is emplacement of radioactive waste in deep underground formations. The goal of geological disposal is long-term isolation of radioactive waste from our living environment in order to avoid exposure of future generations to ionising radiation from the waste. OPERA (OnderzoeksProgramma Eindberging Radioactief Afval) is the Dutch research programme on geological disposal of radioactive waste.

Within OPERA, researchers of different organisations in different areas of expertise will cooperate on the initial, conditional Safety Cases for the host rocks Boom Clay and Zechstein rock salt. As the radioactive waste disposal process in the Netherlands is at an early, conceptual phase and the previous research programme has ended more than a decade ago, in OPERA a first preliminary or initial safety case will be developed to structure the research necessary for the eventual development of a repository in the Netherlands. The safety case is conditional since only the long-term safety of a generic repository will be assessed. OPERA is financed by the Dutch Ministry of Economic Affairs, Agriculture and Innovation and the public limited liability company Electriciteits-Produktiemaatschappij Zuid-Nederland (EPZ) and coordinated by COVRA. Further details on OPERA and its outcomes can be accessed at www.covra.nl.

This report concerns a study conducted in the framework of OPERA. The conclusions and viewpoints presented in the report are those of the author(s). COVRA may draw modified conclusions, based on additional literature sources and expert opinions. A .pdf version of this document can be downloaded from www.covra.nl

OPERA-PU-IBR511A

Title: HLW glass dissolution

Authors: Guido Deissmann (BS), Kirsten Haneke (BS), André Filby (BS), Rob Wieggers (IBR)

Date of publication: 2016

Keywords: HLW glass, dissolution, repository conditions, source term

Summary	1
Samenvatting	1
1. Introduction	3
1.1. Background	3
1.2. Objectives.....	3
1.3. Realisation	3
1.4. Explanation contents	4
2. Nuclear waste glasses.....	5
2.1. Borosilicate glasses	5
2.2. Phosphate glasses	6
2.3. Vitrification technology	6
2.4. Reprocessing of fuels from nuclear power plants in the Netherlands.....	8
2.4.1. Dodewaard.....	9
2.4.2. Borssele	9
3. HLW glasses relevant for OPERA	11
3.1. Characteristics of HLW glass within OPERA	11
3.2. Waste canisters for HLW glass and packaging	12
3.3. Radionuclide inventory.....	13
4. Conditions in the near field.....	15
4.1. OPERA disposal concept.....	15
4.2. Near field evolution	18
4.2.1. Evolution of pH and pore water composition in the HLW section	19
4.2.2. Evolution of redox conditions.....	22
4.2.3. Résumé.....	24
5. Dissolution of HLW glass in the repository environment.....	25
5.1. Mechanisms of nuclear waste glass dissolution	25
5.2. Dissolution of nuclear waste glasses under alkaline conditions	28
5.2.1. Effects of pH and solution composition	28
5.2.2. Effects of glass composition	32
5.2.3. Effects of radiation.....	33
5.3. Reactive surface area of corroding waste glasses.....	35
6. Evaluation	39
6.1. Radionuclide source term.....	40
6.2. Radionuclide migration in the near field	42
6.2.1. Solubility limitation in a cementitious near field.....	43
6.2.2. Sorption of radionuclides in a cementitious near field	44
7. Conclusions.....	47
8. References	49
Appendix 1	1
Appendix 2.....	3
Appendix 3.....	4
Appendix 4.....	12

Summary

The present report summarises the results of the evaluation of the corrosion behaviour of, and the radionuclide release from vitrified high level wastes (HLW) resulting from the reprocessing of spent nuclear fuels from the Dutch nuclear power plants (NPP) Borssele and Dodewaard under disposal conditions expected in a geological repository in Boom Clay in the Netherlands. The results address directly the safety function ‘delay and attenuation of releases (R)’ relevant after the failure of the waste canisters, when the waste forms come into contact with the near field water. Due to the temporal evolution of the cementitious near field in the repository and the uncertainty regarding the lifetime of the waste canisters, different scenarios regarding the composition of the near field water are discussed.

The inventory of vitrified HLW for the OPERA safety case comprises predominantly R7T7 glasses from reprocessing of spent nuclear fuel from the Borssele NPP in La Hague, France, and, to a lesser extent, glasses from the reprocessing of spent nuclear fuels from the Dodewaard NPP in Sellafield, UK. The dissolution behaviour of the waste glasses depends on their composition as well as on the post closure conditions in the near field. Based in particular on the results of the Belgian research programmes into glass dissolution in cementitious environments, ranges and best estimates for the glass dissolution rates and the lifetime of the glass waste forms under repository conditions have been proposed for OPERA. Regarding the release of radionuclides from the glass waste forms, a homogeneous distribution of the radionuclides in the glasses and a congruent release of radionuclides with the glass matrix dissolution were assumed, taking into account the increase in the reactive surface area of the glass monoliths due to fracturing in course of the cooling process.

Samenvatting

Dit rapport bevat de evaluatie over het optredende corrosiegedrag en het daardoor vrijkomen van radionucliden, van in ondergrondse eindberging bevindend verglaasd hoog radioactief afval (HLW). Deze is afkomstig van het opwerken van afgewerkte kernbrandstof van de kerncentrales Borsele en Dodewaard. Het betreft hierbij de veiligheidsfunctie “vertraging en verdunning van vrijkomende radionucliden (R)” welke van belang is wanneer er radionucliden vrijkomen uit de verpakkingen en daarbij in contact komen met zich in de eindberging bevindend water. Aangezien de omstandigheden in de ondergrondse eindberging in de tijd wijzigen alsmede de onzekerheid hoelang de verpakkingen intact blijven, zijn verschillende scenario’s bekeken.

Het verglaasde hoog radioactieve afval bestaat voornamelijk uit het R7T7 type glas afkomstig van kernafval van kerncentrale Borsele dat in La Hague (Fr) opgewerkt is. Een kleiner deel is afkomstig van de opwerking van kernafval van kerncentrale Dodewaard in Sellafield (GB). De wijze waarop het glas in oplossing gaat, is in hoge mate afhankelijk van het soort glas en de omstandigheden in de ondergrondse eindberging. Op basis van voornamelijk op Belgische onderzoekresultaten gebaseerde bandbreedtes worden beste schattingen gegeven voor de snelheid waarmee glas in oplossing gaat alsmede de verwachte levensduur van het glas onder door OPERA aangenomen condities. Ten aanzien van het vrijkomen van radionucliden uit het verglaasde afval wordt uitgegaan van een homogene verdeling van de radionucliden en het daardoor overeenkomstig vrijkomen van radionucliden bij het oplossen van het glas. Hierbij wordt rekening gehouden met de toename van het reactief oppervlak door de bij productie ontstane koelscheuren in het glas.

1. Introduction

1.1. Background

The five-year research programme for the geological disposal of radioactive waste – OPERA – started on 7 July 2011 with an open invitation for research proposals. In these proposals, research was proposed for the tasks described in the OPERA Research Plan [Verhoef 2011b].

The required long-term isolation of radioactive wastes from the biosphere can be achieved by a multiple barrier system, consisting of a combination of a man-made engineered barrier system (EBS) with a suitable geological barrier, the repository host rock. Within a multibarrier concept for the disposal of high-level radioactive wastes (HLW), the waste form acts as the first barrier against the release of radionuclides from the waste into the repository near-field. In as such, the performance of the waste form under repository conditions plays an important role with respect to the isolation of the radioactive waste and the radionuclides contained therein from the biosphere. The understanding of the corrosion behaviour of and the consequent radionuclide release from the disposed HLW forms thus an integral part of a safety assessment for a geological repository. HLW intended for future geological disposal in the Netherlands comprises vitrified wastes (glass) from the reprocessing of light water reactor (LWR) fuels from commercial nuclear reactors, research reactor spent fuels (RRSF), spent uranium targets from molybdenum production as well as non-heat generating wastes such as compacted hulls and ends from fuel assemblies packaged in CSD-C containers and legacy wastes.

1.2. Objectives

In this report, the execution and results of the research proposed for task 5.1.1 with the following title in the Research Plan: *HLW waste matrix corrosion processes* is described. This report refers to the work performed with respect to vitrified HLW (i.e. nuclear waste glasses).

The aim of this report is to provide information on the dissolution behaviour of and the radionuclide release from vitrified HLW in a generic repository in Boom Clay in the Netherlands to assess and quantify the safety function ‘delay and attenuation of releases’ in the context of the envisaged safety case. Based on existing data and information obtained from the literature, relevant dissolution processes under the expected conditions in the repository are investigated and discussed to increase the understanding of waste form evolution (i.e. leaching and dissolution behaviour) with time. The results of these investigations comprise data and ranges for dissolution rates of vitrified HLW under repository conditions and the associated release rates of safety relevant radionuclides that can be used in performance assessments for a geological repository in the Netherlands. In addition to the waste form dissolution rates, processes that may retain the leached radionuclides in the immediate near field by interaction with degradation products from the engineered barrier system (i.e. metal corrosion products, and cement degradation products) will be addressed to derive radionuclide source terms.

1.3. Realisation

The literature study presented in this report was performed by a consortium formed by IBR Consult BV (IBR, Haelen, The Netherlands) and Brenk Systemplanung GmbH (BS, Aachen, Germany). The work reported here was carried out in the period January 2013 to March 2016 and the report is based upon, and solely refers to, information available at that time. Thus, for example, where the report refers to ‘current knowledge’ this should be read to mean ‘knowledge existing at the time the work was carried out’.

1.4. Explanation contents

Chapter 2 provides an overview on the general characteristics of nuclear waste glasses used as a waste matrix for the immobilisation of waste streams from the reprocessing of spent nuclear fuels (SNF) and on the power reactors operated in the Netherlands. Issues concerning the inventory of HLW glass within OPERA are addressed in chapter 3. Chapter 4 discusses bounding conditions for the HLW disposal in the Netherlands with respect to the disposal concept and the environmental conditions to be expected in the repository near field and its evolution. Chapter 5 details the results of the review of literature data and other available information on the dissolution behaviour of HLW glasses in the repository environment. Based on the results of this review, in chapter 6 the available information is analysed to describe the dissolution behaviour of HLW glass and the associated radionuclide release under disposal conditions relevant to OPERA. Conclusions and recommendations resulting from the work performed in the frame of this project are given in chapter 7. References cited throughout this report are compiled in chapter 8.

2. Nuclear waste glasses

Vitrification of HLW streams from spent nuclear fuel reprocessing has been established as a suitable immobilisation route during the last decades. At present, glasses, in particular borosilicate glasses, are used on an industrial scale for the immobilisation of high level wastes in the UK, France, the USA, Russia, Belgium, Germany, and Japan (e.g. [Stefanovsky 2004], [Donald 2007], [Weber 2009], [Donald 2010]). Glasses are non-crystalline (amorphous) solid materials, generally manufactured from mixtures of inorganic compounds that exhibit a (reversible) glass transition when heated towards the liquid state. Basic components of oxide glasses comprise network formers, intermediates, and network modifiers (e.g. [Frizon 2009], [Vernaz 2012]). Glass network formers such as silica (SiO_2), borate (B_2O_3), and phosphate (P_2O_5) build a cross-linked network of chemical bonds in the glass structure. Intermediates like alumina (Al_2O_3), magnesia (MgO), or zirconia (ZrO_2) may act either as network formers or network modifiers, depending on the composition of the glass. Network modifiers like Na_2O , Li_2O , or CaO are added to modify the glass structure and to facilitate glass processability, for example, by lowering the melting temperature and/or decreasing the melt viscosity.

Liquid high level radioactive waste streams (HAW) from both civil and military nuclear programmes are commonly immobilised by vitrification, employing mainly borosilicate and phosphate glasses. These glasses provide suitable media for the majority of the species present in these wastes, due to their capability to accommodate ions with variable charges and radii ([Lutze 1988a], [Stefanovsky 2004], [Ojovan 2005], [Donald 2007], [Weber 2009], [Donald 2010]). Glass waste forms for the immobilisation of HAW streams from nuclear fuel reprocessing have been investigated throughout the last 50 years [Weber 2009]. During this time, a large database has been established for vitrified waste forms for HAW immobilisation (especially regarding borosilicate glasses), with extensive information available on processing characteristics, durability, mechanical behaviour, thermal stability and devitrification behaviour, as well as radiation stability (e.g. [Lutze 1988b], [Weber 1997], [Lee 06], [Donald 2007], [Donald 2010], [Vernaz 2012]). Vitrified HLW is generally accepted as a chemically durable material which reliably retains radioactive species.

2.1. Borosilicate glasses

Borosilicate glass formulations comprising basically silica and boron oxide as network formers and sodium and/or lithium oxide as the main network modifiers, have been in use for the immobilisation of HAW streams since the 1950s (cf. [Lutze 1988a], [Stefanovsky 2004] [Donald 1997, 2010]). This is due to their ability to dissolve and accommodate a wide range of waste compounds and their properties can be easily modified and optimised for special applications [Donald 1997]. Other advantages of silicate-based glass waste forms comprise the extensive experience regarding processing technologies as well as knowledge and understanding of their properties derived from the commercial glass industry.

Vitreous silica (SiO_2) would represent an extremely durable waste form [Donald 1997]. However, the high processing temperatures exceeding $2,000\text{ }^\circ\text{C}$ that would be required proves this material unattractive for this usage. The addition of boron oxide (as well as Na_2O and/or Li_2O) to the glass system is therefore employed to reduce the processing temperature for glass formation leading to glass formulations that still exhibit high durability ([Donald 1997], [Stefanovsky 2004]). Borosilicate glasses are currently used on an industrial scale to immobilise high level wastes in the UK, France, the USA, Russia, and Japan, and have been employed for this purpose in Belgium and Germany in the past ([Grambow 2006], [Weber 2009]).

2.2. Phosphate glasses

Although the majority of glasses developed for the immobilisation of HAW are based on borosilicate compositions, investigations on phosphate-based glasses for immobilisation of reprocessing waste and actinides started as early as the 1960s, due to the perceived advantages of lower melting temperatures and higher potential loadings for some waste compounds (e.g. molybdates or chromates) and especially also actinide oxides compared to borosilicate glasses (e.g. [Sales 1988], [Stefanovsky 1995], [Donald 1997], [Stefanovsky 2004]). However, phosphate melts are usually highly corrosive in nature, significantly more than their silicate equivalents. This factor would seriously limit melter lifetime or would require platinum lined melters. Moreover, many phosphate-based glasses are thermally less stable, are more easily devitrified, and exhibit a lower aqueous chemical durability particularly at higher temperatures compared to silicate glass formulations, although there are exceptions depending on glass formulation ([Donald 1997], [Stefanovsky 2004]). Subsequently a number of variants such as sodium alumino phosphate and iron alumino phosphate glasses have been developed to provide for improved chemical durability and higher thermal stability although remaining more corrosive than silicate melts ([Donald 1997], [Stefanovsky 2004]). Leaching rates reported for these phosphate glasses are (initially) significantly lower than for borosilicate compositions, however, the durability decreases considerably as soon as some initial crystallisation occurs in the phosphate glasses. Iron phosphate glasses developed for the immobilisation of HAW are very resistant to devitrification and exhibit a high chemical durability. Investigations aimed at the feasibility of vitrification of HAW arising from commercial reprocessing in Japan using iron phosphate glasses showed that waste loadings of (simulated) HAW of 20 wt.% were achievable at melting temperatures of 1200 °C, without any crystalline phases being present in the final waste form [Fukui 2003]. Sodium alumino phosphate glasses for HAW conditioning are produced in Russia on an industrial scale [Stefanovsky 2004].

2.3. Vitrification technology

A variety of processes have been developed for the vitrification of HAW [Vernaz 2012]. Most processes follow the same basic steps where liquid HAW first undergoes evaporation followed by a calcination step and subsequently vitrification, to produce a homogeneous waste form. The melting temperatures are usually in the range of 1,100 to 1,200 °C to minimize the loss of volatile fission products. The first industrial scale vitrification process initially commenced in 1968 in Marcoule, France, with full scale operation starting in 1978. This process (AVM Process) is operating on a continuous basis and is used with slight modifications also in La Hague (France) and at Sellafield in the UK. In the AVM process, the feed of liquid HAW is mixed with LiNO₃, dried and calcined in a rotary kiln (Figure 2-1). The produced oxides are fed together with the glass frit to the glass melter, consisting of an inductively heated metal crucible. The molten glass is directly poured from the furnace into metal storage canisters, which are sealed after cooling.

Alternative continuous processes have been developed using Joule-heated ceramic melters, where the glass is heated via electrodes (Joule melter or JCM Process) [Donald 2007]. In this process, the liquid waste and the glass frit may be fed directly into the melter in form of a slurry, with evaporation and calcination occurring within the melter. Alternatively, dried and calcined HAW mixed with glass frit is fed into the melter from a rotary calciner, similar as in the AVM process. In the JCM process a highly viscous glass layer forms at the walls of the ceramic melter vessel so that the melt does not contact the crucible directly, reducing the number of contaminated crucibles. Moreover, losses of volatile fission products such as caesium and ruthenium are minimized because the surface of the glass melt is covered by cold materials. Joule-heated ceramic melters for HAW vitrification are used in the USA, where the first large-scale pilot plant was commissioned in 1984, in Japan, Russia, and China [Donald 2007]. A similar process (Pamela process) was employed in the vitrification plant of Eurochemic at Mol, Belgium.

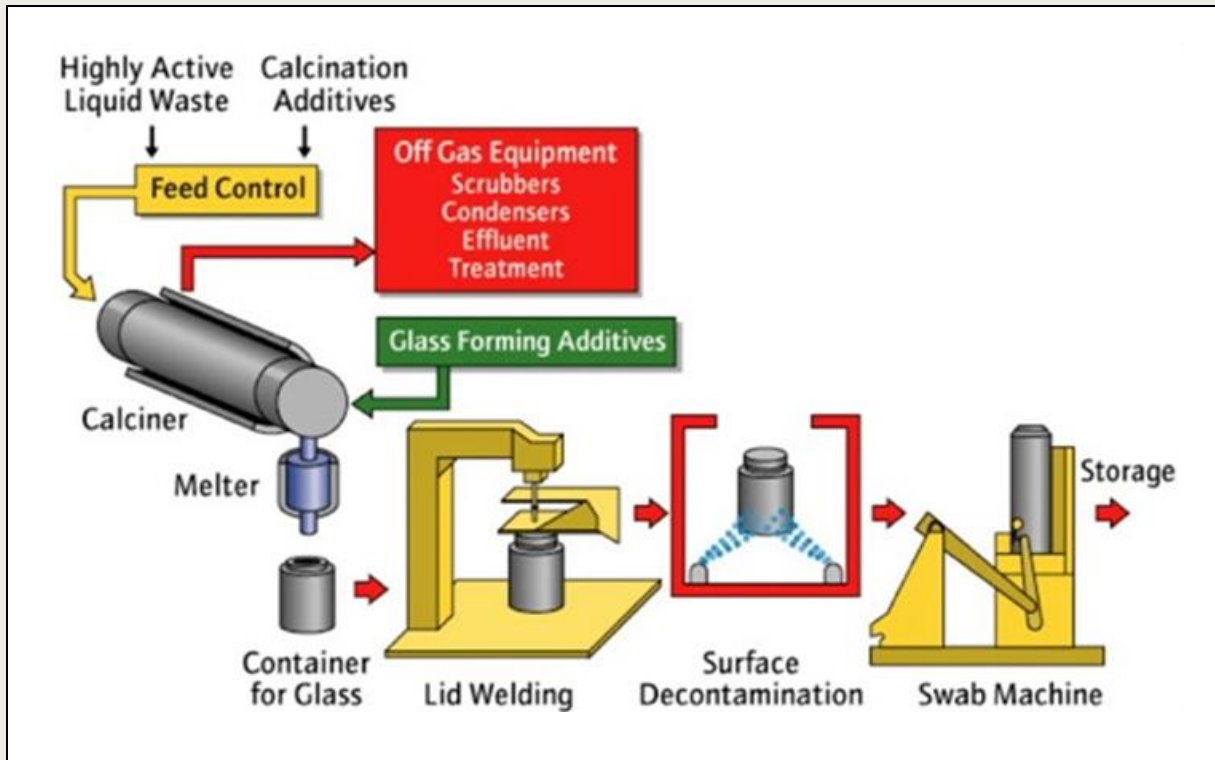


Figure 2-1 Continuous vitrification process scheme [Gribble 2009]

As a related vitrification process, the cold crucible melter (CCM) technology that employs a cold crucible induction melter has been developed in France ([Grambow 2006], [Boen 2010]). This process is based on the use of water-cooled metallic melters and allows for greater flexibility with respect to waste composition and the load of corrosive waste compounds. The melter wall is protected by a layer of solidified glass so, similar to the JCM process, the melt does not come into direct contact with the crucible wall. The design of the melter allows for either the direct feeding of calcined waste and glass frit or for feeding liquid HAW and glass-forming additives. The CCM allows for higher glass melting temperatures thus enabling higher waste loads and/or the production of more durable glasses by increasing the amounts of refractory elements such as zirconium, silicon and aluminium in the glass formulation [Petitjean 2002].

The composition of glass frits employed for the vitrification of HAW from spent nuclear fuel reprocessing in the vitrification plants in La Hague, France, and Sellafield, UK, as well as a glass frit used in the Eurochemic plant in Mol, Belgium are given in Table 2-1. Table 2-2 summarises the composition of some common nuclear waste glasses resulting from the immobilisation of HAW waste streams from spent nuclear fuel reprocessing.

Table 2-1 Composition of selected glass frits used for vitrification of HAW from spent nuclear fuel reprocessing ([Donald 1997], [Donald 2010])

Component		R7T7 (La Hague)	MW (Sellafield WVP)	SM513 (Eurochemic)	SM539 (Eurochemic)
SiO ₂	wt.%	54.9	61.7	58.6	45.5
B ₂ O ₃	wt.%	16.9	21.9	14.7	33.0
Al ₂ O ₃	wt.%	5.9		3	
CaO	wt.%	4.9		5.1	6.5
Na ₂ O	wt.%	11.9	11.1	6.5	10.5
Li ₂ O	wt.%	2.4	5.3	4.7	4.5
ZnO	wt.%	3.0			
TiO ₂	wt.%			5.1	
MgO	wt.%			2.3	

Table 2-2 Typical compositions of nuclear waste glasses (borosilicate glasses) from the vitrification of waste streams from spent nuclear fuel reprocessing

		Cogema	Sellafield WVP MW glass			PAMELA
		R7T7	Magnox	Blend75/25 ¹⁾	AGR/Oxide ²⁾	SM513
SiO ₂	wt.%	45.6	46.0	45.0	49.2	52.2
B ₂ O ₃	wt.%	14.1	16.8	17.0	18	13.1
Al ₂ O ₃	wt.%	4.7	5.1	1.5	<0.1	3.6
Na ₂ O	wt.%	9.9	8.3	8.3	8.9	9.1
Li ₂ O	wt.%	2.0	4.0	4.4	4.0	4.2
MgO	wt.%		5.6	1.5	<0.1	2.1
CaO	wt.%	4.0				4.5
Fe ₂ O ₃	wt.%	1.1	1.7		0.7	1.7
TiO ₂	wt.%					4.5
ZnO	wt.%	2.5				
FP/Zr/An-oxides ³⁾	wt.%	17.0	12.0	22.3	18.7	4.5
Source		[Boen 2010]	[Harrison 2009]	[Brookes 2010]	[Harrison 2009]	[Ferrand 2008]

¹⁾ 25% Magnox waste/75% Oxide waste; ²⁾ 100% Oxide waste; ³⁾ FP: fission products

2.4. Reprocessing of fuels from nuclear power plants in the Netherlands

Within the nuclear programme of the Netherlands, there is currently one nuclear power plant (NPP) in operation: the Borssele NPP (Kernenergiecentrale Borssele), a pressurised water reactor (PWR) located near Vlissingen in the Zeeland Province [MEAAI 2014]. The boiling water reactor (BWR) at Dodewaard (Kernenergiecentrale Dodewaard, Gelderland Province) was permanently shut down in 1997 and is now in Safe Enclosure. The following sections provide a brief overview on these NPP, their basic characteristics are summarised in Table 2-3.

Table 2-3 Nuclear power plants in the Netherlands [WNA 2016a,b]

Reactor	Operator	Type	Design	Criticality	Capacity net/gross	Capacity thermal	Status
Dodewaard	EPZ	BWR	GE	24/06/1968	55/60 MW _e	183 MW _t	shut down
Borssele	GKN	PWR	KWU	20/06/1973	482/515 MW _e	1366 MW _t	operating

2.4.1. Dodewaard

The Dodewaard NPP was the first nuclear power plant established in the Netherlands, intended mainly as a means for the national nuclear power industry to gain know-how about the construction of NPP and exploitation of nuclear power. The construction of the relatively small natural circulation BWR commenced in 1965 and commercial operation started in March 1969 [WNA 2016b]. The Dodewaard NPP was shut down permanently in March 1997 for economic reasons, about 7 years ahead of the originally planned end of service life. After removal of all fissionable material, the plant was brought into Safe Enclosure for a period of 40 years ending in 2045, since the plant reached the state of Safe Enclosure in 2005 [MEAAI 2014].

The spent nuclear fuel unloaded from the Dodewaard NPP was mainly reprocessed at the ThORP facility (Thermal Oxidation Reprocessing Plant) at Sellafield, UK. Between 1978 and 2003, about 57 tons of spent nuclear fuel from the Dodewaard NPP was shipped to Sellafield for reprocessing ([TKSG 1997], [MEAAI 2014]). The resulting vitrified waste (28 waste canisters) was returned from Sellafield to the Netherlands in April 2010, and transferred to COVRA for long-term storage [MEAAI 2014]. About 8.5 tons of spent nuclear fuel from Dodewaard had been reprocessed during the 1970s in the Eurochemic plant in Dessel/Mol, Belgium ([Wolf 1996], [TKSG 1997]). The vitrified product from the Eurochemic plant (PAMELA glass) was not returned to the Netherlands and is therefore not relevant for the Dutch waste inventory within OPERA.

2.4.2. Borssele

The Borssele PWR is the only nuclear power plant operational for electricity production in the Netherlands. It was designed and built by Siemens/KWU. The construction of the plant started in July 1969, commercial operation commenced in October 1973. The originally intended life span of the Borssele NPP of 40 years was extended to 2033 by the Dutch Government in 2006. Following the extension of the operating life, an upgrade of the steam turbine increased the capacity from the original 452 MW_e to 485 MW_e. In 2011, a licence was granted for the use of MOX fuels with 5.4% fissile Pu content as 40% of the fuel load in the Borssele NPP ([WNN 2011], [MEAAI 2014]). The first MOX fuels were loaded into the reactor during the annual refuelling outage in June 2014 [ENS 2014].

Spent nuclear fuels unloaded from Borssele NPP are kept in wet storage for about 3 years in the spent fuel pool at the reactor site prior to reprocessing. Spent nuclear fuel from Borssele is reprocessed by Areva NC at La Hague, France. About 375 tonnes of spent fuel from Borssele have been reprocessed there up to mid-2014. The vitrified wastes and the compacted hulls and ends from the reprocessing process are returned from France to the Netherlands and stored at COVRA. According to the treaty signed by the Republic of France and the Kingdom of the Netherlands in 2012 regulating the reprocessing of Dutch spent fuels produced after 2015, all radioactive wastes from reprocessing will be returned to the Netherlands before 31 December 2052 [MEIAA 2014].

3. HLW glasses relevant for OPERA

The release rates of radionuclides from wastes disposed in a geological repository depend, inter alia, on the processes controlling waste form dissolution and the mechanisms leading to a release of radionuclides from the waste matrices. The release of radionuclides from the waste into the repository near field strongly depends on the distribution and speciation of the radionuclide in the waste form. The matrix compositions and the radiological inventories of the various waste categories included in the OPERA disposal concept [Verhoef 2014a] are addressed in [Meeusen 2014] and [Hart 2014], respectively. In order to determine reliable radionuclide source terms for the safety assessments within OPERA, waste families were defined as groups of radioactive wastes from the same origin, with similar nature, and identical or rather close conditioning characteristics, while belonging to the same category of the current waste classification used in the Netherlands [Verhoef 2016]. For each of these waste families, standardised compositions were derived to be used in the further analysis and assessments of waste form corrosion/dissolution and radionuclide release mechanisms within OPERA. These standardised compositions include inventories of radionuclides per waste container, the expected distribution of the radionuclides in the respective waste matrices and the chemical composition of the wastes as well as the dimensions/properties of the waste containers and – if relevant – the expected heat output in 2130. The information and the level of detail match the requirements of the various tasks within OPERA and reflect the available information [Verhoef 2016]. The following sections summarise the information on the standardised composition and the waste inventories with respect to the waste family vitrified HLW (HLW glass).

3.1. Characteristics of HLW glass within OPERA

HLW glasses to be considered within OPERA comprise the vitrified wastes from the reprocessing of spent nuclear fuels from the two Dutch nuclear power plants that were and are to be returned from the reprocessing plants in Sellafield and La Hague, respectively, and are stored at COVRA (cf. section 2.4). Due to the significantly larger amounts of spent fuel from the Borssele NPP reprocessed at La Hague, the vast majority of the waste glasses will have the characteristics of the French waste glass (R7T7). Waste glasses produced in the Sellafield waste vitrification plant represent less than 10% of the total inventory of HLW glasses in the Netherlands (cf. [Verhoef 2016]).

The technical specifications for the nuclear waste glasses laid down in contracts with the waste producers (i.e. the reprocessing facilities) comprise, inter alia, maximum values for the activities of selected radionuclides, upper limits for the masses of actinides, as well as ranges for glass matrix compositions. Guarantee values for the compositions of waste glasses returned from France and the UK to the Netherlands are summarised in Table 3-1 (cf. [Verhoef 2016]). Regarding the information on the UK waste glasses provided in [Verhoef 2016] (cf. Table 3-1), it should be noted that the ranges for the glass matrix components (i.e. SiO_2 , B_2O_3 and the alkali oxides) refer to the glass frits and not to the produced waste glass, in contrast to the information provided by AREVA for the French waste glasses. Table 3-2 provides additional information on the composition of the waste glasses produced by BNFL in Sellafield, based on data for a batch of 28 waste glass canisters produced in 2004.

Table 3-1 Guaranteed compositions of the waste glass matrices of vitrified reprocessing wastes returned from France and the UK, respectively, and stored in the Netherlands [Verhoef 2016]

		France	UK
SiO ₂	wt.%	42.4 ... 51.7	54 ... 65
B ₂ O ₃	wt.%	12.4 ... 16.5	21 ... 31
Al ₂ O ₃	wt.%	3.6 ... 6.6	
Na ₂ O	wt.%	8.1 ... 11	12 ... 18
Li ₂ O	wt.%	1.6 ... 2.4	
CaO	wt.%	3.5 ... 4.8	
ZnO	wt.%	2.2 ... 2.8	
Fe ₂ O ₃	wt.%	0 ... 4.5	
NiO	wt.%	0 ... 0.5	
Cr ₂ O ₃	wt.%	0 ... 0.6	
P ₂ O ₅	wt.%	0 ... 1	
RuO ₂ +Rh+Pd	wt.%	0 ... 3	
FP/Zr/An-oxides ¹⁾	wt.%	4.2 ... 18.5 ²⁾	7.5 ... 19

¹⁾ FP: fission products; ²⁾ incl. dispersed metal particles

Table 3-2 Composition of waste glass produced in 2004 by BNFL in Sellafield, based on data from a batch of 28 canisters [Verhoef 2016]

		Minimum	Maximum
SiO ₂	wt.%	44.76	46.22
B ₂ O ₃	wt.%	16.33	16.93
Al ₂ O ₃	wt.%	1.54	2.11
Na ₂ O	wt.%	7.99	8.25
Li ₂ O	wt.%	3.87	4.13
MgO	wt.%	1.43	1.57
FP-oxides ¹⁾	wt.%	12.50	13.65
An-oxides	wt.%	0.42	0.68

¹⁾ FP: fission products

3.2. Waste canisters for HLW glass and packaging

In the vitrification plants, the molten glasses are poured into stainless steel waste canisters, containing each about 150 L of waste glass (approximately 400 kg). Figure 3-1 depicts the French canister for waste glasses CSD-V (Colis Standard de Déchets Vitriifiés), which has an internal diameter of 420 mm and a wall thickness of 5 mm, identical in construction to the waste canisters used in the UK. The waste canisters are allowed to cool down for 24 h before being closed by welding on the canister top. According to [Verhoef 2016], there are no guaranteed parameters for the steel used for the waste canisters. In the waste specifications in the Netherlands, stainless steel type X12 CrNi 23.13 as per NF EN 10095 with additional specified values (or equivalent) is presented as typical.

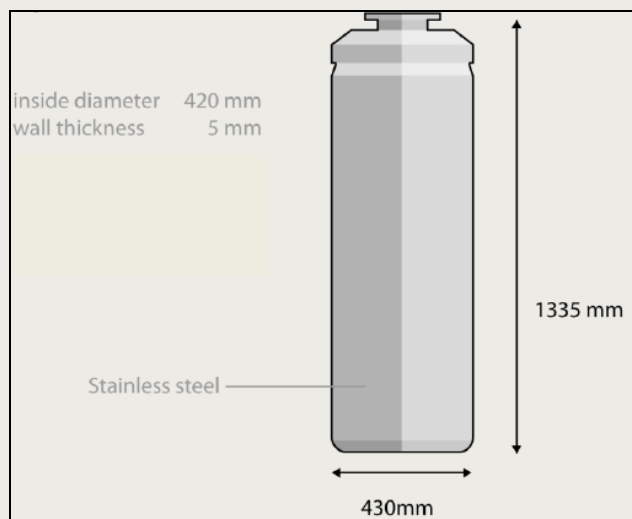


Figure 3-1 Schematic sketch of a CSD-V canister used for storage and disposal of vitrified HLW [Verhoef 2016]

According to the waste inventory provided in the OPERA disposal concept [Verhoef 2014a], 625 waste canisters (CSD-V) containing vitrified HLW are intended for final disposal. The maximum heat production of each waste canister at disposal time (i.e. after a storage period of at least 100 years) is expected to be less than 200 W [Verhoef 2016]. Within the OPERA disposal concept in clay, it is assumed that each CSD-V canister is placed into one supercontainer (cf. section 4.1) for final disposal [Verhoef 2014a].

3.3. Radionuclide inventory

A reference radionuclide inventory for CSD-V canisters containing vitrified HLW at the time of disposal was derived in [Verhoef 2016], based in particular on the technical specifications for wastes processed in La Hague [AREVA 2007] and Sellafield [BNFL 2001]. It was assumed that this inventory applies to the vitrified wastes from both sources [Verhoef 2016]. The activity of radionuclides per CSD-V canister at disposal time is summarised in Table A-1 in Appendix 1. Table 3-3 summarises the guaranteed maximum values for uranium, plutonium, caesium-137 and strontium-90 per canister of vitrified waste stored in the Netherlands. For the vitrified HLW it is generally expected that the radionuclides are homogeneously distributed in the waste matrix [Verhoef 2016].

Table 3-3 Guaranteed maximum inventories of selected actinides and fission products per waste canister of vitrified HLW produced in France and the UK and stored in the Netherlands [Verhoef 2016]

		France	UK
U	g	4,500	2,000
Pu	g	110	200
¹³⁷ Cs	TBq	6,600	8,000
⁹⁰ Sr	TBq	4625	5,500

The total radionuclide inventory of the wastes to be considered for final disposal within OPERA was estimated in [Hart 2014]. [Hart 2014] derived the radionuclide inventories in the various waste categories included in the OPERA disposal concept [Verhoef 2014a] such as low and intermediate level waste (LILW), non-heat generating HLW, RRSF or vitrified HLW in the year 2130. Only radionuclides with half-lives greater than 10 years were taken into account as relevant for the long-term safety of the repository [Hart 2014]. The

inventories of radionuclides relevant for the long-term safety contained in the HLW glasses in the year 2130 are provided in Table A-2 in Appendix 1. The inventories of selenium-79 and iodine-129 in the vitrified HLW provided in [Hart 2014] were derived from information on the respective inventories in HLW-glass canisters used in the NAGRA Model Inventory [McGinnes 2002].

4. Conditions in the near field

The evaluation of the long-term behaviour of nuclear wastes in a deep geological disposal facility requires an understanding of the environmental conditions to which the material will be exposed. The durability of the waste forms and the long-term radionuclide release are affected by intrinsic properties of the waste forms as well as by the interaction with the disposal environment, i.e. the engineered barriers system and the geological environment, and the near-field conditions that may evolve over time. Thus with respect to the disposability of the waste forms and the safety case for a repository, assessments and predictions of the long-term durability of the waste forms in the repository environment, and radionuclide release rates under realistic repository conditions are essential.

Near field characteristics that affect waste form performance and radionuclide source terms include hydrogeological (e.g. groundwater flow regimes and flow rates) as well as geochemical conditions (e.g. pH, redox potential, temperature, ionic strength, and groundwater composition), which both depend on the repository design and the geological environment. The deep geological disposal of LILW and HLW addressed within OPERA is at present at a site-generic stage, i.e. no potential repository site has been selected. However, the preselection of a potential geological formation (Boom Clay) for the repository and the development of a disposal concept [Verhoef 2014a] for the OPERA safety case allow constraining the near field conditions in the repository to some degree. The following section 4.1 provides an overview on the disposal concept pursued within OPERA. Aspects regarding the expected evolution of the repository near field are discussed in section 4.2.

4.1. OPERA disposal concept

The disposal concept pursued within OPERA considers the installation of a multi-barrier repository system within the poorly indurated Boom Clay formation in the Netherlands. A multi-barrier system intended for the long-term isolation of radioactive wastes from the biosphere typically comprises a combination of a man-made engineered barrier system (EBS) with a suitable geological barrier, the repository host rock. An outline of the disposal system in clay has been provided by [Verhoef 2011a] and [Verhoef 2014a]. The generic disposal concept for HLW pursued within this context is based on the Belgian ONDRAF/NIRAS supercontainer concept (cf. [ONDRAF 2004], [Bel 2006], [ONDRAF 2013]).

The OPERA disposal facility consists of both surface and underground facilities, connected by two vertical shafts and (optionally) an inclined ramp [Verhoef 2014a]. The surface facilities comprise the waste conditioning facilities required for receiving, inspecting, and conditioning of the different waste types and the construction and supply facilities, i.e. the support infrastructure for construction, operation, and closure of the underground disposal facilities.

The underground disposal facilities contain separate disposal sections for different types of wastes, a pilot facility and a workshop for maintenance work, all connected by the main gallery, which is an orbicular structure. The disposal drifts are horizontal boreholes supported by wedge-shaped concrete blocks. The disposal drifts used for vitrified HLW and RRSF have a length of 45 m and are directly connected to the main gallery. The dimensions of the disposal tunnels in the different sections of the OPERA disposal facility are provided in Table 4-1.

Table 4-1 Dimensions of the disposal drifts in different sections of the OPERA disposal facility [Verhoef 2014a]

Waste section	Number of drifts [-]	Length [m]	Diameter (outer/inner) [m]	Concrete support thickness [m]	Spacing [m]
heat-generating HLW	47	45	3.2/2.2	0.50	50
RRSF	6	45	3.2/2.2	0.50	50
non-heat-generating HLW	36	200	3.2/2.2	0.50	50
LILW and DU	65	200	4.8/3.7	0.55	50

The functions and compositions of various cementitious materials utilised within the OPERA disposal concept in clay (e.g. for mechanical support, waste conditioning, backfilling) are discussed in [Verhoef 2014b].-The mechanical support during the constructional and operational phase of the geological disposal facility is provided by the gallery lining. In [Verhoef 2014b] concrete segments made with Portland fly ash cement (CEM II) are proposed for this purpose. The suggested composition of the concrete used for the gallery lining and the mechanical support of the disposal tunnels is provided in Table 4-2.

Table 4-2 Suggested composition of concrete used for the mechanical support of the disposal tunnels [Verhoef 2014b]

Component/Parameter	Type	
cement	CEM II/A to B-(V)	386 kg m ⁻³
water		125 kg m ⁻³
plasticiser	Woermann BV 514	1.33 kg m ⁻³
superplasticiser	Woermann FM 30	3.65 kg m ⁻³
fine aggregate	quartz sand: 0-2 mm	615 kg m ⁻³
coarse aggregate	quartz gravel: 2-8 mm	612 kg m ⁻³
coarse aggregate	quartz gravel: 8-16 mm	700 kg m ⁻³
w/c-ratio		0.39

Prior to disposal, the CSD-V canisters with vitrified HLW (as well as CSD-C canisters and ECN canisters with RRSF and non-heat generating HLW) will be overpacked in supercontainers [Verhoef 2014a]. In the supercontainer concept, the waste canister, overpack and buffer are transported and disposed of as one entity. The OPERA supercontainer, adopted from the Belgian supercontainer concept (cf. [Bel 2006]), consists of a carbon steel overpack (30 mm), a concrete buffer (600 to 700 mm) and a stainless steel envelope (4 mm) [Verhoef 2016]. Supercontainers with a length of 2.5 m will contain one CSD-V canister with vitrified HLW or one CSD-C canister with compacted reprocessing wastes, respectively, whereas supercontainers with a length of 3.0 m will contain two ECN-canisters with either RRSF or other non-heat generating HLW [Verhoef 2014a]. Taking into account the length of a single disposal drift in the HLW section of the OPERA disposal facility, each disposal drift can hold 15 supercontainers with a length of 2.5 m containing vitrified HLW (CSD-V) and/or compacted wastes (CSD-C). For the supercontainers with a length of 3 m used for RRSF and other (non-heat generating) HLW packaged in ECN-canisters, the emplacement of 12 supercontainers in each disposal drift are considered in [Verhoef 2014a]. The provisional properties of the OPERA supercontainer for vitrified wastes and compacted reprocessing wastes are shown in Table 4-3.

Table 4-3 Provisional properties of the OPERA supercontainer for reprocessing wastes [Verhoef 2014a]

Property	
outer container diameter	1.9 m
outer container length	2.5 m
waste container(s)	1 CSD-V or CSD-C canister
steel overpack thickness	3 cm
concrete buffer thickness	0.6-0.7 m
steel envelope thickness	0.4 cm
weight	approx. 20,000 to 24,000 kg
maximum dose rate at container surface	≤10 mSv/h

Potential compositions of the concrete to be used in the OPERA supercontainer are discussed in [Verhoef 2014b], based on compositions studied by the Belgian waste management organisation ONDRAF/NIRAS. In [Verhoef 2014b] concrete made with sulphate-resistant Portland cement (CEM I) and limestone aggregates is proposed for the OPERA supercontainer (cf. Table 4-4). As an alternative, self-compacting concrete investigated by ONDRAF/NIRAS (cf. [van Humbeeck 2007]) was suggested in [Verhoef 2014b].

Table 4-4 Suggested composition of concrete used for the OPERA supercontainer [Verhoef 2014b]

Component/Parameter	Type	
cement	CEM I/42.5 N HS LA (LH)	350 kg m ⁻³
water		175 kg m ⁻³
filler	Calcitec 2001 ME	50 kg m ⁻³
plasticiser	Glenium 27/20	4.41 kg m ⁻³
fine aggregate	limestone: 0-4 mm	708 kg m ⁻³
coarse aggregate	limestone: 2-6 mm	414 kg m ⁻³
coarse aggregate	limestone: 6-14 mm	191 kg m ⁻³
coarse aggregate	limestone: 6-20 mm	465 kg m ⁻³
w/c-ratio		0.50

N usual initial strength, HS High Sulphate resistance, LA Low Alkali content, (LH Low Hydration heat)

After the emplacement of the waste packages in the disposal drifts, the tunnels are backfilled with grout to fill the voids between the gallery linings and emplaced waste packages and hydraulically sealed off using a plug [Verhoef 2014a]. For simplicity it is presumed in OPERA that the type of backfill is independent of the type of emplaced waste, i.e. the same mortar is used as backfill in all waste sections of the disposal facility. Foam concrete made either with Portland cement (CEM I) or blast furnace slag cement (CEM III) and fine aggregates is proposed and investigated within OPERA for the backfill providing the enclosure of the emplaced waste packages [Verhoef 2014a, b]. The composition of the foam concrete for the backfill suggested in OPERA is given in Table 4-5 for two different densities [Verhoef 2014b].

Table 4-5 Suggested composition of the foam concrete used for the backfill in OPERA [Verhoef 2014b]

Component/Parameter	Type	Density 1200	Density 1600
cement	CEM I	360 kg m ⁻³	400 kg m ⁻³
water		140 kg m ⁻³	160 kg m ⁻³
foaming agent	TM 80/23 (synthetic)	1 kg m ⁻³	1 kg m ⁻³
water		21.3 kg m ⁻³	13.6 kg m ⁻³
fine aggregate	quartz sand: 0-4 mm	750 kg m ⁻³	1100 kg m ⁻³
w/c-ratio		0.45	0.43

4.2. Near field evolution

The long-term performance of a waste form in a deep geological repository cannot be assessed without an understanding of the conditions to which the material will be exposed. Besides intrinsic properties of the waste matrix (e.g. material composition, chemical and mechanical properties), the interaction with the disposal environment, i.e. the engineered barriers system and the geological environment, and the conditions prevailing in the near field affect the waste form durability and the radionuclide release. Near field factors substantially affecting the radionuclide source term for a waste form comprise hydrogeological (e.g. groundwater flow/exchange rates) and geochemical conditions (notably pH, redox potential, temperature, gas partial pressures, groundwater salinity/composition, microbial activity), which essentially depend on the repository design and the geological environment. In general after closure of the repository, the near-field will be influenced by a number of complex, inter-related processes such as (i) heat generation from the emplaced high-level wastes, (ii) resaturation of the repository, (iii) consumption of oxygen, (iv) gas generation due to corrosion, microbial degradation, and radiolysis of water and organic materials, (v) corrosion of waste containers, and (vi) the evolution/degradation of engineered barriers by interaction with the local groundwater (e.g. [Beattie 2012]). The extent and chronology of these processes will vary between different repository concepts [Beattie 2012].

The hydraulic conductivity of the host rock is important with respect to a variety of aspects related to the performance of the repository, e.g. the time required for the resaturation of the repository after closure, the mass transport to and from the disposal tunnels and waste containers (including the transport/flow of potentially deleterious groundwater constituents into the near field, and the transport of radionuclides released from the wastes into the far field), or the time frame for the leaching of cementitious backfill or buffer materials. Furthermore, the porosity and permeability affect the gas flow out of the near field (e.g. mode and rate of transport of H₂ generated by metal corrosion) and the potential for the formation of a separate gas phase in the repository. The composition of the groundwater in the surrounding host rock formation can affect the chemical conditions within the repository near-field as well as the degradation rates of cementitious barriers and the corrosion of metallic waste containers, due to the presence of potentially deleterious components (e.g. sulphate and magnesium with respect to cement degradation; sulphides and chloride with respect to metal corrosion, etc.) in elevated concentrations.

Although the properties of the Boom Clay and the groundwater composition at a potential repository site in Boom Clay in the Netherlands cannot be defined in detail at this time due to the inherent variability of the Boom Clay formation throughout the Netherlands (i.e. no

"reference" conditions are available), the general evolution of the repository near-field and the expected overall conditions relevant to the performance of the disposed high level wastes can be constrained to a certain degree. Section 4.2.1 discusses the probable evolution of pH and pore water composition in the near-field of the HLW-section of the OPERA disposal facility resulting from the interaction between the cementitious barriers and the Boom Clay groundwater. The expected evolution of the redox conditions in the repository near-field is addressed in section 4.2.2. Section 4.2.3 summarises the main conclusions regarding the near-field evolution relevant to the long-term behaviour of high-level radioactive wastes to be disposed in the Netherlands.

4.2.1. Evolution of pH and pore water composition in the HLW section

Within the OPERA disposal concept, cementitious materials are the main constituents of the near-field in the planned repository, e.g. in the supercontainer buffer, the backfill and the gallery linings (cf. section 4.1). The chemical and physical conditions in the repository near-field will thus be determined by the large amounts of hydrated cements for long periods of time (e.g. [Berner 1992], [Atkins 1992], [Glasser 2011], [Drace 2013]). The degradation of the engineered barriers and the evolution of the geochemical conditions will occur due to the disequilibrium between the chemical conditions in the cementitious materials and the groundwater infiltrating into the near-field (cf. [Wieland 2001]), and the cementitious materials will be leached in order to adjust the geochemical conditions in the near field to the groundwater conditions in the long-term.

The cementitious materials in the EBS will contain a number of hydrated cement phases, with the exact mineral assemblage depending on the cement formulation, curing time and temperature. The evolution of the cementitious materials, pore water pH and chemistry in the repository near field under leaching conditions in the post-closure phase is commonly described by various stages, defined by different pH ranges in the pore water and associated buffering phases (cf. [Atkins 1992], [Glasser 2011], [Drace 2013]). In addition to the changes in the chemical conditions and the pH buffering capacity due to the sacrificial dissolution of the hydrated cement phases, also the physical/hydraulic properties (porosity, permeability, and tortuosity) of the cementitious barrier materials are affected (cf. [Drace 2013]).

Initially, the main components of the cementitious materials are expected to be calcium-silica-hydrate (CSH) gels, portlandite ($\text{Ca}(\text{OH})_2$), hydrated calcium aluminates, and alkali (i.e. Na, K) hydroxides/sulphates (e.g. [Glasser 2011], [Hoch 2012]). In stage I, the initial cement pore water composition is dominated by the dissolution of the alkali hydroxides (NaOH and KOH) that will condition the pore water to a high pH (i.e. $\text{pH} > 13$) (cf. [Wieland 2002], [Glasser 2011]). As groundwater gradually replaces the initial pore water, in stage II the chemistry will be dominated by the dissolution of portlandite, which will maintain a pH of about 12.5 in the pore water. After portlandite depletion, in stage III the pH will be buffered in the range between 10 and 12 by the incongruent dissolution of CSH-phases (i.e. preferential release of calcium), lowering the Ca/Si-ratio over time and reducing the pH value at which the pore water is buffered (e.g. [Berner 1988], [Harris 2002], [Glasser 2011]). The formation of secondary minerals (e.g. calcite, brucite, hydrogarnet, ettringite, and/or hydrotalcite) may occur due to reactions between groundwater constituents and cement phases [Hoch 2012]. After complete depletion of the CSH, the pore water composition and pH can be controlled by secondary phases such as calcite (e.g. [Wang 2013a]) and the pH can continue to decrease to a value buffered by the groundwater in the host rock formation (e.g. [Krupka 1998], [Glasser 2011], [Drace 2013]).

The duration of the different stages and the timescales of pore-water evolution depend on various factors, including the pore volume of the cementitious materials and the connectivity of pore spaces, the hydraulic conductivity of the host rock and the hydraulic

potentials, and the groundwater composition and the concentration of potentially deleterious components (e.g. magnesium and sulphate). Generally it is expected to take thousands to tens of thousands of years until the pH of the cement pore water decreases to values below pH 10 and approaches the pH of the contacting groundwater. In general, a diffusion controlled system, such as in a clay host rock, is expected to maximise the duration of the high pH period [NAGRA 2002]. Simulations performed for the Belgian supercontainer concept indicate that highly alkaline conditions with a pH above 12.5 remain for at least 80,000 years (cf. [Wickham 2008], [Wang 2009a]). [Diomidis 2014] expected highly alkaline conditions to prevail for a considerably longer period of time in the near field of a Swiss L/ILW repository due to larger amounts of cementitious materials in the caverns and thus higher availability of alkalis and portlandite. According to [Wersin 2003] stage II (portlandite stage, pH 12.5) will persist over very long time periods (many hundred thousand to millions of years) in a cementitious repository in Opalinus Clay, due to the very low water exchange rate. Calculations made for the geological disposal programme in the UK indicated a pH above 12.5 for over 100,000 years and a pH above 10.5 for over a million years in a cementitious repository [Kursten 2004].

Based on scoping calculations of the near field evolution in concrete in contact with Boom Clay ground water for a repository according to the supercontainer concept in Boom Clay in Mol, Belgium [Wang 2009a], [Lemmens 2012] described the evolution of the concrete pore water with a decrease from pH 13.5 (young cement water) to 12.5 (evolved cement water) and further to about pH 12 (old cement water). [Lemmens 2012] expected the first two stages (pH 13.5 to 12.5) to last up to several 10^5 years, due to the expected slow transport by diffusion. Figure 4-1 depicts the expected evolution of the pH at the interface between cement and Boom Clay. The simulated cement pore water compositions are provided in Table 4-6 ([Wang 2009a], [Ferrand 2013]). For comparison, the expected cement pore water compositions resulting from the interaction between Opalinus Clay pore water and cementitious materials in a proposed LILW repository in Switzerland are provided in Appendix 2.

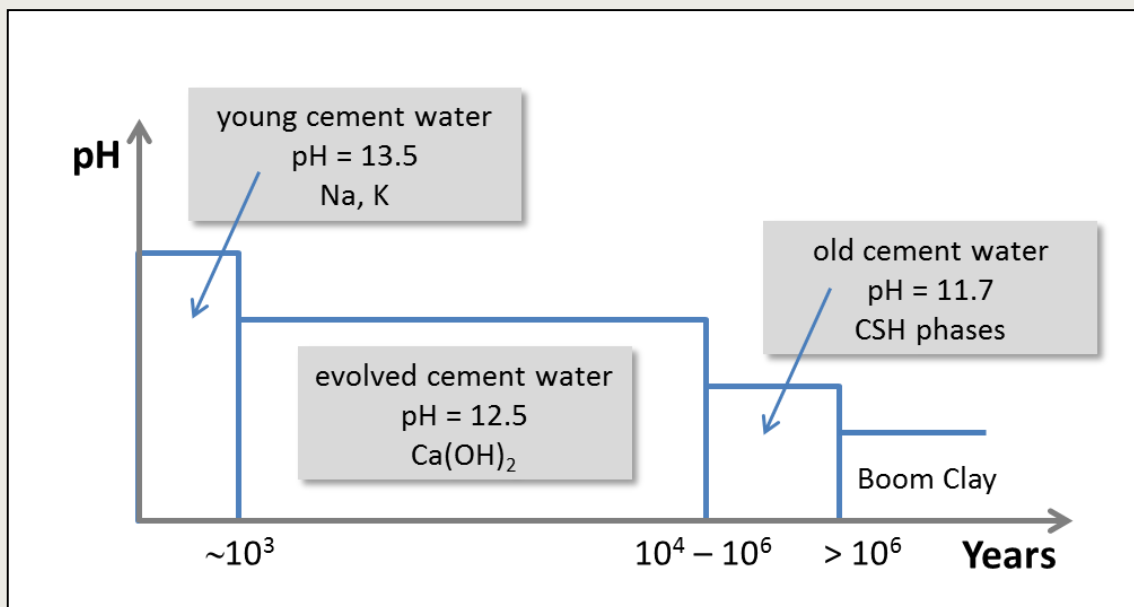


Figure 4-1 Evolution of the pH in the pore water at the interface between cement and Boom Clay (modified after [Ferrand 2013]).

Table 4-6 Simulated pore water composition in the near-field concrete of a cementitious repository in Boom Clay in Mol (adapted from [Wang 2009a], [Ferrand 2013] and [Cachoir 2015]; Boom Clay pore water from [De Craen 2004]) - concentrations in mmol L⁻¹)

	Young cement water	Evolved cement water	Old cement water	Boom Clay pore water
pH	13.5	12.5	11.7	8.5
Eh	--800 mV	--800 mV	--800 mV	-274 mV
Na	141	15.1	15.1	15.6
K	367	0.2	0.2	0.2
Ca	0.7	15.3	0.8	0.05
Mg	$\sim 10^{-7}$	$\sim 10^{-7}$	$\sim 4 \cdot 10^{-6}$	0.06
Si	$3 \cdot 10^{-4}$	$3 \cdot 10^{-6}$	$8 \cdot 10^{-4}$	0.1
Al	0.06	0.005	9.4	$2.4 \cdot 10^{-5}$
CO ₃ ⁻²	0.3	0.008	0.02	14.4
Cl ⁻	0.2 ... 12	0.2	0.2	0.7
SO ₄ ²⁻	2	0.007	0.05	0.02

Within OPERA, the evolution of the near-field conditions (e.g. regarding water saturation of the repository components, temperature evolution, and pH conditions) in the HLW/SF-section of the OPERA disposal facility have been addressed by [Kursten 2015] and [Seetharam 2015]. The timescale of resaturation of the repository is mainly dependent on the unsaturated hydraulic properties of the EBS materials and the Boom Clay, the porosity/permeability of the cementitious materials, the hydraulic conductivity of the Boom Clay and the hydraulic gradient (cf. [Wickham 2008]). The calculations of [Kursten 2015] indicate that the concrete buffer of the supercontainer becomes fully water saturated soon after the disposal tunnels are backfilled (i.e. in less than 10 years). However, these calculations were performed without the presence of a stainless steel envelope. One of the main reasons being that it is very difficult to simulate water transport through a single hole, since the envelope will be fabricated from stainless steel, which, under repository conditions, will mainly be susceptible to localized corrosion (e.g. high chloride concentrations could lead to pitting corrosion) [Kursten 2016]. Thus the time frame of resaturation of the supercontainer concrete and thus the arrival of deleterious species at the carbon steel overpack will depend on the lifetime and failure mechanisms of the steel envelope.

Simulations of the temperature evolution in the OPERA disposal facility for the disposal of vitrified HLW show that the surface temperature of the respective supercontainers will not exceed 40 °C, due to the 100 years cooling time of the HLW prior to disposal [Kursten 2015]. The temperature at the surface of the overpack in the simulations reached a peak temperature of 50 °C after about 10 years that decreased to below 30 °C after 100 years [Kursten 2015].

Scoping calculations of the pH evolution in the cementitious pore water of the concrete buffer at the interface to the carbon steel overpack indicate a decrease of the initial pH (13.5, controlled by the dissolved alkalis) to a minimum value of 12.14 after 9 years when temperature reaches its peak value of 50 °C. It is expected that high pH conditions (i.e. pH 13.5) will be resumed in the concrete after the short thermal phase [Kursten 2015]. The further long-term evolution of the pH under isothermal conditions at ambient temperature is shown in Figure 4-2. Conditions with pH ~ 13.5 will prevail up to about 1,000 years until the concrete buffer gets depleted in Na- and K-hydroxides [Kursten 2015]. Afterwards, the

pH will be determined by portlandite dissolution at about 12.5; this pH is predicted to persist for at least 80,000 years after which it will drop to a value of about 11.3 [Kursten 2015]. The predicted pH evolution is very conservative due to the neglect of (i) pore clogging in the cementitious materials due to calcite precipitation, and (ii) transport limitations in the Boom Clay. Thus it is expected that a pH of 12.5 could be maintained in the concrete buffer for much longer time spans than 80,000 years [Kursten 2015].

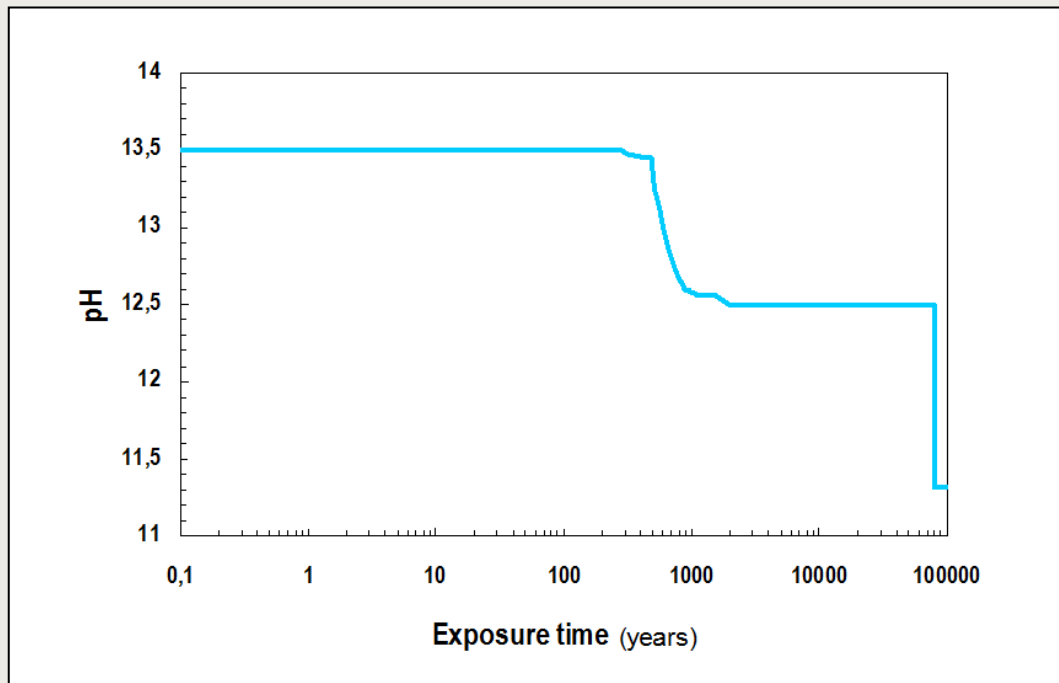


Figure 4-2 Long-term evolution of the pH in the pore water at the cement/overpack interface of the supercontainer as function of time after repository closure [Kursten 2015]

4.2.2. Evolution of redox conditions

The presence of oxygen plays a paramount role with respect to the evolution of the redox conditions in the repository in the post-closure phase. Initially after operation and closure of the disposal facility, some oxygen will be trapped in voids in the excavation-disturbed zone and in pores in the buffer/backfill materials, leading to aerobic conditions during resaturation. However, the oxygen remaining after closure will be consumed comparatively fast by a number of processes, such as corrosion of metallic canister materials, oxidation of ferrous iron bearing minerals and sulphides present in the host rocks, reaction with organic matter, and aerobic microbial respiration or other mechanisms (e.g. [Diomidis 2014]). Thus after an initial aerobic phase, anoxic conditions will prevail in the repository near field that are expected to persist indefinitely (cf. [Diomidis 2014], [Kursten 2015]). The duration of the aerobic phase depends on the amount of oxygen present and the rates of the oxygen consuming reactions [Neill 1994]. In general, the rates of oxygen consumption and metal corrosion are strongly dependent on the water saturation which itself depends on the temperature and the hydraulic properties of the host rock formation and the cementitious materials (cf. [Wersin 2003]). The generation of H₂ due to anoxic corrosion of container materials or other metals present can further enhance the reducing conditions in the repository, depending on the nature of the metals and their anoxic corrosion rates.

According to [Diomidis 2014], during the initial oxic phase in which oxygen is still available, a redox potential in the range of 200 mV can be expected. Once oxygen is consumed the only available oxidant is water, and thus a redox potential as low as -750 mV vs. SHE is expected in highly alkaline environments (cf. [Smart 2004], [Diomidis 2014]). The redox conditions will be influenced by various reactions occurring between dissolved and solid redox-active species under cementitious conditions (e.g. [Wersin 2003]). Due to the amounts of iron/steel in the repository environment and the ease of electron transfer between Fe(II) and Fe(III) compared to other redox couples, it is mainly assumed that iron phases control redox conditions in the repository near-field (cf. [Wersin 2003] and references therein, e.g. [Jobe 1997], [King 2000]).

[Berner 2003] estimated the redox conditions in the reference pore water of a cementitious LILW repository in the Opalinus Clay in Switzerland. A possible range of redox conditions was estimated for different combinations of iron bearing solids (including sulphides), assuming that the redox conditions are generally defined by the Fe^{2+}/Fe^{3+} -couple and magnetite is the major corrosion product in equilibrium with the cementitious pore fluid. The calculations based on these assumptions resulted in redox potentials ranging from -750 to -230 mV at a pH of 12.55. For an initial stage pore water at pH ~13.4, a redox potential of -430 mV was calculated [Berner 2003].

More recently, [Berner 2014] derived a pore solution composition for radionuclide solubility calculations in the repository environment based on the equilibration of a cement/concrete system with Opalinus Clay water for 10,000 years due to diffusion processes. The redox potential of the system of about -500 mV was calculated from the thermodynamic equilibrium with Fe-monocarbonate ($Ca_4Fe^{III}_2(CO_3)(OH)_{12}(H_2O)_5$), Fe-ettringite ($Ca_6Fe^{III}_2(SO_4)_3(OH)_{12}(H_2O)_{26}$), Fe-hydroxalcalite ($(MgO)_4Fe^{III}_2O_3(H_2O)_{10}$) and hydrous magnetite ($Fe_3O_4 \cdot 2H_2O$) [Berner 2014].

[Wang 2009a] performed scoping calculations of the geochemical evolution in the cementitious repository near-field relevant for the Belgian supercontainer concept, taking into account the reference pore water composition in the Boom Clay at Mol, Belgium. Depending on the dominant corrosion products of the metallic barriers under anaerobic conditions, i.e. either magnetite or $Fe(OH)_2$, redox potentials were estimated at the surface of the metallic barriers (cf. Table 4-7). The redox potentials are assumed to be around or below -800 mV as long as some uncorroded iron/steel remains [Wang 2009a]. [Wang 2009a] expected this phase to be followed by the establishment of redox conditions controlled by the E_H of the in-diffusing Boom Clay pore water at about -300 mV.

Table 4-7 Estimated redox conditions in the cementitious near-field of a HLW-repository in Boom Clay in Mol as function of dominant metal corrosion products and pH in the presence of uncorroded metals (after [Wang 2009a])

Corrosion product	pH	Redox potential
Magnetite (Fe_3O_4)	13.5	-884 mV
	12.5	-825 mV
$Fe(OH)_2$	13.5	-850 mV
	12.5	-800 mV

More recently within the context of radionuclide solubilities in the pore water of the supercontainer buffer concrete, [Wang 2013a] discussed again the redox conditions in the different stages of cement degradation in a deep geological repository for HLW in Boom Clay in Belgium. Based on the approach of [Wersin 2003], three different mechanisms were proposed that could control the redox conditions in the cementitious system:

- (1) the dissolved iron concentration is controlled by iron-cement interactions resulting in a total dissolved iron concentration of 10^{-7} mol kg⁻¹ in equilibrium with magnetite as corrosion product;
- (2) the dissolved iron concentration is controlled by the solubility of iron oxihydroxides (Fe(OH)₃) and magnetite is one of the corrosion products;
- (3) the dissolved iron concentration is controlled by the solubility of goethite (FeOOH) and magnetite is one of the corrosion products.

The redox potentials calculated using the NAGRA/PSI 01/01 thermodynamic database [Hummel 2002] ranged between -90 to -800 mV in stage I (pH 13.5) and between -30 and -741 mV in stage II (pH 12.5) [Wang 2013a], depending on the mechanism controlling the total dissolved iron concentration in the cementitious pore water. Moreover it was noted by [Wang 2013a] that distinctively different redox potentials were calculated when using the ANDRA Thermochimie v7b database [Giffaut 2014] instead of the NAGRA/PSI database. [Wang 2013a] concluded that an accurate estimation of the redox potential in the engineered barrier system is difficult due to the uncertainties regarding the mechanisms controlling the redox conditions and the thermodynamic data, but in general the redox potential in the near field of the supercontainer is expected to be reducing.

4.2.3. Résumé

Although representative (“reference”) conditions regarding the hydraulic properties and the pore water composition of the Boom Clay for the generic OPERA disposal facility are not available yet (cf. [Seetharam 2015]), the overall evolutionary pathway for the near-field conditions can be described, in which conditions gradually evolve from unsaturated to water saturated and from aerobic to anaerobic/reducing. After a fast resaturation of the system within a few years after closure and a brief thermal phase with peak temperatures not exceeding 50 °C at the cement/overpack interface of the supercontainer, the repository near-field will further evolve under ambient conditions [Kursten 2015]. The chemical evolution of the repository system will be characterised – on the timescale of thousands to hundred thousands of years – by the continuous interaction of the cementitious near-field materials with the Boom Clay pore water and the accompanying mineralogical changes that will buffer the pH to values >12 under anoxic/reducing conditions. The time frame for saturation of the supercontainer concrete will depend on the lifetime and failure mode of the stainless steel envelope, but starting with the failure of the envelope, a similar chemical evolution in the concrete in the supercontainer buffer as in the other cementitious materials (i.e. long-lasting anoxic/reducing conditions at high pH) can be expected.

5. Dissolution of HLW glass in the repository environment

The prediction of the performance of nuclear waste glasses in the repository environment requires an understanding of the processes that determine the glass dissolution rate within the context of the geochemical conditions the glass is exposed to. Generally, the dissolution of glasses in aqueous environments is a complex process depending on the intrinsic properties of the glass (e.g. glass composition, surface area, structure, etc.) as well as on the hydrogeochemical conditions, such as solution composition and pH, temperature, and water exchange rates and prevailing solute/mass transport mechanisms. A number of studies were performed in the recent years focussing on an understanding of glass alteration mechanisms as function of glass composition and environmental variables (cf. [Gin 2013a] and references therein). The long-term behaviour of nuclear waste glasses under repository conditions has been investigated intensely in the last decades (e.g. in the EC funded projects GLAMOR, GLASTAB, CORALUS, and NF-PRO), especially for disposal in clay formations, increasing the comprehension of the key processes relevant to the long-term behaviour of nuclear waste glasses under geological disposal conditions (e.g. [van Iseghem 2006], [Valcke 2006a,b], [van Iseghem 2007], [van Iseghem 2012]). Key issues addressed in this context comprised the measurement of glass dissolution rates, the characterisation of the alteration layer, the interaction of glasses with near field materials, and the behaviour of radionuclides during waste glass dissolution. Therefore, the following section 5.1 provides an overview of the general processes relevant to glass dissolution in aqueous environments followed by a more detailed coverage of the available information and data on glass dissolution rates under highly alkaline and cementitious conditions in section 5.2.

5.1. Mechanisms of nuclear waste glass dissolution

The alteration and dissolution of nuclear waste glass in contact with water is controlled by several inter-related processes at the glass surface. Independent of the glass composition and the alteration conditions, the most important processes comprise (e.g. [Gin 2013a]):

- Water diffusion,
- Ion exchange between hydrogenated species and alkalis (interdiffusion),
- Hydrolysis of covalent and iono-covalent bonds in the glass matrix,
- Formation and evolution of a surface alteration layer (gel layer),
- Silica saturation of the solution,
- Precipitation of secondary phases,
- Retention of radionuclides in the gel layer and secondary phases
- Removal of silicon from the solution by sorption, chemical reaction or transport.

The contribution of these processes to the (apparent) glass dissolution rate (measured by the release of mobile species into solution) depend on glass composition and on the physical and chemical conditions at and near the glass surface. At neutral pH, these processes cause fast initial glass dissolution, followed by the formation of an alteration layer and a significant decrease of the dissolution rate. As a consequence of these processes and depending on solubility, the glass matrix components and the radionuclides can either remain at the glass surface and form an amorphous, hydrated layer (gel layer), precipitate as crystalline secondary phases, or are released into the bulk solution.

Based on extensive studies on the dissolution of nuclear waste glasses and in particular simulated HLW borosilicate glasses, a general picture on the typical dissolution behaviour of HLW borosilicate glasses under conditions representative for geological disposal environments has been established (Figure 5-1, cf. [van Iseghem 2006], [Gin 2013a], [Gin 2014]).

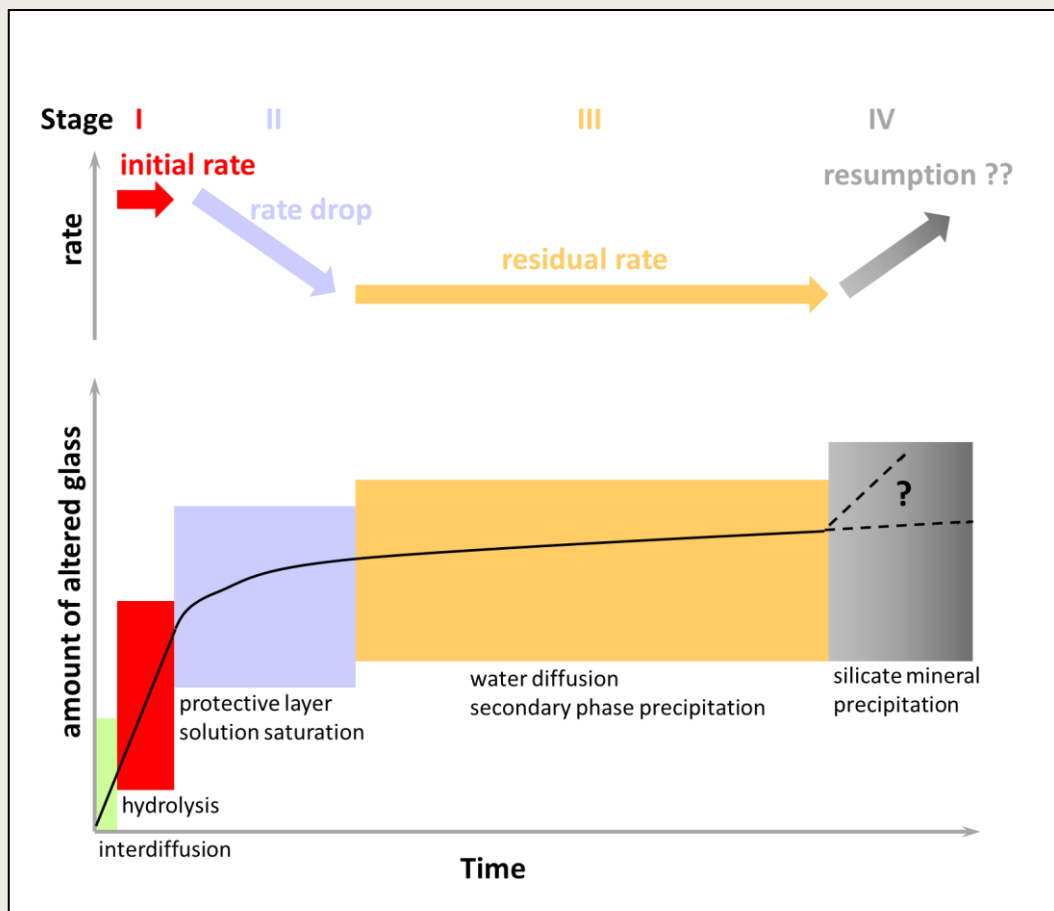


Figure 5-1 Stages of nuclear glass dissolution and related potential rate-limiting mechanisms (after [van Iseghem 2006], [Gin 2013], [Gin 2014])

The (fast) initial rate corresponds to interdiffusion and hydrolysis of the silicate network bonds. Interdiffusion (ion exchange) leads to a leaching of alkali ions from the glass network via ion exchange with H^+ ions in the aqueous solution, resulting in an increase in solution pH. Competitive to the hydrolysis of the silicate network, the interdiffusion results in the dissolution of the glass network [van Iseghem 2007]. Due to the formation of surface layers, the release of glass components at neutral to slightly alkaline conditions appears to be incongruent, i.e. boron, which is not retained in the surface layer, is released at higher rates compared to other glass components (e.g. silicon). During later stages the dissolution rate drops under closed-system conditions. This rate drop may be either related to the formation of a reaction layer or be due to affinity effects related to the increasing activity of silica in solution and the progressive silica saturation of the solution. After this rate drop, a (low) long-term residual dissolution rate persists. The formation of secondary phases or the interaction of dissolved silica with near field materials in a geological repository (e.g. steel corrosion products, bentonite clays) may act as a sink for silica. This effect may lead to the resumption of alteration and an increase in the glass dissolution rate during the later stages.

According to [Gin 2013a], there is general agreement that the (fast) initial dissolution rate is controlled by the hydrolysis of Si-O-metal bonds, whereas the debate concerning the mechanisms limiting the residual rate remains open. The mechanisms deemed relevant in this context comprise [Gin 2013a] (i) a slow transformation of amorphous phases into more stable crystalline phases (e.g. [Curti 2006], [Gin 2011]), changes in local solution composition (e.g. [Ojovan 2006]), water diffusion into the glass (e.g. [Ferrand 2006]), or

transport limitations in a passivating layer (e.g. [Gin 2011]). However, at present there is no consensus on the relative importance of the individual processes or their interrelation (cf. [Gin 2013a], [Gin 2014]). The potential for the resumption of a relatively rapid glass dissolution rate (potentially approaching the fast initial dissolution rate) is suggested to depend on a combination of glass composition and physico-chemical conditions and seems to be favoured especially by high temperatures and/or highly alkaline conditions ([Ribet 2004a], [Gin 2013a]).

The above described processes contributing to the dissolution of glasses in aqueous environments are all influenced by the high pH and the conditions typical in cementitious systems:

- Glass dissolution tends to become congruent at high pH (cf. [Utton 2011], [Cassingham 2015]).
- The hydrolysis of Si-O-metal bonds is accelerated at high pH ([Ferrand 2008], [Utton 2011]);
- The changing silica speciation (i.e. dissociation of H_4SiO_4) at high pH increases glass solubility (e.g. [Paul 1990], [Utton 2011]);
- The gel layer seems to be thinner and less protective at high pH (cf. [Gin 2001], [Ferrand 2013]);
- The precipitation of secondary phases on the glass surface at high pH (e.g. CSH phases, zeolites) can accelerate glass dissolution (e.g. [Ferrand 2008], [Utton 2013], [Fournier 2014]).
- The silica saturation of the solution can be lowered due to reaction with cement phases (e.g. reaction with portlandite to form CSH) increasing the glass dissolution rate.

Due to these effects, glass dissolution may progress at a rate close to the maximum initial rate (stage I in Figure 5-1) in cementitious environments [Seetharam 2015]. At pH above ~11.5 the glass dissolution rate can remain relatively high and there is a risk for a resumption of dissolution (stage IV in Figure 5-1), even after a (temporary) rate decrease [Gin 2001]. According to [Gin 2013], the environmental conditions in cementitious systems could maintain the glass dissolution in stage I or IV, due to the precipitation of CSH and zeolite phases, as long as the pore water composition contacting the glass is dominated by the cementitious material.

The model of glass dissolution described above and generally accepted in the (nuclear waste) glass community is based on diffusion-coupled hydration and selective cation release, producing an altered zone at the glass surface, whose formation is controlled by solid-state interdiffusion involving the inward diffusion of hydrogen species (H_3O^+ , H_2O) coupled to the outward diffusion of mobile cations. However, based on recent investigations on the structural and chemical interface between the pristine glass and the altered zone, and the observed sharp gradients in the nanometre to sub-nanometre range, a new dissolution mechanism, namely interfacial dissolution-reprecipitation, applicable to both, silicate glass dissolution and mineral weathering, has been proposed (cf. [Geisler 2010], [Hellmann 2012], [Hellmann 2015], [Putnis 2015]).

However, irrespective of the mechanism that leads to the formation of the altered layer, either interdiffusion or interfacial precipitation, glass dissolution rates that are measured in the laboratory (or observed in nature) will be invariable [Hellmann 2016]. I.e. the glass will dissolve at a given rate depending on its composition, the composition of the fluid (e.g. pH, chemistry, ionic strength), and the alteration conditions (e.g. temperature, flow rate, etc.) independent of the correct interpretation of the mechanism [Hellmann 2016]. Nevertheless, knowledge of the mechanism will support the understanding of the reaction progress, and can aid in the development of predictive tools to model or to better understand the long-term glass dissolution.

5.2. Dissolution of nuclear waste glasses under alkaline conditions

The measured dissolution rates of nuclear waste glasses depend on a number of variables, including glass composition, temperature, pH and solution composition, as well as on the experimental methods employed for their determination (e.g. [Ebert 1994], [Strachan 2001]). The dissolution rates of nuclear waste glasses have in many cases been determined in neutral to slightly alkaline conditions. However, various researchers systematically evaluated the pH dependency of glass dissolution rates in the alkaline region (e.g. [Knauss 1990], [Advocat 1991], [Abraitis 1998], [Abraitis 2000a], [Gin 2001], [Pierce 2008]). More recently, a number of studies addressed the dissolution behaviour of different waste glasses under conditions relevant to disposal in a cementitious repository near field (e.g. [Corkhill 2013], [Depierre 2013], [Utton 2013], [Cassingham 2015]). Especially in the context of research related to the Belgian supercontainer concept, glass dissolution studies with leachants representative for various stages of concrete degradation in the presence and absence of cementitious materials were performed, using in particular the standardised borosilicate glass SON68, an inactive reference glass simulating the AREVA R7T7 borosilicate waste glass (cf. [Ferrand 2008], [Ferrand 2012], [Lemmens 2012b], [Ferrand 2013a,b], [Ferrand 2014]). Data on glass dissolution rates in alkaline environments are compiled in Table A-5 in Appendix 3 and discussed in the following sections.

5.2.1. Effects of pH and solution composition

The kinetics of glass dissolution are typically described using the Transition State Theory (TST) (cf. [Lasaga 1981], [Aagaard 1982], [Grambow 1985]), which, in a simplified form, can be written as:

$$r_i = k v_i e^{-E_a/RT} a_{H^+}^{-\eta} \left[1 - \left(\frac{Q}{K} \right)^\sigma \right] \prod_j a_j^{\eta_j} = k v_i e^{-E_a/RT} 10^{\eta \text{pH}} \left[1 - \left(\frac{Q}{K} \right)^\sigma \right] \prod_j a_j^{\eta_j}$$

In this equation r_i is the release rate of glass component i , k an intrinsic (forward) rate constant, v_i the stoichiometric coefficient for the component i in the glass matrix, E_a the activation energy, R the gas constant and T the absolute temperature, a_{H^+} the hydronium ion activity and $-\eta$ the reaction order with respect to a_{H^+} , Q the activity product of the rate-limiting reaction, K the equilibrium constant for the reaction, σ the Temkin coefficient, and a_j is the activity of the j^{th} aqueous species that acts as an inhibitor or catalyst. However, a glass phase will never be in equilibrium with the aqueous phase because glasses are thermodynamically unstable with respect to an assemblage of crystalline phases with a similar bulk composition [van Iseghem 2007].

Values for the power law coefficient η that describes the dependency of the reaction rate on the activity of H^+ or pH, respectively, have been determined by various authors (cf. Table 5-1, for details see Table A-6 in Appendix 3). Data for η compiled for the alkaline region indicate that the glass dissolution rates typically increase as $10^{-0.4\text{pH}}$. Thus in general, borosilicate glasses become more susceptible to dissolution under high pH conditions when the silica network becomes subject to direct chemical attack (cf. [Utton 2011]). Similar values for η (~ -0.4) were obtained for natural basaltic glasses and pure silica glasses [Brady 1996]. Taking into account the range of glass compositions addressed in the various studies, the values of η are rather consistent, suggesting that the pH dependency of the dissolution rate in basic conditions does not depend strongly on glass composition (cf. [Frizon 2009], [Utton 2011]). According to the observations of [McGrail 1997] and [Pierce 2008], the power law coefficient η does not depend on temperature within experimental error.

The activation energy E_a for the dissolution of glasses in alkaline solutions have been calculated for a variety of glasses and dissolution conditions. [Ferrand 2008] determined a mean activation energy of 86 kJ mol^{-1} for the dissolution of SON68 borosilicate glass in KOH

solutions (pH 9 to 11.5). More recently, an E_a value of 76 kJ mol^{-1} was applied to the modelling of SON68 glass dissolution in cementitious environments ([Ferrand 2013], [Ferrand 2014]), based on data from [Frugier 2008]. According to [Jollivet 2012], the activation energy determined for the dissolution of SON68 glass in neutral to slightly alkaline conditions ($\sim 77 \text{ kJ}\cdot\text{mol}^{-1}$) is very near to that for the dissolution of quartz (72 kJ mol^{-1} [Dove 1999]) and amorphous silica (83 kJ mol^{-1} [Icenhower 2000]), suggesting that the dissolution of the SON68 glass network and of other simple borosilicate glasses is controlled by the hydrolysis of Si-O bonds (cf. [Pierce 2008]). [Abraitis 2000a] calculated E_a for the dissolution of a British Magnox waste glass in alkaline solutions (pH 12) to be between 56 and 64 kJ mol^{-1} . The E_a values for the dissolution of Magnox-Oxide waste blend glasses at pH 12 were found to range between 83.1 and 96.4 kJ mol^{-1} (MT25 blend) and between 70.8 and 86.2 kJ mol^{-1} (MT30 blend), respectively, depending on the element selected for the determination of the dissolution rates [Cassingham 2015]. [McGrail 1997] obtained an activation energy value E_a of 74.8 kJ mol^{-1} for the dissolution of a sodium-calcium-aluminoborosilicate glass studied for the immobilisation of low-activity waste under alkaline conditions, using the normalised silicon release. [Pierce 2008] calculated the activation energy of simulant aluminoborosilicate waste glasses to be between 52 and 56 kJ mol^{-1} in the pH range from 7 to 12, based on boron release. Similar activation energies were also determined for the dissolution of various natural glasses in alkaline conditions (pH 10.6) (cf. [Wolff-Boenisch 2004]). The activation energy values determined in the various studies are in the range proposed by [Lasaga 1981] to be consistent with a surface-controlled dissolution mechanism (typically between 42 and 84 kJ mol^{-1}).

Table 5-1 Power law coefficients η for pH dependence of nuclear waste glass dissolution rates in the alkaline region

Glass type	pH range	η	Source
R7T7	7 ... 10	0.41	[Advocat 1991a]
R7T7	7 ... 11.5	0.39	[Advocat 1991b]
SON68	7 ... 11.5	0.39	[Gin 2001]
SON68	6 ... 10	0.40	[Frugier 2008]
SON68	9 ... 14	0.32	[Ferrand 2013]
Magnox MW	9 ... 12	0.40	[Abraitis 1998]
Magnox MW	7 ... 10	0.43	[Abraitis 2000a]
Magnox-Oxide blend	8 ... 12	0.35 ... 0.58	[Cassingham 2015]
Aluminoborosilicate	7 ... 13	0.40 ... 0.51	[Knauss 1990]
Aluminoborosilicate	6 ... 12	0.40	[McGrail 1997]
Aluminoborosilicate	5 ... 11	0.35	[McGrail 2001]
Aluminoborosilicate	7 ... 12	0.34 ... 0.40	[Pierce 2008]
ILW-glass	7 ... 11.7	0.38	[Mercado-Depierre 2013]

In studies addressing glass dissolution in alkaline conditions, often test solutions containing potassium, sodium or lithium hydroxides and salts, or buffered solutions were used (e.g. [Advocat 1991a], [Abraitis 2000a], [Ferrand 2008], [Cassingham 2015]). These (cat)ions generally do not affect the glass dissolution process significantly, for example, by enhancing the preferential precipitation of secondary phases [Utton 2011]. In contrast, (evolved) porewaters in cementitious systems contain calcium, due to dissolution of portlandite and CSH-gels, which can react with the silicon released during glass dissolution. The extent of reactions, which can sustain glass alteration at its initial dissolution rate, is related to the capacity of the surrounding medium and near field materials (e.g. cements, clays, metallic corrosion products) to consume the silicon released during glass dissolution and maintaining a low silicon concentration in solution, i.e. below saturation (cf. [Gin 2001], [Vernaz 2001], [Utton 2011], [Gin 2013a]).

In Figure 5-2 the measured dissolution rates of French R7T7/SON68 and UK Magnox type glasses in the alkaline regime are depicted as function of pH and solution type, based mainly on the data on the release of mobile elements compiled in Appendix 3 (Table A-5). As expected, the rates show a large spread due to the compositional differences of the glasses, and the different experimental conditions and methodologies adopted in the various studies, generally indicating the increase of the glass dissolution rates with increasing pH. Dissolution rates of SON68 borosilicate glasses for specific selected solution conditions, which were obtained in the context of research related to the Belgian supercontainer concept (e.g. [Ferrand 2008], [Ferrand 2013a,b], [Ferrand 2014]), are provided in Figure 5-3.

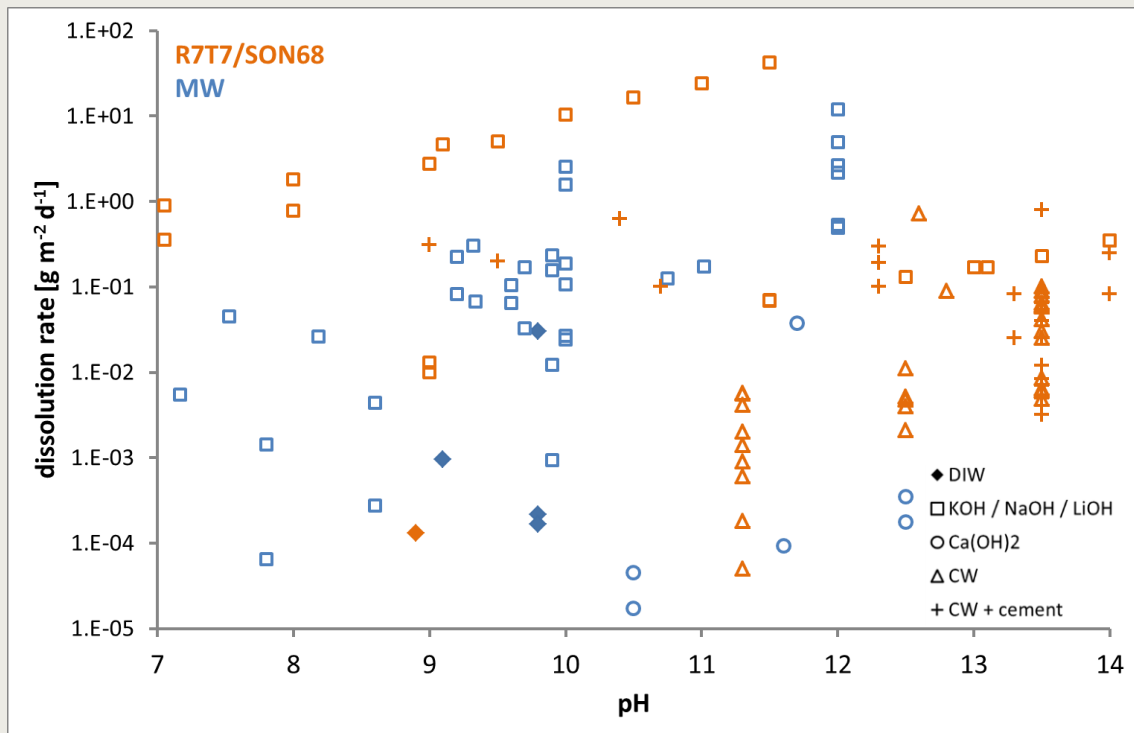


Figure 5-2 Dissolution rates of nuclear waste glasses under alkaline and cementitious conditions (CW: cement water)

Regarding the availability of data for the different nuclear waste glasses relevant within OPERA, no studies were found addressing the dissolution rates of UK Magnox type waste glasses in (simulated) cement wasters (other than $\text{Ca}(\text{OH})_2$ -solutions) and in the presence of cementitious materials. Investigations addressing the glass durability in the presence of cementitious materials seem to be limited to experiments on SON68 glass dissolution rates in stage I of concrete degradation (i.e. alkali-rich young cement water at pH 13.5), obtained within research for the Belgian supercontainer concept to date. More details on the effects of glass composition on glass durability are provided in the following section 5.2.2.

The evaluation of the available data and studies on glass alteration in highly alkaline and cementitious conditions can be generally summarised as follows:

- The dissolution rates depend on glass type, temperature, pH, solution composition, and the presence/absence of cementitious materials;
- Generally, the glass durability decreases with increasing pH in alkaline conditions;
- The highest dissolution rates are observed in KOH (NaOH, LiOH) solutions (e.g. [Lemmens 2012b], [Ferrand 2013a]);

- The presence of calcium in the solution has an antagonistic effect on the glass alteration rate due to the inclusion of calcium into the altered glass layer and/or CSH precipitation on the glass surface (cf. [Utton 2013], [Corkhill 2013], [Depierre 2013], [Mercado-Depierre 2013]);
- The presence of cementitious materials decreases the silicon concentration in solution due to CSH-formation by reaction with portlandite, resulting in higher dissolution rates, as long as portlandite is available (e.g. [Ferrand 2013a,b], [Ferrand 2014]).

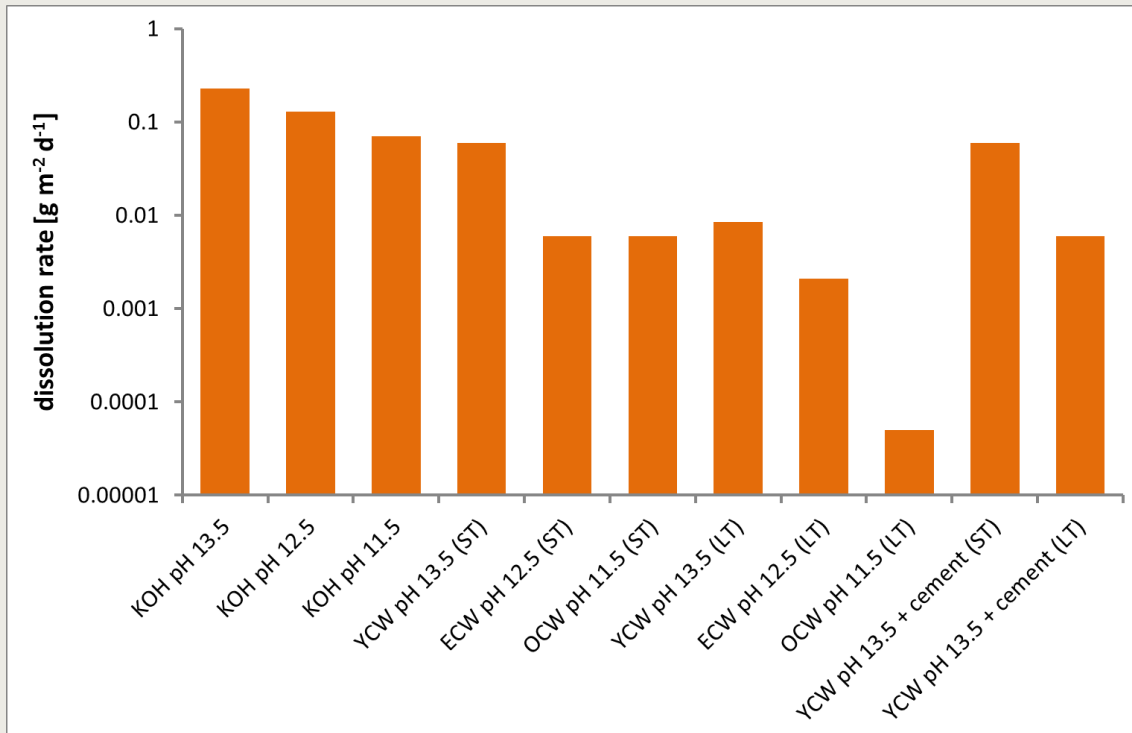


Figure 5-3 Dissolution rates for SON68 glasses determined in the context of the Belgian supercontainer disposal concept (data from [Ferrand 2013a] YCW: young cement water, ECW: evolved cement water, OCW: old cement water; ST: short-term, LT: long-term)

[Ferrand 2013a] proposed the following model for the alteration of nuclear waste glasses in supercontainer conditions as a working hypothesis, with different alteration mechanisms prevailing in the three main environmental stages expected in a (degrading) supercontainer buffer:

Stage I: Young Cement Water (YCW) with high potassium and sodium concentrations at pH 13.5 and portlandite available in the cement. In a first stage, silicon released during glass dissolution is consumed by portlandite to form CSH, aluminium reacts with CSH to form CASH phases. The resulting low silicon and aluminium concentrations in solution trigger the glass to dissolve congruently at a high constant rate, slightly suppressed by the integration of calcium into the surface layer [Ferrand 2013a]. After consumption of portlandite and CSH close to the glass surface, the silicon and aluminium concentrations will increase, with the further glass dissolution triggered by secondary phase formation at a lower rate, as measured in static tests without cement [Ferrand 2013a].

Stage II: Evolved Cement Water (ECW) with low potassium and sodium concentrations at pH 12.5 and portlandite present. In this stage, [Ferrand 2013a] assumes that the glass dissolution is also triggered by reactions with portlandite, although the dissolution rate may be lower than the initial rate in stage I at pH 13.5, due to the lower pH. However,

experimental evidence to corroborate this hypothesis is lacking to date [Ferrand 2013a]. According to [Ferrand 2013a] both in stage I and II, the glass dissolution is driven by the formation of secondary phases, with the glass surface continuously undersaturated with respect to the solution composition.

Stage III: Old Cement Water (OCW) with pH ~11.7 controlled by the solubility of CSH phases. After consumption of available portlandite, the glass is assumed to be much more stable than in stages I and II with much lower glass dissolution rates prevailing, due to the formation of a protecting reaction layer in equilibrium with the silicon and aluminium leached from the glass [Ferrand 2013a]. Nevertheless, a continued reaction of the glass with CSH (e.g. forming CASH) that could trigger further glass dissolution and prevent the formation of a protective layer could not be ruled out [Ferrand 2013a]. Experimental data to support these hypotheses are however lacking to date.

Thus the glass dissolution rates in the repository environment will depend on the stage of supercontainer concrete degradation and the availability of portlandite at the time of waste canister failure. The evolution of the near-field chemistry/mineralogy resulting from the exchange of cementitious materials with Boom Clay pore water directly impacts glass dissolution rates, formation of glass alteration layers and secondary phases, and thus the lifetime of the glass waste forms as well as the radionuclide release with time (source term).

5.2.2. Effects of glass composition

The overall durability of the glass matrix is affected by the composition of the glass in all stages of glass dissolution, i.e. in the region of the initial dissolution rate and rate drop, as well as in the residual rate regime and resumption regimes. Some glass components can promote durability, whereas others, such as mobile alkalis are known to reduce the durability in aqueous environments (cf. [Harrison 2014]). Moreover, some species can provide for an increased glass durability specifically under acidic or alkaline conditions, respectively (cf. [Utton 2011]). The addition of zirconia (ZrO_2) is generally thought to improve the durability of glasses in alkaline conditions, at least by reducing the initial dissolution rate, although some studies suggest that this may not be true for the residual dissolution rate [Cailleteau 2008]. The oxides of transition metals such as iron, manganese, and chromium, as well as tin or lanthanum are also thought to improve the resistance of glasses to alkaline attack (cf. [Utton 2011], [Gin 2013b]). However, [Gin 2014] pointed out that the glass dissolution rate in each kinetic regime has a specific composition dependency, i.e. the effect of the glass composition on the aqueous durability cannot be anticipated for different kinetic regimes. According to [Gin 2013b], higher ZnO concentrations significantly decrease the initial dissolution rate of borosilicate glasses, but can also increase the residual dissolution rates. Moreover, the effects of glass composition on the durability are generally thought to be nonlinear and strong synergetic effects have been observed. In as such the effects of glass composition on glass durability and dissolution behaviour are still not fully understood at present ([Gin 2014], [Harrison 2014]).

[Pierce 2008] studied the dissolution behaviour of different glasses of varying composition at high pH in flow through experiments. The remarkably similar durability of the glasses and the similarity in the initial glass dissolution rates was thought to be due to the behaviour of glass at high pH, where (above pH 9) the rate limiting step for dissolution is the rupture of Si-O bonds. The chemical durability of the glasses in the alkaline regime is thus strongly related to the polymerisation of the silicate network, i.e. number and type of Si-O bonds. Therefore, the dissolution rate under alkaline conditions may be less dependent on the overall glass composition, but rather be coupled to the degree of Si-O polymerisation and the rupture of Si-O bonds [Utton 2011].

The differences in the composition of the HLW borosilicate glasses to be disposed of in the Netherlands, i.e. the French R7T7 and the UK Magnox type (blend) glasses, can impede the direct comparison of dissolution rates presented in the literature (cf. [Harrison 2009]). The French R7T7 glass contains about 4.0 wt.% CaO, 2.5 wt.% ZnO and practically no MgO, whereas the UK Magnox type glasses contain negligible CaO and ZnO but up to 5.5 wt.% MgO, depending on the blend rate with oxide wastes (cf. Table 2-2). Additional differences comprise the higher proportions of ZrO₂ and Na₂O in R7T7 glasses, and the higher B₂O₃ and Li₂O content in UK Magnox glasses.

With respect to the different waste glasses relevant within OPERA, comparative dissolution studies under identical experimental conditions are rare. In a study comparing the durability of the French R7T7-type glass SON68 and a simulated UK Magnox glass over 12 years at 90 °C in de-ionised water, the dissolution rate of Magnox glass ($9.6 \cdot 10^{-4} \text{ g m}^{-2} \text{ d}^{-1}$), based on the release of boron and lithium at >500 days, was found to be about 10 times greater than that of SON68 ($1.3 \cdot 10^{-4} \text{ g m}^{-2} \text{ d}^{-1}$) [Curti 2006]. The lower durability of the UK HLW glass was attributed in particular to the large amount of magnesium in the UK Magnox glass, promoting the formation of secondary magnesium-aluminium clay minerals (cf. [Curti 2006], [Harrison 2010]). The results show that, whilst the general dissolution behaviour of both glasses in aqueous environments is similar, the compositional differences result in significantly different long-term dissolution rates. [Curti 2006] concluded that R7T7 glass has more favourable alteration properties than magnesium-bearing MW glasses regarding corrosion rates and radionuclide retention.

Regarding the compositional variations in UK vitrified HLW (i.e. ‘Magnox’ glass from feeds containing >90 % Magnox HAW, and ‘Blend’ glass from feeds containing typically a mix of 75 % Oxide and 25 % Magnox HAW), [Harrison 2014] noted significantly different responses in standard durability tests regarding the short- and long-term glass dissolution rates in de-ionised water. In MCC-1 tests (90 °C, monolithic sample, SA/V 10 m²; for details of methods see e.g. [Strachan 2001]) performed for up to 42 days, the Magnox glass appeared to have significantly lower boron and sodium releases (i.e. about a factor 5) than the Blend glass. In contrast, in product consistency tests (PCT, 90 °C, powdered sample, SA/V ~2,000 m²), both Magnox and blend glasses with waste loadings of ~25 wt.% revealed similar elemental releases (e.g. with respect to boron, lithium, or sodium) for up to 112 days. However, at higher waste loading (~38 wt.%) the Magnox glass showed an initially lower dissolution rate than the blend glass for up to 42 days [Brookes 2010], but higher residual rates in the longer-term [Harrison 2014]. In summary [Harrison 2014] concluded that for UK HLW glass, the aqueous durability generally improves with increasing waste incorporation. Cassingham [2015] investigated the dissolution behaviour of simulant Magnox-Oxide (ThORP) blend glasses with waste loadings of 25 wt.% and 30 wt.% in single-path flow-through experiments in the an alkaline pH range of pH 8.0 to 12.0 and a temperature range from 23 to 70 °C. It was found that the dissolution rate (based on the release of silicon, boron, and sodium) and the dissolution mechanism under these conditions were not sensitive to the variation in glass composition resulting from the different HLW incorporation rates [Cassingham 2015]. Based on the similarity of the measured boron release rates to those obtained by [Abraitis 2000b] in single-path flow-through tests of Magnox glass under alkaline conditions, it was suggested by [Cassingham 2015] that the dependence of the dissolution rates on glass composition is weak in the case of Magnox and Magnox-ThORP blend glasses under alkaline conditions.

5.2.3. Effects of radiation

Although borosilicate glasses are known to be self-healing materials with respect to α -, β - and γ -radiation [Gin 2014], radioactive decay of the incorporated radionuclides can potentially reduce the durability of nuclear waste glasses due to different mechanisms, such as (i) radiation induced structural changes, (ii) microfracturing that increases the

surface area accessible for dissolution, and (iii) by radiolysis of the aqueous medium associated with changes in the local pH and chemistry. Generally, radiation effects on the structure and durability of nuclear waste glasses depend on the type of radiation. Initially the internal radiation source will be dominated by β - and γ -decay of short-lived fission products (e.g. ^{137}Cs , ^{90}Sr), whereas in the longer term the major radiation effect will be from the α -decay of plutonium and minor actinides (i.e. neptunium, americium, and curium). Each α -decay involves the ejection of an α -particle (He^{2+}) and the recoil of the daughter nucleus, producing displacement damage in the atomic structure of the waste form that leads to significant numbers of atomic displacements in the waste glasses [Ewing 1995]. Self-irradiation from β - and γ -decaying radionuclides may cause excitation and ionisation processes in the glasses, leading to the formation of point defects, electron-hole pairs, ion radicals, and holes, and may disrupt Si-O or B-O bonds in borosilicate glasses [Stefanovsky 2004]. Self-irradiation damage from α -decay in glasses containing short-lived actinides, in particular ^{238}Pu and ^{244}Cm , has been investigated for several decades. Therefore radiation effects resulting from α -decay in nuclear waste glasses are relatively well known (e.g. [Weber 1997], [Deschanel 2007], [Weber 2009]).

In general, the effects of α -decay in glass waste forms are thought to be limited at the ambient temperatures that are expected over the relevant decay times for actinides (e.g. [Weber 1997], [Weber 2009]). However, the structure and many physical and mechanical properties of the glass evolve slightly, mainly due to ballistic effects associated with α -decay [Gin 2014]. Doses of less than $10^{17} \alpha \text{ g}^{-1}$ result in an increase in stored energy associated with the formation of defect centres in the structure of the glass. Higher doses lead to more global modifications of the network structure and result in volume expansions or contractions, and changes in density and hardness. These effects seem to saturate at certain doses (about 2 to $4 \cdot 10^{18} \alpha \text{ g}^{-1}$ for R7T7 glasses, e.g. [Peuget 2006], [Fillet 2008], [Gin 2014], [Peuget 2014]). Volume changes resulting from α -decay damage in nuclear waste glasses are generally limited to about 1 % (cf. [Wronkiewicz 1993], [Ewing 1995], [Peuget 2006], [Deschanel 2007], [Donald 2010]). At extreme doses (i.e. $> 8 \cdot 10^{18} \alpha \text{ g}^{-1}$) the formation of helium bubbles in simulated nuclear waste glasses doped with ^{238}Pu and ^{244}Cm was observed ([Inagaki 1992], [Weber 1997], [Weber 2014]), which might result in a loss of mechanical integrity at extreme long times [Weber 2009]. However, due to the relatively small effects of the internal irradiation regarding changes in stored energy, glass structure, and volume, it is generally thought that the chemical durability of the glass waste forms is not significantly impaired due to α -decay from incorporated actinides (cf. [Weber 1997], [Donald 1997], [Weber 2009]). In the absence of appropriate experimental evidence, [Ewing 1995] estimated a conservative factor of 10 to allow for the enhancement of the glass dissolution rate due to radiation induced changes in the glass structure. Data obtained from short-term testing of actinide doped nuclear waste glasses indicated that dissolution rates may increase by a factor of 3 to 4 due to radiation effects from α -decay (cf. [Wronkiewicz 1994], [Stefanovsky 2004]).

A number of studies were carried out on the dissolution behaviour of radioactive or irradiated glasses, showing little or no effect of internal or external radiation on the initial dissolution rates, though studies of radiation effects on the residual glass dissolution rates are still rare (cf. [Fillet 2008], [Gin 2014]). [Peuget 2006] found no changes in the initial alteration rate of R7T7 type glasses doped with varying levels of $^{244}\text{CmO}_2$ in pure water. [Peuget 2007] studied the effect of α -radiation on the chemical reactivity of R7T7 glass in pure water, using various glass samples doped with ^{237}Np , ^{238}Pu , ^{239}Pu , ^{241}Am , or ^{244}Cm , covering a range of alpha activity from 10^5 to $10^{11} \text{ Bq g}^{-1}$. The results showed no significant impact of α -activity or α -decay dose, respectively, on the initial glass alteration rates [Peuget 2007]. According to [Deschanel 2007], the initial dissolution rate of a borosilicate glass demonstrating a potential for conditioning of plutonium was not increased by a

cumulative α -decay up to doses of $2 \cdot 10^{18} \alpha \text{ g}^{-1}$ (evoked by incorporation of 1.5 wt.% CmO_2 in the glass matrix) within the measurement uncertainty. [Advocat 2001] performed dissolution tests with radioactive ($\alpha\beta\gamma$) French waste glasses, including industrially produced nuclear waste glasses from the R7 and T7 vitrification units at La Hague and α -doped SON68 glass, in initially pure water. It was found that the $\alpha\beta\gamma$ -radiation field did neither affect the initial dissolution rates nor the low long-term (residual) alteration rates, although the time required to reach the low final rate was longer for the highly radioactive glass samples than for inactive glass. Similarly, in a recent dissolution study (static conditions, 90 °C, pure water) on R7T7-type glass specimens doped with 0.85 wt.% $^{239}\text{PuO}_2$ and 0.24 wt.% $^{99}\text{TcO}_2$ to simulate α/β -dose rates corresponding to long-term disposal conditions, [Rolland 2013] could show that there was not significant effect of the dose rates (150 Gy h^{-1} for ^{239}Pu -doped glass and 0.06 Gy h^{-1} for ^{99}Tc -doped glass) and local irradiation fields in water on the residual glass dissolution rates.

Only very few studies could be found that consider both irradiation and the chemical durability of glasses under alkaline conditions. [Abdelouas 2004] performed dissolution tests on SON68 glass under external α - or γ -irradiation in synthetic solutions rich in silicon, boron, and sodium with an initial pH of 9.8 to mimic saturation conditions. Under α -irradiation ($\sim 1,800 \text{ Gy}$) or lower dose γ -irradiation ($\sim 2,000$ to $4,000 \text{ Gy}$), no changes in the dissolution behaviour were observed. Higher γ -doses ($\sim 58,000 \text{ Gy}$) led to a (temporary) decrease in pH thus favouring ion-exchange between water and soluble glass constituents, resulting in a slight increase in the release of alkalis [Abdelouas 2004]. [Wellman 2005] studied the effects of self-irradiation on the dissolution kinetics of plutonium-containing borosilicate glasses between pH 9 and 12 at 80 to 88 °C, using single pass through flow experiments. The proportions of ^{238}Pu to ^{239}Pu in the glasses (MCC defense reference glass) were varied, yielding accumulated doses ranging from $1.3 \cdot 10^{16}$ to $2.6 \cdot 10^{18} \alpha \text{ g}^{-1}$ at the time of testing. It was found that the effect of self-irradiation on the glass dissolution rate was insignificant compared to the effect of the high pH on dissolution, despite the exposure to internal radiation for more than 20 years [Wellman 2005]. No other studies were found during the literature survey that address the effect of irradiation on glass durability under high pH conditions. Moreover, in many of the aforementioned studies on irradiation effects on nuclear waste glasses, the French waste glasses (R7T7 or SON68) were investigated, whereas recent investigations on the impact of internal radiation on the aqueous durability of British Magnox type waste glasses seem to be lacking. [Boult 1991] investigated the radiation effects in MW glasses doped with 2.5 wt.% ^{238}Pu . Besides a slight loss of density ($\sim 0.5 \%$) incurred at an α -dose of $2 \cdot 10^{18} \alpha \text{ g}^{-1}$ it was noted that the Soxhlet leach rates of the MW glass were largely unaffected by the α -decay.

5.3. Reactive surface area of corroding waste glasses

The performance of nuclear waste glasses disposed in a geological repository is generally assessed by assuming that the radionuclides are homogeneously distributed in the glass and that the release of radionuclides is limited by the alteration of the (homogeneous) glass matrix (e.g. [Mallants 2001], [Frizon 2009], [Poinsot 2012]). The source term, i.e. the radionuclide flux over time, can then be estimated from the quantity of altered glass (QAG) that is given by

$$QAG = \iint_{t,S} r(t,S) \cdot dS \cdot dt$$

where r is the glass dissolution rate, S the reactive surface area, and t the time (cf. [Frizon 2009], [Verney-Carron 2010], [Poinsot 2012]).

Glass alteration in aqueous environments can be treated as a surface reaction at the macroscopic scale. However, it has to be taken into account that nuclear waste glass blocks are fractured by mechanical stresses due to rapid cooling after pouring (cf. [Verney-Carron 2010], [Ojovan 2011], [Poinsot 2012]). Thus the reactive surface area of the waste glass available for leaching and dissolution in the repository can be significantly greater than the geometric surface area of the original moulded glass block (cf. [Frizon 2009], [Poinsot 2012], [Gin 2013a], [Vienna 2013]). The cracking occurs during the cooling phase due to mechanical stresses incurred from the temperature gradient between the hot core and the cool outer surface of the waste package [Ribet 2009]. The temperature gradient itself is a result of a combination of the thermal cooling scenario of the melt, the thermal power resulting from the decay of short-lived radionuclides in the waste matrix, and the low thermal conductivity of the waste glass [Ribet 2009]. The resulting crack network depends on a variety of parameters such as the geometry of the waste canister, the vitrification process parameters, the cooling scenario, and the density of defects like bubbles, metal fines, and crystals within the nuclear waste glass [Vienna 2013].

Thus in estimating the dissolution rate of nuclear waste glasses in the repository environment from surface normalised dissolution rates (cf. section 5.2) the degree of cracking of the glass as well as the accessibility of the crack surfaces to the aqueous phase have to be considered. Various empirical and experimental methods such as X-ray tomography, leaching tests under initial rate and residual rate regimes, or particle size analysis after removal of (inactive) glass blocks from a waste canister have been employed to estimate the reactive surface area of nuclear waste glasses (cf. [Ferrand 2011], [Poinsot 2012], [Gin 2013a]). Moreover, these estimates have recently been supported by thermomechanical simulations taking into account the viscoelasticity of the glass, mechanical parameters, and threshold and critical stresses (e.g. [Barth 2014]). As an outcome of these studies, "cracking factors" or "fracture ratios" that relate the actual reactive surface of a glass block to its nominal geometrical surface area have been defined.

A number of studies have been performed with respect to the accessible surface area relevant to French R7T7-type glass packages in the long-term, using inactive SON68 glasses (e.g. [Sené 1999], [Minet 2003]). Generally consistent results were obtained, giving a total surface area equivalent to about 40 times the geometric surface area of 1.7 m^2 , i.e. about 70 m^2 (cf. [Ribet 2004b], [Ribet 2009], [Verney-Carron 2010], [Poinsot 2012]). The characterisation of the crack network in a fractured Roman glass block altered for about 1800 years in seawater suggested a cracking factor of 86, i.e. about a factor 2 higher than the cracking factor determined for SON68 glass ([Verney-Carron 2008], [Verney-Carron 2010]). Thus with respect to the French R7T7 waste glass, [Vienna 2013] concluded that the exposed surface area of glass canister filled with 400 kg of waste glass could be 10 to 100 times larger than the geometric surface of the glass waste form (1.7 m^2), depending on the process parameters and the cooling scenario.

[Ferrand 2011] performed a detailed assessment of the effective surface area of vitrified HLW to be expected in supercontainer disposal conditions, i.e. in a highly alkaline near-field. The selected cracking factors were based in particular on literature data for SON68 glasses obtained under neutral conditions, due to a lack of experimental data regarding evolution and behaviour of fractured glasses under high pH conditions. [Ferrand 2011] proposed effective cracking factors (i.e. the ratio of the effective surface area altered by glass-water-interaction to the external geometric surface area of the glass monolith) of 5 for initial rate conditions, and 40 for residual rate conditions as reference values for the expert range minimum and maximum (i.e. the range within which the experts expect the parameter value to lie). The source range (i.e. the range outside of which the experts do not expect the parameter value to lie) for the effective cracking factor was calculated by the expert range minus the 95% confidence interval, and the expert range maximum

multiplied by a factor of 3, respectively, resulting in a source range for the effective cracking factor between 3 and 120 [Ferrand 2011]. This approach should account for the possibilities that (i) the cracking factors of the glass waste forms to be disposed of in supercontainers could be lower than the experimentally determined average values, and (ii) the effective surface area increases after disposal [Ferrand 2011].

The effects of cracking on the accessible reactive surface area of Magnox type waste glasses was addressed in a review on the development and properties of UK vitrified HLW products by [Dunnett 2007]. From earlier experimental assessments of the increase in glass surface area by the presence of cracking using surface area measurements, leaching tests, or computerised tomography, it was noted that the surface area of cooled cracked glass blocks was about a factor 11 to 12 larger compared to a monolithic block [Dunnett 2007]. Regarding the reactive surface of the waste glasses and the life time of glass waste forms under disposal conditions, [Harrison 2010] used a cracking factor of 12 for UK Magnox waste glasses as a best estimate, and a worse case cracking factor of 27 for a mechanically stressed container.

Glass cracking factors have previously been used in performance assessment models in various countries to evaluate the performance of nuclear waste glasses in the repository environment. The performance assessment model used for the former Belgian repository design in the SAFIR 2 safety case considered a cracking factor between 5 and 27, using a best estimate value of 10 in the reference case [Mallants 2001]. NAGRA assumed a factor of 15 relative to the original geometric surface of the glass waste form, to account for the effect of cracking on the surface area available for leaching [NAGRA 2002]. The value applied in [NAGRA 2002] was slightly higher than the value of 12.5 used in previous safety assessments ([NAGRA 1994], [Curti 2003]). CEA developed an operational model for glass dissolution using different cracking factors for initial dissolution rate conditions (5 ± 1) and residual rate conditions (40 ± 17) applicable for R7T7 glasses between pH 7 and 10 and a temperature range from 25 to 100 °C (cf. [Ribet 2004b], [Ribet 2009]).

In performance assessment models generally a constant reactive surface area of the glass waste forms is assumed to date (e.g. [Gin 2013a]). Open questions with respect to the reactive surface area of degrading glass waste forms in a geological repository and its evolution over time (i.e. increase or decrease of reactive surface area) that are currently under debate comprise, inter alia, effects of (i) the slow release of residual stresses, (ii) stress corrosion, (iii) external stress loads (e.g. lithostatic pressure) in a geological repository, and (iv) the precipitation of secondary minerals in cracks (cf. [Poinssot 2012], [Gin 2013a], [Vienna 2013]).

6. Evaluation

Within a multibarrier concept for the disposal of HLW, the waste form acts as the first barrier against the release of radionuclides from the waste into the repository near-field. In as such, the performance of the waste form under repository conditions is an important issue with respect to the isolation and containment of the radioactive waste and the radionuclides therein from the biosphere. The safety assessment methodology throughout the repository development within OPERA is based on safety functions that are defined as actions or roles that the natural and engineered barriers must perform to prevent the radionuclides present in the disposed wastes posing an unacceptable hazard to humans or the environment (cf. [ONDRAF 2004], [Verhoef 2011a], [Verhoef 2011b]). The five safety functions defined in [Verhoef 2011b] for the OPERA reference concept (incl. inter alia ‘physical containment’, ‘resistance to leaching’, and ‘transport and retention’) were later on replaced by the updated safety functions published in 2009 by ONDRAF/NIRAS [Smith 2009] (cf. [Verhoef 2014a]). The safety functions in [Smith 2009] related to the waste forms and the EBS comprise – with respect to the disposal of HLW – (i) the safety function ‘engineered containment (C)’, which describes the isolation of the radionuclides from their immediate environment (i.e. the near field water) provided by the supercontainer, and (ii) the safety function ‘delay and attenuation of releases (R)’. The latter safety function that is relevant following the engineered containment phase once the physical containment by the supercontainer is impaired and the wastes come into contact with water, includes (i) the ‘limitation of contaminant releases from the waste forms (R1)’ describing the slow release of radionuclides from the waste, and (ii) the ‘retardation and spreading in time of contaminant migration (R3)’ related to the radionuclide sorption capacity and the slow diffusive transport in the EBS and the Boom Clay host rock.

The loss of integrity of the engineered containment provided by the supercontainer in the post-closure phase requires a number of subsequent steps and processes, such as

- (fast) resaturation of the repository backfill,
- corrosion/failure of the stainless steel envelope,
- re-saturation of the concrete buffer,
- corrosion/failure of the carbon steel overpack, and finally
- corrosion/failure of the CSD-V-canister,

before the vitrified HLW in the failed waste canisters can come into contact with the near field water at some point in the (far) future. The radionuclides contained in the nuclear waste glasses can be leached, when the vitrified HLW becomes accessible to the near field water.

In the following section 6.1 the glass dissolution rates of and the radionuclide release from vitrified HLW under repository conditions relevant to OPERA are discussed to assess and quantify the safety function R1: ‘limitation of contaminant releases from the waste forms’ in the context of the envisaged OPERA safety case. Section 6.2 provides an overview on processes that affect the radionuclide migration and may contribute to the retention of the leached radionuclides in the immediate near field (e.g. due to solubility constraints and/or interaction with degradation products from the engineered barrier system) addressing thus the safety function R3: ‘retardation and spreading in time of contaminant migration’.

6.1. Radionuclide source term

The performance of a nuclear waste form in the repository environment is dependent on the environmental conditions to which the material will be exposed. Near field factors affecting substantially the radionuclide source term for a waste include the hydrogeological regime and the geochemical conditions (notably pH, redox potential, temperature, gas partial pressures, groundwater/pore water composition), which themselves will evolve over time in the post-closure phase (cf. section 4.2). Due to the uncertainties with respect to the time scales of the engineered containment phase and the degradation stages of the cementitious materials at the time of canister failure, i.e. when the vitrified HLW can come into contact with water, different scenarios with respect to the composition of the near-field water resulting from the interaction of Boom Clay pore water with the cementitious materials are addressed.

As reference scenario, it is assumed here that the conditions in the supercontainer pore water at the time of canister failure are representative for the stage II of concrete degradation (i.e. portlandite stage), based on the expected lifetime of the overpack and the long duration of stage II of up to several 100,000 years (cf. [Lemmens 2012a], [Kursten 2015]). Due to the relatively low heat output of the heat-generating wastes in the OPERA concept and the rather insignificant temperature excursion in the HLW section during the first decades (cf. [Kursten 2015]), ambient conditions (i.e. about 25 °C in 500 m depth in the Netherlands) are assumed at the time of canister failure. Moreover, the oxygen available at the time of repository closure will have been consumed, for example due to corrosion of metals during the degradation of EBS, leading to anoxic or reducing conditions at that time. The relevant environmental conditions for this scenario can thus be described by an anoxic/reducing near field water at pH 12.5 controlled by portlandite dissolution (i.e. the near field water can be described as a saturated Ca(OH)_2 solution) at ambient temperature. Alternatively to the reference scenario, in case of an early canister failure scenario, it might be assumed that the conditions in the near field are representative for concrete during degradation stage I, depending at the time of the loss of physical containment of the waste. In this scenario, the pH in the near field water would be higher compared to the reference scenario (up to pH ~13.5, cf. section 4.2) and the pore water composition dominated by KOH and NaOH. Potential deleterious effects of the co-disposal of HLW and LILW in the OPERA disposal concept (e.g. ingress of oxidising species or complexing organic ligands released from the LILW) are disregarded at that point by assuming an appropriate design and layout of the disposal facility (e.g. by placing low permeability seals and plugs between the different repository sections).

For the evaluation of the performance and life time of the nuclear waste glasses in a geological repository in Boom Clay in the Netherlands and the radionuclide source term, it is assumed that the radionuclides are homogeneously distributed in the waste glasses, that the release of radionuclides is limited by the alteration of the (homogeneous) glass matrix (i.e. congruent release of radionuclides at the rate of glass dissolution), and that the glass dissolution can be described as a surface process at the macroscopic scale. The quantity of altered glass can then be calculated by

$$QAG = r \cdot S \cdot \tau \cdot t$$

where r is the dissolution rate, S the geometric surface area of the glass waste package, τ the effective cracking factor, and t the time.

The majority of the waste glasses relevant within the Dutch disposal programme are French R7T7 glasses. The most relevant data regarding their behaviour for OPERA are the

Belgian studies on SON68 glass dissolution under supercontainer conditions, which will form the basis for the following evaluation. However, to date, no experimental data on the long-term dissolution rates for R7T7/SON68 glass for the aforementioned reference scenario (stage II, evolved cement water with pH 12.5) in the presence of cementitious are available. [Ferrand 2013a] proposed to use the measured long-term dissolution rates in the tests using young cement waters at pH 13.5 with cement as ‘expert range’ for performance assessments, due to the lack of experimental evidence that the long-term dissolution rates in stages II and III in the presence of aged cement will be lower. According to [Ferrand 2013a] the measured dissolution rates for the lower pH (i.e. 12.5 and ~11.5) scenarios without cement could not be defended as long-term rates for stages II and III, because the effect of the presence of aged cement in the system was not known. Since the glass dissolution rates are expected to be (at least) slightly higher in “young” cementitious systems than in the later stages due to the higher pH and the higher alkali contents in the pore water, the rate data proposed by [Ferrand 2013a] can be deemed as conservative in our opinion.

Thus the starting point for calculating a best estimate plus upper and lower bounding values for the glass lifetime in the repository are the measured long-term dissolution rates at pH 13.5 in presence of cement ($0.0032 \dots 0.0094 \text{ g m}^{-2} \text{ d}^{-1}$; [Ferrand 2013a]), using here a mid-range value of $0.006 \text{ g m}^{-2} \text{ d}^{-1}$ as long-term rate. The density of the waste glass is $\sim 2.7 \text{ kg dm}^{-3}$ (cf. [Harrison 2010]), the internal diameter of the waste canister (i.e. the diameter of the monolith) 0.42 m (cf. [Verhoef 2016]), and the geometric surface of the (uncracked) glass monolith 1.7 m^2 (cf. [Poinsot 2012], [Vienna 2013]). Using the glass cracking factor of 40 as maximum of the expert range from [Ferrand 2011] (i.e. the cracking factor for the residual regime proposed, i.a., by [Ribet 2009] and [Poinsot 2012]) gives a glass package dissolution rate of $32.4 \mu\text{m a}^{-1}$, leading to glass package lifetime of 6,500 years, when assuming a linear dissolution along the 0.21 m radius of the glass block (cf. [Harrison 2010]). Applying the minimum value of the expert range for the cracking factor of [Ferrand 2013a] would yield a waste package lifetime of about 50,000 years.

For a (non-conservative) lower bound, a cracking factor of 5 as the minimum of the expert range proposed by [Ferrand 2011], and a long-term glass dissolution rate of $5 \cdot 10^{-5} \text{ g m}^{-2} \text{ d}^{-1}$ as determined in static experiments with “old” cement water (pH 11.5; [Ferrand 2013a]) are assumed. With these assumptions, a lifetime of the waste glass of $6.2 \cdot 10^6$ years results. For the upper bound, it is assumed that the glass dissolves completely at its initial rate in high pH cement waters. Taking the initial rate of $0.06 \text{ g m}^{-2} \text{ d}^{-1}$ measured in “young” cement water at pH 13.5 [Ferrand 2013a] and applying a cracking factor of 100 (upper value for R7T7 glass from [Vienna 2013]) yields a glass package dissolution rate of $\sim 800 \mu\text{m a}^{-1}$ and a glass package lifetime of ~ 260 years. This is a rather pessimistic approach, based on the assumption that as well as maintaining the dissolution rate at its high initial value, the reactive surface area of the glass as expressed by the cracking factor is and remains high. The waste glass performance data suggested for OPERA are summarised in table 6-1.

Table 6-1 Summary of glass waste form performance data suggested for OPERA

	Best estimate (realistic- conservative)	Lower bound (non-conservative)	Upper bound (conservative)
Glass dissolution rate	$0.006 \text{ g m}^{-2} \text{ d}^{-1}$	$0.00005 \text{ g m}^{-2} \text{ d}^{-1}$	$0.06 \text{ g m}^{-2} \text{ d}^{-1}$
Cracking factor	40	5	100
Glass package dissolution rate	$32.4 \mu\text{m a}^{-1}$	$0.03 \mu\text{m a}^{-1}$	$811 \mu\text{m a}^{-1}$
Glass package lifetime	$\sim 6,500 \text{ a}$	$6.2 \cdot 10^6 \text{ a}$	260 a
Waste form dissolution rate	$1.5 \cdot 10^{-4} \text{ a}^{-1}$	$1.6 \cdot 10^{-7} \text{ a}^{-1}$	$3.9 \cdot 10^{-3} \text{ a}^{-1}$

Regarding the performance of UK Magnox type waste glasses, larger uncertainties have to be taken into account here, since so far no dissolution rate data in the presence of cementitious materials are available. Generally, from the database no clear picture regarding the durability of Magnox type glasses in alkaline environments in relation to that of R7T7/SON68 glass emerges. Long term dissolution experiments (12 years) in initially pure water revealed a dissolution rate for simulant Magnox glass that is about an order of magnitude higher than that of SON68 [Curti 2006]. In contrast, rather similar initial dissolution rates of SON68 and simulated Magnox Oxide blend glasses in the range of some tens $\text{g m}^{-2} \text{d}^{-1}$ were obtained in alkali buffer solutions at pH 11.5 to 12 at elevated temperatures (cf. [Gin 2001], [Cassingham 2015]). Dissolution rates of simulant UK HLW glasses in saturated $\text{Ca}(\text{OH})_2$ solutions at pH 11 to 12 (cf. [Utton 2012], [Corkhill 2013]) span about the same range as the data for SON68 dissolution in old cement water (pH ~11.5) from [Ferrand 2013a], however, large differences (about a factor 100) exist between the two datasets for the UK glass.

The effective cracking factors for UK waste glasses provided by [Dunnett 2007] fall inside the expert range for R7T7/SON68 glass proposed by [Ferrand 2011]. Thus in a first approach, a durability and lifetime similar to R7T7 (cf. Table 6-1) can be applied also to the UK waste glasses. Assuming that the relation between the long-term dissolution rates of the two glass types determined by [Curti 2006] holds through also in cementitious conditions, surface specific dissolution rates (best estimate) that are one order of magnitude higher might be assumed for UK Magnox type waste glass in a worse case scenario. With respect to the different UK HLW glasses (i.e. "pure" Magnox waste glasses vs. Magnox-Oxide waste blend glasses) used in the various studies, a similar performance is assumed here, since it was suggested by [Cassingham 2015] that the dependence of the dissolution rates on glass composition is weak in the case of Magnox and Magnox-ThORP blend glasses under alkaline conditions.

It should be noted that the best estimate lifetime of the glass waste packages under supercontainer conditions calculated above are considerably shorter than the best estimates for glass package lifetimes used in various international HLW disposal programmes for non-cementitious environments. For example, in previous safety assessments in Belgium (SAFIR-2), a glass package lifetime of about 70,000 years was provided for R7T7 glass as best estimate [Mallants 2001]. The parameters used in [NAGRA 2002] yield a best estimate value for the lifetime of R7T7 and Magnox MW glass packages in the repository environment of 530,000 years and 70,000 years, respectively (cf. [Harrison 2010]). Based on the V_0 - V_r model applicable to R7T7 glasses produced in La Hague, it was concluded in the safety assessment for geological disposal of HLW in clay in France that the glass matrix lifetime would be "*at least several hundreds of millennia*" [ANDRA 2005]. [Harrison 2010] derived a best estimate for the lifetime of a Magnox MW glass package of 150,000 years for a generic repository in the UK.

6.2. Radionuclide migration in the near field

The radionuclides released due to dissolution or leaching of a waste form, i.e. in this case nuclear waste glasses, are not necessarily in a mobile form that can readily migrate in the EBS or the repository host rock. The released radionuclides may precipitate in a less soluble secondary phase or may be incorporated in or sorbed by crystalline or amorphous phases formed during the degradation of the waste form, depending on the chemical environment and the secondary phases present. In case of glass waste forms degrading in an alkaline environment, CSH-phases and zeolites newly formed on the glass surface (cf. [Gin 2013a], [Utton 2013]) may act as sinks for radionuclides due to sorption or uptake processes. In addition, compounds like powellite (CaMoO_4) and clay-like silicate minerals often observed as secondary phases during the alteration of nuclear waste glasses under repository conditions (e.g. [Bosbach 2009]) may retain certain radionuclides (e.g. trivalent

actinides and lanthanides). Moreover, the (degrading) near field materials may provide sinks for various radionuclides, for example due to sorption onto container corrosion products such as magnetite, including also reduction of radionuclides in higher valence states to less soluble forms in lower valence states and their precipitation. In the expected highly alkaline cementitious near field within the supercontainer buffer, the various cement phases may limit the radionuclide mobility due to sorption (e.g. on CSH-phases) or structural uptake (e.g. in AF_m -phases); furthermore the concentrations of certain radionuclides may be limited by the low solubility of their hydroxides under high pH conditions.

In general, it can be expected that the highest radionuclide concentrations will occur in the repository near-field and will decrease along the migration path to the far-field, due to further retardation processes, such as sorption on materials present in the engineered or natural barriers (i.e. in this case the Boom Clay), or due to dilution. In section 6.2.1 approaches to the evaluation of maximum radionuclide concentration in the repository near field are discussed, section 6.2.2 provides some information on the sorption of radionuclides in a cementitious near field.

6.2.1. Solubility limitation in a cementitious near field

The dissolved concentrations of radionuclides in the cementitious near field are determined by a variety of processes such as the release rates from the degrading waste forms, the potential formation of secondary solid phases when exceeding a solubility limit, and/or the sorption onto or uptake by solid repository materials (e.g. also by solid solution formation). Due to the complex interactions of the various processes and the large number of parameters that may affect the radionuclide behaviour (e.g. pH, Eh, solution composition and presence of complexing ligands, nature and availability of solid phases and their surfaces/interfaces), it is difficult to accurately determine the maximum radionuclide concentrations in the repository near field. One possible approach to the determination of maximum concentrations of radionuclides in a geological repository is the calculation of the solubility of radionuclides by using chemical thermodynamic data and assuming potential solubility limiting phases (cf. [Wanner 2007]). According to [Wang 2013a], it is justified within the radioactive waste community that the solubility determined by equilibrium calculations represents the maximum released radionuclide concentration.

[Wang 2013a] evaluated the solubility of various radionuclides in the pore water of the concrete buffer of a supercontainer used for the disposal of HLW in Boom Clay in Belgium. The solubility limits were mainly derived using a thermodynamic approach by calculation of the equilibrium with a solubility controlling solid phase, and are partly based on the review of experimental data in the literature for cementitious conditions. In a first step, [Wang 2013a] modelled the interaction of the cement buffer with Boom Clay pore water, using the reference Boom Clay pore water from the Mol site [de Craen 2004], to derive the pore water composition in the concrete buffer for the different cement degradation stages (cf. section 4.2.1). The pore water compositions simulated by this approach for the various stages of cement degradation (i.e. Stage I: NaOH and KOH pore water; stage II: portlandite stage, stage III: buffering by CSH-phases) are provided in Table 6-2.

Table 6-2 Simulated pore water composition in the near field concrete at 25 °C [Wang 2013a] - concentrations in mmol L⁻¹

Parameter	Stage I	Stage II	Stage III
pH	13.5 ... 12.5	12.5	12.5 ... 10.5
Na	141 ... 15	15	15
K	370 ... 0.2	0.2	0.2
Ca	0.7 ... 15.4	15.4	15.4 ... 1.4
Mg	10 ⁻⁷ ... 10 ⁻⁶	10 ⁻⁶	10 ⁻⁶ ... 10 ⁻⁴
Al	0.08 ... 0.008	0.008	0.008 ... 0.5
Si	0.01 ... 0.002	0.002	0.002 ... 5
CO ₃	0.4 ... 7 10 ⁻³	7 10 ⁻³	7 10 ⁻³ ... 0.02
SO ₄	8 ... 0.04	0.04	0.04 ... 5.7

According to [Wang 2013a], the estimation of the redox potential within the supercontainer buffer is difficult due to uncertainties regarding the redox controlling mechanisms and the thermodynamic data. In general, it is expected that the conditions in the repository near field in the HLW repository in Boom Clay are reducing [Wang 2013a]. The radionuclide solubilities evaluated by [Wang 2013a] for the supercontainer near field are summarised in Table 6-3. According to [Wang 2013a] the most influential chemical parameter on the solubility was the pH. With respect to the maximum solubility of uranium provided by [Wang 2013a] it should be noted that these concentrations were derived for U^{VI}, assuming that the repository conditions might be to oxidising for uranium to prevail as U^{IV}. In the case that the redox potential would be negative enough to favour U^{IV} in solution (i.e. less than ~670 mV in stage I and less than about ~550 mV in stage II), significantly lower uranium solubilities (10⁻⁸ to 10⁻⁹ mol L⁻¹) might occur (cf. [Berner 2003]).

With respect to the proposed Swiss cementitious repository for ILW in the Opalinus Clay, [Berner 2003] carried out solubility calculations for various radionuclides in the cementitious stage II pore water (cf. Table A-3), which are provided in Table A-7 for comparison. More recently, [Berner 2014] re-evaluated the solubility limits for safety relevant elements in the pore water of a concrete system for use in the provisional safety analysis for deep geological repository for long-lived ILW (cf. Table A-8). The solubility calculations were performed for the degradation stage characterised by portlandite saturation (Stage II, cf. Table A-4 for the pore water composition) using the updated NAGRA/PSI Chemical Thermodynamic Database 12/07 [Thoenen 2014], whereas the evaluations in [Berner 2003] were based on the NAGRA/PSI Chemical Thermodynamic Database 01/01 [Hummel 2002].

6.2.2. Sorption of radionuclides in a cementitious near field

The mobility of radionuclides in cementitious materials depends on the chemical behaviour of the particular element in high pH systems as well as on the chemical, physical and mineralogical properties of the solid material (e.g. pore water pH, degradation state, amount and nature of cement minerals, aggregates and accessory phases, specific surface areas, interface properties, etc.) and the presence of complexing ligands and competing ions. The retardation of radionuclides by sorption onto cementitious materials can encompass processes like ion exchange (e.g. radium and/or strontium uptake by CSH, e.g. [Tits 2006]), surface complexation (e.g. caesium sorption by CSH, e.g. [Heath 2000], [Iwaida 2002]) or structural uptake and solid solution formation (e.g. uptake of selenium or iodine by AF_m phases, e.g. [Baur 2003], [Aimoz 2012]) or combinations thereof.

Table 6-3 Solubilities of selected elements in a cementitious supercontainer near field [Wang 2013a] - concentrations in mol kg⁻¹ (VL: very low, NL: not limited)

Element	Stage	Upper bound	95% confidence limit for upper bound	Lower bound	95% confidence limit for lower bound	
Ag	I	6E-5		VL		
	II	6E-6		VL		
	III	6E-6		VL		
Am	I - III	3E-9	3E-10 ... 3E-8	3E-9	3E-10 ... 3E-8	
	Be	I	1E-4		<1E-4	
		II	<1E-4		<1E-4	
III		<1E-4		<1E-4		
C	I	3E-4		8E-6		
	II	8E-6		8E-6		
	III	1E-5		8E-6		
Ca	I	1.5E-2		7E-4		
	II	1.5E-2		1.5E-2		
	III	1.5E-2		1.4E-3		
Cl	I - III	NL		NL		
Cm	I - III	3E-9	3E-10 ... 3E-8	3E-9	3E-10 ... 3E-8	
	Cs	I - III	NL		NL	
		I	I - III	NL		NL
I			9E-4		5E-6	
Mo	II		5E-6		5E-6	
	III	4E-5		5E-6		
	I	1.1E-5	2E-6 ... 2E-5	7E-9	4E-9 ... 8E-9	
Nb	II	7E-9	4E-9 ... 8E-9	7E-9	4E-9 ... 8E-9	
	III	8E-7	1.8E-7 ... 4.2E-7	7E-9	4E-9 ... 8E-9	
	I - III	2.9E-7	2.4E-7 ... 3.4E-7	2.9E-7	2.4E-7 ... 3.4E-7	
Ni	I - III	2.9E-7	2.4E-7 ... 3.4E-7	2.9E-7	2.4E-7 ... 3.4E-7	
Np (IV)	I - III	1E-8		1E-9		
Pa	I - III	1E-8		1E-8		
	Pb	I	NL		NL	
		II	NL		5E-2	
III		NL		1E-4		
Pd	I	1E-4		1E-5		
	II	1E-5		1E-5		
	III	1E-5		4E-6		
Pu (IV)	I - III	1E-8		1E-11		
	Ra	I	1E-6		7E-9	
		II	1E-6		1E-6	
III		1E-6		1E-8		
Se	I	NL		5E-4		
	II	NL		2E-5		
	III	NL		1E-11		
Sn	I	2E-6		1E-8		
	II	1E-8		1E-8		
	III	1E-7		1E-8		
Sr	I	2.5E-3		1E-4		
	II	2.5E-3		2.5E-3		
	III	2.5E-3		3.4E-4		
Tc	I	NL		1E-6 Tc ^{IV}		
	II	NL		1E-7 Tc ^{IV}		
	III	NL		NL		
Th	I - III	1E-8	1E-9 ... 1E-7	1E-8	1E-9 ... 1E-7	
	U(VI)	I	3E-6	2.6E-7 ... 7E-6	2E-6	1E-6 ... 6E-6
		II	2E-6	1E-6 ... 6E-6	2E-6	1E-6 ... 6E-6
III		3E-5		2E-6	1E-6 ... 6E-6	
Zr	I	3E-8	5E-9 ... 1E-7	2E-8	3.6E-10 ... 1E-6	
	II - III	2E-8	3.6E-10 ... 1E-6	2E-8	3.6E-10 ... 1E-6	

The sorption of radionuclides to cementitious materials and radionuclide retardation under cementitious near-field conditions has been intensively discussed within the context of nuclear waste disposal and is still in the focus of international research activities, for example in the EC-Horizon 2020 research project CEBAMA (www.cebama.eu). Various case specific sorption databases for radionuclide-cement interactions have been developed in the past decades (e.g. [Wieland 2002], [Wang 2009b], [Suyama 2012], [Wang 2013b], [Wieland 2014]), which can provide an overview on the radionuclide retardation expected in various cementitious systems under different environmental conditions. However, at present no directly applicable data sets are at hand to describe the sorption of radionuclides in a cementitious repository in Boom Clay in the Netherlands.

7. Conclusions

The inventory of vitrified HLW to be disposed of in a deep geological repository in the Netherlands comprises predominantly R7T7 glasses from reprocessing of spent nuclear fuel from the Borssele NPP in La Hague, France, and, to a lesser extent, waste glasses from the reprocessing of spent nuclear fuels from the Dodewaard NPP in Sellafield, UK. The generic disposal concept for HLW in Boom Clay being pursued in the context of OPERA is based on the Belgian supercontainer concept. In this concept, the EBS makes extensive use of cementitious materials as buffer within the supercontainer, as backfilling grout, and in the construction material for the disposal gallery linings. Thus the near-field chemistry will be governed by the degradation of cementitious materials in the long-term and an anoxic and highly alkaline repository near field will prevail probably for some hundreds of thousands of years post closure.

Experimental investigations on the dissolution behaviour of nuclear waste glasses in cementitious environments have been performed especially in the context of the Belgian research programmes related to the supercontainer concept, focussing in particular on the French waste glass R7T7 and its inactive surrogate SON68, respectively. Comparatively fewer data and information on the performance of UK waste glasses under cementitious conditions are available; experimental data on the dissolution of UK waste glasses in the presence of cementitious materials seem to be lacking to date. Based on a review of the literature and a compilation of a database on glass dissolution rates under alkaline conditions, focussing on French R7T7/SON68 and UK Magnox MW type glasses, the following conclusions can be drawn:

- Glass dissolution rates generally depend on glass type, temperature, pH, solution composition, and the presence of cementitious materials;
- Glasses are generally less durable under high pH conditions;
- The highest dissolution rates are observed in alkali-rich KOH (NaOH/LiOH) solutions;
- Elevated calcium concentrations in solution such as in evolved cement pore waters have an antagonistic effect on the glass alteration rate due to the inclusion of calcium into the altered glass layer and/or CSH-precipitation on the glass surface;
- The presence of cementitious materials leads to a decrease of the silicon concentration in solution, for example due to CSH-formation by reaction with portlandite (Ca(OH)_2) resulting in higher glass dissolution rates, as long as portlandite is available.

Thus the glass dissolution rates in the repository will depend on the stage of supercontainer concrete degradation and the availability of portlandite at the time of waste canister failure. The evolution of the near-field chemistry and the extent of cement alteration resulting from the exchange of cementitious materials with Boom Clay pore water will directly impact glass dissolution rates, the formation of glass alteration layers and secondary phases, as well as the radionuclide release with time (source term).

The design of the multi-barrier system within the OPERA disposal concept for HLW, that is the supercontainer concept, emphasises on the one hand the protection of the overpack material, i.e. the safety function 'engineered containment (C)', through the engineering of a highly alkaline environment. However, once the overpack and the CSD-V canister are breached, this high pH environment could sustain glass dissolution to proceed in the initial (or resumption) regimes (i.e. at higher rates), due to precipitation of CSH-phases and/or zeolites, thus adversely affecting the safety function R1: 'limitation of contaminant releases from the waste forms'.

Taking into account in particular the results of the Belgian research programmes into glass dissolution under supercontainer conditions, ranges and best estimates for the glass dissolution rates and the lifetime of the glass waste forms under repository conditions have been proposed here for OPERA. Regarding the release of radionuclides from the glass waste forms, a homogeneous distribution of the radionuclides in the glasses and a congruent release of radionuclides with the glass matrix dissolution were assumed, taking into account the increase in the reactive surface area of the glass monoliths due to fracturing in course of the cooling process. Larger uncertainties regarding the performance of UK Magnox MW type glasses under cementitious repository conditions compared to R7T7 glasses were noted. As a best estimate, a waste package dissolution rate of $32 \mu\text{m a}^{-1}$ and a glass package lifetime of about 6,500 years are suggested.

However, the dissolution of the glass waste forms in the repository does not necessarily imply that all radionuclides released from the glass matrix will be mobile and can migrate into the repository near and far field, since the radionuclides might be retained by amorphous and/or crystalline secondary phases formed as a consequence of the alteration process on the glass surface. Moreover, the migration of radionuclides released from the HLW glasses may further be delayed by sorption to other near field materials such as corrosion products from the metallic waste canisters/overpacks or retention/uptake in the cementitious materials present in the supercontainer buffer or the repository backfill.

In order to better constrain the dissolution behaviour of nuclear waste glasses under OPERA disposal conditions, to build further confidence in the OPERA safety case, and to evaluate safety margins with respect to the geological disposal of vitrified HLW in the Netherlands, in our opinion the following issues should be addressed in more detail in future research activities:

- Near field conditions at the time of canister failure: The geochemical conditions the wastes are exposed to after canister failure should be further constrained, for example, by coupled reactive transport simulations of the interaction of typical Boom Clay groundwaters expected in various regions of the Netherlands with the cementitious EBS materials. In this context it is suggested to look in more detail on the effect of the stainless steel envelope on the timescales of the resaturation of the supercontainer buffer and the lifetime of the overpack/waste canister.
- Glass dissolution rates in evolved cementitious systems: The glass dissolution rates proposed here for OPERA are based on data for systems with young cement pore waters at pH 13.5. It is suggested to further evaluate future international research activities, i.e. especially experimental work envisaged within the Belgian repository programme, addressing glass dissolution behaviour in stages II and III of concrete degradation in the presence of cementitious materials, to better constrain long-term glass dissolution rates for the respective scenarios in OPERA and potentially reduce conservative assumptions.
- Performance of UK waste glasses: The performance of UK Magnox type waste glasses in the presence of cementitious materials is poorly constrained to date, due to the lack of respective experimental data. Thus it is suggested to conduct selective experiments similar to those performed in the Belgian programme, to constrain and envelope the performance of UK waste glasses relative to SON68 glasses in supercontainer conditions.
- Glass alteration products/secondary phases: To constrain the radionuclide retention by alteration products and secondary phases forming on the corroding glass surface under alkaline conditions, experiments are suggested to determine the nature of secondary products formed during waste glass alteration under supercontainer conditions and evaluate their thermodynamic stability and their radionuclide retention potential.
- Reactive surface area: Investigations on the effects of cracking and the evolution of the effective surface area of waste glasses under disposal conditions could reduce existing uncertainties regarding waste form performance in the repository.

8. References

- [Aagaard 1982] Aagaard P, Helgeson HC, *Thermodynamic and kinetic constraints on reaction rates among minerals and aqueous solutions I: theoretical considerations*, Amer J Sci 282 (1982) 237-285.
- [Abdelouas 2004] Abdelouas A, Ferrand K, Grambow B, Mennecart T, Fattahi M, Blondiaux G, Houée-Lévin C, *Effect of gamma and alpha irradiation on the corrosion of the French borosilicate glass SON68*, Mat Res Soc Symp Proc 807 (2004) 175-180.
- [Abraitis 1998] Abraitis PK, Vaughan DJ, Livens FR, Monteith J, Trivedi DP, Small JS, *Dissolution of a complex borosilicate glass at 60 °C: The influence of pH and proton adsorption on the congruence of short-term leaching*, Mat Res Soc Symp Proc 506 (1998) 47-54.
- [Abraitis 2000a] Abraitis PK, Livens FR, Monteith JE, Small JS, Trivedi DP, Vaughan DJ, Wogelius RA, *The kinetics and mechanisms of simulated British Magnox waste glass dissolution as a function of pH, silicic acid activity and time in low temperature aqueous systems*, Appl Geochem 15 (2000) 1399-1416.
- [Abraitis 2000b] Abraitis PK, McGrail BP, Trivedi DP, Livens FR, Vaughan DJ, *Single-pass flow-through experiments on a simulated glass in alkaline media at 40°C. I. Experiments conducted at variable solution flow rate to glass surface area*, J Nucl Mater 280 (2000) 196-205.
- [Abraitis 2000c] Abraitis PK, McGrail BP, Trivedi DP, Livens FR, Vaughan DJ, *Single-pass flow-through experiments on a simulated glass in alkaline media at 40°C. II. Experiments conducted with buffer solutions containing controlled quantities of Si and Al*, J Nucl Mater 280 (2000) 206-215.
- [Advocat 1991a] Advocat T, Crovisier JL, Vernaz E, Ehret G, Charpentier H, *Hydrolysis of R7T7 nuclear waste glass in dilute media: Mechanisms and rate as a function of pH*, Mat Res Soc Symp Proc 212 (1991) 57-64.
- [Advocat 1991b] Advocat T, *Les mécanismes de corrosion en phase aqueuse du verre nucléaire R7T7: Approche expérimentale, Essai de modélisation thermodynamique et cinétique*, PhD thesis, University Louis Pasteur, Strasbourg, France (1991) 1-229.
- [Advocat 2001] Advocat T, Jollivet P, Crovisier JL, Del Nero M, *Long-term alteration mechanisms in water for SON68 radioactive borosilicate glass*, J Nucl Mater 298 (2001) 55-62.
- [Aimoz 2012] Aimoz L, Wieland E, Taviot-Gueho C, Dähn R, Vespa M, Churakov SV, *Structural insight into iodide uptake by AFm phases*, Environ Sci Technol 46 (2012) 3874-3881.
- [Andriambololona 1992] Andriambololona Z, Godon N, Vemaz E, *R7T7 glass alteration in the presence of mortar*, Mat Res Soc Symp Proc 257 (1992) 151-158.
- [ANDRA 2005] ANDRA, *Dossier 2005 Argile - Synthèse - Evaluation of the feasibility of a geological repository in an argillaceous formation*, Châtenay-Malabry (2005) 1-238.
- [AREVA 2007] AREVA, *Specification for standard vitrified waste residue (CSD-V) with high actinide content produced at la Hague* (2007) 1-23 (Confidential document not published openly).
- [Atkins 1992] Aktins M, Glasser F, *Application of Portland cement-based materials to radioactive waste immobilization*, Waste Manage 12 (1992) 105-131.
- [Barth 2014] Barth N, George D, Ahzi S, Rémond Y, Joulaee N, Khaleel MA, Bouyer F, *Simulation of cooling and solidification of three-dimensional bulk borosilicate glass: effect of structural relaxations*, Mech Time-Depend Mater 18 (2014) 81-96.
- [Baur 2003] Baur I, Johnson CA, *The solubility of selenate-AF_t (3CaO·Al₂O₃·3CaSeO₄·37.5H₂O) and selenate-AF_m (3CaO·Al₂O₃·CaSeO₄·xH₂O)*, Cem Concr Res 33 (2003) 1741-1748.
- [Beattie 2012] Beattie TM, Williams SJ, *An overview of near-field evolution research in support of the UK geological disposal programme*, Min Mag 76 (2012) 2995-3001.
- [Bel 2006] Bel JJP, Wickham SM, Gens RMF, *Development of the supercontainer design for deep geological disposal of high-level heat emitting radioactive waste in Belgium*, Mat Res Soc Symp Proc 932 (2006)

- [Berner 1988] Berner UR, *Modelling the incongruent dissolution of hydrated cement minerals*, Radiochim Acta 44/55 (1988) 387-393.
- [Berner 1992] Berner UR, *Evolution of pore water chemistry during degradation of cement in a radioactive waste repository environment*, Waste Manage 12 (1992) 201-219.
- [Berner 2003] Berner U, *Radionuclide concentration limits in the cementitious near-field of an ILW repository*, NAGRA Technical Report NTB 02-22 (2003) 1-48.
- [Berner 2014] Berner U, *Solubility of radionuclides in a concrete environment for provisional safety analyses for SGT-E2*, NAGRA Technical Report NTB 14-07 (2014) 1-81.
- [BNFL 2001] British Nuclear Fuels Ltd, *Manual of determination methods for guaranteed parameters of vitrified residue* (2001) 1-74 (Confidential document not published openly).
- [Boen 2010] Boen R, *Cold-crucible fabrication of nuclear glasses*, Clefs CEA 59 (2010) 17-21.
- [Bosbach 2009] Bosbach D, Luckscheiter B, Brendebach B, Denecke MA, Finck N, *High level nuclear waste glass corrosion in synthetic clay pore solution and retention of actinides in secondary phases*, J Nucl Mater 385 (2009) 456-460.
- [Boult 1991] Boult KA, Dalton JT, Hough A, Marples JAC, Robertson GP, Wilkins RI, *Radionuclide release from solidified high level waste - Task 3 Characterization of radioactive waste forms*, Contract No F11W/0097 Final report EUR-13604 (1991) 1-70.
- [Brady 1996] Brady PV, House WA, *Surface-controlled dissolution and growth of minerals*, in: Brady PV (ed) *Physics and Chemistry of Mineral Surfaces*, CRC Press, New York (1996) 249-256.
- [Brookes 2010] Brookes C, Harrison M, Riley A, Steele C, *The effect of increased waste loading on the durability of High Level Waste glass*, Mat Res Soc Symp Proc 1265 (2010) 1265-AA03-05, 1-6.
- [Cachoir 2015] Cachoir C, Mennecart T, *Spent fuel dissolution in supercontainer conditions - Reporting period 2009-2012*, External Report SCK•CEN ER-231 (2015) 1-140.
- [Cailleteau 2008] Cailleteau C, Angeli F, Devreux F, Gin S, Jollivet P, Spalla O, *Insight into silicate-glass corrosion mechanisms*, Nature Mater 7 (2008) 978-983.
- [Cassingham 2015] Cassingham N, Corkhill CL, Backhouse DJ, Hand RJ, Ryan JV, Vienna JD, Hyatt NC, *The initial dissolution rates of simulated UK Magnox-ThORP blend nuclear waste glass as a function of pH, temperature and waste loading*, Min Mag 79 (2015) 1529-1542.
- [Chave 2011] Chave T, Frugier P, Gin S, Ayrat A, *Glass-water interphase reactivity with calcium rich solutions*, Geochim Cosmochim Acta 75 (2011) 4125-4139.
- [Corkhill 2013] Corkhill CL, Cassingham NJ, Heath PG, Hyatt NC, *Dissolution of UK High-Level Waste glass under simulated hyperalkaline conditions of a colocated geological disposal facility*, Int J Appl Glass Sci 4 (2013) 341-356.
- [Curti 2003] Curti E, *Glass dissolution parameters: Update for Entsorgungsnachweis*, NAGRA Technical Report NTB 02-21 (2003) 1-46.
- [Curti 2006] Curti E, Crovisier JL, Morvan G, Karpoff AM, *Long-term corrosion of two nuclear waste reference glasses (MW and SON68): A kinetic and mineral alteration study*, Appl Geochem 21 (2006) 1152-1168.
- [de Craen 2004] de Craen M, Wang L, van Geet M, Moors H, *Geochemistry of Boom Clay pore water at the Mol site*, Scientific Report SCK•CEN-BLG-990 (2004) 1-179.
- [Depierre 2013] Depierre S, Frizon F, Gin S, Angeli F, *Leaching of nuclear waste glass in cement pore water: Effect of calcium in solution*, in: Bart F, Cau-dit-Coumes C, Frizon F, Lorente S (eds) *Cement based materials for nuclear waste storage*, Springer (2013) 161-168.
- [Deschanel 2007] Deschanel X, Peugeot S, Cachia JN, Charpentier T, *Plutonium solubility and self-irradiation effects in borosilicate glass*, Prog Nucl Energy 49 (2007) 623-634.
- [Diomidis 2014] Diomidis N, *Scientific basis for the production of gas due to corrosion in a deep geological repository*, NAGRA Arbeitsbericht NAB 14-21 (2014) 1-64.

- [Donald 1997] Donald IW, Metcalfe BL, Taylor RNJ, The immobilization of high level radioactive wastes using ceramics and glasses, *Jour Mat Sci* 32 (1997) 5851-5887.
- [Donald 2007] Donald IW, Immobilisation of radioactive and non-radioactive wastes in glass-based systems: an overview, *Glass - Part A* 48 (2007) 155-163.
- [Donald 2010] Donald IW, Waste immobilization in glass and ceramic based hosts - Radioactive, toxic and hazardous wastes, Wiley (2010) 1-507.
- [Dove 1999] Dove P, *The dissolution kinetics of quartz in aqueous mixed cation solutions*, *Geochim Cosmochim Acta* 63 (1999) 3715-3727.
- [Drace 2013] Drace Z, Ojovan MI, *A summary of IAEA coordinated research project on cementitious materials for radioactive waste management*, in: Bart F, Cau-dit-Coumes C, Frizon F, Lorente S (eds) *Cement-based materials for nuclear waste storage*, Springer (2013) 3-11.
- [Dunnett 2007] Dunnett BF, *Review of the development of UK High Level Waste vitrified product*, Nexia Solutions Report NS(06)7926, Issue 4 (2007) 1-56.
- [Ebert 1994] Ebert WL, Mazer JJ, *Laboratory testing of waste glass aqueous corrosion; effects of experimental parameters*, *Mat Res Soc Symp Proc* 333 (1994) 27-40.
- [ENS 2014] European Nuclear Society, *First MOX loading in Borssele*, ENS News 45 (2014) www.euronuclear.org/e-news/e-news-45/borssele.htm, accessed on 01.03.2016.
- [Ewing 1995] Ewing RC, Weber WJ, Clinard jr FW, *Radiation effects in nuclear wastefoms for high level radioactive waste*, *Prog Nucl Energy* 29 (1995) 63-127.
- [Ferrand 2006] Ferrand K, Abdelouas A, Grambow B, *Water diffusion in the simulated French nuclear waste glass SON 68 contacting silica rich solutions: Experimental and modeling*, *J Nucl Mater* 355 (2006) 54-67.
- [Ferrand 2008] Ferrand K, Lemmens K, *Determination of the forward rate of dissolution for SON68 and PAMELA glasses in contact with alkaline solutions*, *Mat Res Soc Symp Proc* 1107 (2008) 287-294.
- [Ferrand 2011] Ferrand K, *Assessment of the effective surface area of vitrified waste in supercontainer disposal conditions*, External Report SCK•CEN-ER-155 (2011) 1-24.
- [Ferrand 2012] Ferrand K, Lemmens K, Gielen B, Vercauter R, *Determination of dissolution rates in vitrified high and medium level waste in a cementitious environment*, in: *Cementitious materials in safety cases for geological repositories for radioactive waste: role, evolution and interaction*. NEA/RWM/R(2012)3 (2012) 155-158.
- [Ferrand 2013a] Ferrand K, *Topical report on tests on vitrified (V)HLW waste in supercontainer disposal conditions (status 2011)*, External Report SCK•CEN-ER-195 (2013) 1-464.
- [Ferrand 2013b] Ferrand K, Liu S, Lemmens K, *The interaction between nuclear waste glass and Ordinary Portland Cement*, *Int J Appl Glass Sci* 4 (2013) 328-340.
- [Ferrand 2014] Ferrand K, Liu S, Lemmens K, *The effect of Ordinary Portland Cement on nuclear waste glass dissolution*, *Proc Mat Sci* 7 (2014) 233-229.
- [Fillet 2008] Fillet C, Ribet I, Gin S, Peugeot S, Vernaz E, *Long term behaviour of French R7T7 glass: a short review*, *Glass Technol: Europ J Glass Sci Technol A* 49 (2008) 302-306.
- [Fournier 2014] Fournier M, Gin S, Frugier P, *Resumption of nuclear glass alteration: State of the art*, *J Nucl Mat* 448 (2014) 348-363.
- [Frizon 2009] Frizon F, Gin S, Jégou C, *Mass transfer phenomena in nuclear waste packages*, in: Wang LQ (ed) *Advances in Transport Phenomena 2009, ADVTRANS 1*, Springer (2009) 31-133.
- [Frugier 2008] Frugier P, Gin S, Minet Y, Chave T, Bonin B, Godon N, Lartigue JE, Jollivet P, Ayrat A, De Windt L, Santarini G, *SON68 nuclear glass dissolution kinetics: Current state of knowledge and basis of the new GRAAL model*, *J Nucl Mater* 380 (2008) 8-21.
- [Fukui 2003] Fukui T, Ishinomori T, Endo Y, Sazarashi M, Ono S, Suzuki K, *Iron phosphate glass as potential waste matrix for high-level radioactive waste*, Waste Management '03 Conference, February 23 - 27, 2003, Tucson, AZ (2003) 1-11.

- [Geisler 2010] Geisler T, Janssen A, Scheiter D, Stephan T, Berndt J, Putnis A, *Aqueous corrosion of borosilicate glass under acidic conditions: A new corrosion mechanism*, J Non-Cryst Solids 356 (2010) 1458-1465.
- [Giffaut 2014] Giffaut E, Grivé M, Blanc P, Vieillard P, Colàs E, Gailhanou H, Gaboreau S, Marty N, Madé B, Duro L, *Andra thermodynamic database for performance assessment: ThermoChimie*, Appl Geochem 49 (2014) 225-236.
- [Gin 1994] Gin S, Godon N, Mestre JP, Vernaz EY, *Experimental investigation of aqueous corrosion of R7T7 nuclear glass at 90 °C in the presence of organic species*, Appl Geochem 9 (1994) 255-269.
- [Gin 2001] Gin S, Mestre JP, *SON68 nuclear glass alteration kinetics between pH 7.5 and 11*, J Nucl Mat 295 (2001) 83-96.
- [Gin 2011] Gin S, Guittonneau C, Godon N, Neff D, Rebiscol D, Cabié M, Mostefaoui S, *Nuclear glass durability: New insight into alteration layer properties*, J Phys Chem C115 (2011) 18696-18706.
- [Gin 2013a] Gin S, Abdelouas A, Criscenti LJ, Ebert WL, Ferrand K, Geisler T, Harrison MT, Inagaki Y, Mitsui S, Mueller KT, Marra JC, Pantano CG, Pierce EM, Ryan JV, Schofield JM, Steefel CI, Vienna JD, *An international initiative on long-term behavior of high-level nuclear waste glass*, Mater Today 16 (2013) 243-248.
- [Gin 2013b] Gin S, Frugier P, Jollivet P, Bruguier F, Curti E, *New insight into the residual rate of borosilicate glasses: effect of S/V and glass composition*, Int J Appl Glass Sci 4 (2013) 371-382.
- [Gin 2014] Gin S, *Open scientific questions about glass corrosion*, Proc Mat Sci 7 (2014) 163-171.
- [Glasser 2011] Glasser FP, *Application of inorganic cements to the conditioning and immobilisation of radioactive wastes*, in: Ojovan MI (ed) Handbook of advanced radioactive waste conditioning technologies, Woodhead, Oxford (2011) 67-135.
- [Grambow 1985] Grambow B, *A general rate equation for nuclear waste glass corrosion*, Mat Res Soc Symp Proc 44 (1985) 15-27.
- [Grambow 2006] Grambow B, *Nuclear waste glasses - How durable?* Elements 2 (2006) 357-364.
- [Gribble 2012] Gribble N, Short R, Turner E, Riley AD, *The impact of increased waste loading on vitrified HLW quality and durability*, Nucl Future 5 (2012) 211-216.
- [Harris 2002] Harris AW, Manning MC, Tearle WM, Tweed CJ, *Testing of models of the dissolution of cements - leaching of synthetic C-S-H gels*, Cem Concr Res 32 (2002) 731-746.
- [Harrison 2009] Harrison MT, Dunnet BF, Morgan S, Scales CR, Small JS, *International research on vitrified HLW long term behaviour: State of the art*, National Nuclear Laboratory NNL (09) 8864 Issue 4 (2009) 1-90.
- [Harrison 2010] Harrison MT, *Review of glass dissolution rates for use in the Disposal System Safety Case performance assessment models*, National Nuclear Laboratory NNL (10) 10734 Issue 3 (2010) 1-36.
- [Harrison 2014] Harrison MT, *The effect of composition on short- and long-term durability of UK HLW glass*, Proc Mat Sci 7 (2014) 186-192.
- [Hart 2014] Hart J, *Determination of the inventory Part A: Radionuclides*, OPERA report OPERA-PU-NRG1112A (2014) 1-47.
- [Heath 2000] Heath TG, Illet DJ, Tweed CJ, *Development of a near-field sorption model for a cementitious repository*, UK Nirex report AEAT/R/ENV/0229 (2000) 1-41.
- [Hellmann 2012] Hellmann, Wirth R, Daval D, Barnes JP, Penisson JM, Tisserand D, Epicier T, Florin B, Hervig RL, *Unifying natural and laboratory chemical weathering with interfacial dissolution-reprecipitation: A study based on the nanometer-scale chemistry of fluid-silicate interfaces*, Chem Geol 294/295 (2012) 203-216.
- [Hellmann 2015] Hellmann R, Cotte S, Cadel E, Malladi S, Karlsson LS, Lozano-Perez S, Cabié M, Seyeux A, *Nanometre-scale evidence for interfacial dissolution-reprecipitation control of silicate glass corrosion*, Nat Mater (2015) 307-311.
- [Hellmann 2016] Hellmann R, *pers comm* (2016)

- [Hoch 2012] Hoch AR, Baston GMN, Glasser FP, Hunter FMI, Smith V, *Modelling evolution in the near field of a cementitious repository*, *Min Mag* 76 (2012) 3055-3069.
- [Hummel 2002] Hummel W, Berner U, Curti E, Pearson FJ, Thoenen T, *Nagra/PSI Chemical Thermodynamic Data Base 01/01*, NAGRA Technical Report NTB 02-16 (2002) 1-565.
- [Hunter 2015] Hunter FMI, Hoch AR, Heath TG, Baston GNM, *Review of glass dissolution models and application to UK glasses*, *AMEC/103498/02 Issue 2*, 2015, 1-58.
- [Icenhower 2000] Icenhower J, Dove P, *The dissolution kinetics of amorphous silica into sodium chloride solutions: effects of temperature and ionic strength*, *Geochim Cosmochim Acta* 64 (2000) 4193-4203.
- [Inagaki 1992] Inagaki Y, Furuya H, Idemitsu K, Banba T, Matsumoto S, Muraoka S, *Microstructure of simulated high-level waste glass doped with short-lived actinides, ²³⁸Pu and ²⁴⁴Cm*, *Mat Res Soc Symp Proc* 257 (1992) 199-206.
- [Iwaida 2002] Iwaida T, Nagasaki S, Tanaka S, Yaita T, Tachimori S, *Structure alteration of C-S-H (calcium silicate hydrated phases) caused by sorption of cesium*, *Radiochim Acta* 90 (2002) 677-681.
- [Jobe 1997] Jobe DL, Lemire RJ, Taylor P, *Iron oxide redox chemistry and nuclear fuel disposal*, *AECL-11667, COG-96-487-1* (1997) 1-48.
- [Jollivet 2012] Jollivet P, Gin S, Schumacher S, *Forward dissolution rate of silicate glasses of nuclear interest in clay-equilibrated groundwater*, *Chem Geol* 330/331 (2012) 207-217.
- [King 2000] King F, Stroes-Gascoyne S, *An assessment of the long-term corrosion behavior of C-steel and the impact on the redox conditions inside a nuclear fuel waste disposal container*, Ontario Power Generation Report No 06819-REP-01200-10028-R00 (2000).
- [Knauss 1990] Knauss KG, Bourcier WL, McKeegan KD, Merzbacher CI, Nguyen SN, Ryerson FJ, Smith DK, Weed HC, Newton L, *Dissolution kinetics of a simple analogue nuclear waste glass as a function of pH, time and temperature*, *Mat Res Soc Symp Proc* 176 (1990) 371-381.
- [Kosakowski 2013] Kosakowski G, Berner U, *The evolution of clay rock/cement interfaces in a cementitious repository for low- and intermediate level radioactive waste*, *Phys Chem Earth* 64 (2013) 65-86.
- [Krupka 1998] Krupka KM, Serne RJ, *Effects on radionuclide concentrations by cement/ground-water interactions in support of performance assessment of low-level radioactive waste facilities*, Pacific Northwest National Laboratory PNNL-11408 (1998) 1-142.
- [Kursten 2004] Kursten B, Smailos E, Azkarate I, Werme L, Smart NR, Santarini G, *State-of the-art document on the CORrosion BEhaviour of COntainer MATerials (COBECOMA)*, European Commission, Contract No FIKW-CT-20014-20138, Final Report (2004) 1-299.
- [Kursten 2015] Kursten B, Druyts F, *Assessment of the uniform corrosion behavior of carbon steel radioactive waste packages with respect to the disposal concept in the geological Dutch Boom Clay formation*, OPERA-PU-SCK513 (2015) 1-107.
- [Kursten 2016] Kursten B, *pers comm* (2016)
- [Lasaga 1981] Lasaga AC, *Rate laws of chemical reactions*, in: Lasaga AC, Kirkpatrick R (eds) *Kinetics of geochemical processes*, *Rev Miner* 8 (1981) 1-68.
- [Lee 2006] Lee WE, Ojovan MI, Stennett MC, Hyatt NC, *Immobilisation of radioactive waste in glasses, glass composite materials and ceramics*, *Adv Appl Ceram* 105 (2006) 1-12.
- [Lemmens 2012a] Lemmens K, Mennecart T, Cachoir C, *Spent fuel dissolution in Belgian supercontainer conditions: source term and compatibility*, *Mat Res Soc Symp Proc* 1475 (2012) 131-136.
- [Lemmens 2012b] Lemmens K, Cachoir C, Ferrand K, Mennecart T, Gielen B, Vercauter R. *Interaction of cementitious materials with high-level waste matrices*, in: *Cementitious materials in safety cases for geological repositories for radioactive waste: role, evolution and interaction*, NEA/RWM/R(2012)3 (2012) 80-81.
- [Lutze 1988a] Lutze W, *Silicate glass*, in: Lutze W, Ewing RC (eds) *Radioactive waste forms for the future*, North-Holland, Amsterdam (1988) 1-159.

- [Lutze 1988b] Lutze W, Ewing RC, *Summary and evaluation of nuclear waste forms*, in: Lutze W, Ewing RC (eds) *Radioactive waste forms for the future*, North-Holland, Amsterdam (1988) 699-740.
- [Mallants 2001] Mallants D, Marivoet J, Sillen X, *Performance assessment of the disposal of vitrified high-level waste in a clay layer*, *J Nucl Mater* 298 (2001) 125-135.
- [McGinnes 2002] McGinnes DF, *Model radioactive waste inventory for reprocessing waste and spent fuel*, NAGRA Technical Report NTB 01-01 (2002) 1-42.
- [McGrail 1997] McGrail BP, Ebert WL, Bakel AJ, Peeler DK, *Measurement of kinetic rate law parameters on a Na-Ca-Al borosilicate glass for low-activity waste*, *J Nucl Mater* 249 (1997) 175-189.
- [McGrail 2001] McGrail BP, Bacon DH, Icenhower JP, Mann FM, Puigh RJ, Schaef HT, Mattigod SV, *Near-field performance assessment for a low-activity waste glass disposal system: laboratory testing to modeling results*, *J Nucl Mater* 298 (2001) 95-111.
- [MEAAI 2014] Ministry of Economic Affairs, Agriculture and Innovation & Ministry of Foreign Affairs, *National report of the Kingdom of the Netherlands for the fifth review conference on the Joint Convention of the safety of spent fuel management and on the safety of radioactive waste management* (2014) 1-112.
- [Meeussen 2014] Meeussen JCL, Rosca-Bocancea E, *Determination of the inventory Part B: Matrix composition*, OPERA report OPERA-IR-NRG1112B (2014) 1-23.
- [Mercado-Depierre 2013] Mercado-Depierre S, Angeli F, Frizon F, Gin S, *Antagonist effects of calcium on borosilicate glass alteration*, *J Nucl Mat* 441 (2013) 402-410.
- [Minet 2003] Minet Y, Godon N, *Leaching full-scale fractured glass blocks*, *Ceramic Transactions* 143 (2003) 275-282.
- [NAGRA 1994] NAGRA, *Kristallin-I safety assessment report*, NAGRA Technical Report NTB 93-22 (1994) 1-396.
- [NAGRA 2002] NAGRA, *Project Opalinus Clay Safety Report. Demonstration of disposal feasibility for spent fuel, vitrified high-level waste and long-lived intermediate-level waste (Entsorgungsnachweis)*, NAGRA Technical Report NTB 02-05 (2002) 1-360.
- [Neall 1994] Neall F, *Modelling of the near-field chemistry of the SMA repository at the Wellenberg site: Application of the extended cement degradation model*, NAGRA Technical Report NTB 94-03 (1994) 1-45.
- [Ojovan 2005] Ojovan MI, Lee WE, *An introduction to nuclear waste immobilisation*. Elsevier Science, Amsterdam (2005) 1-250.
- [Ojovan 2006] Ojovan MI, Pankov A, Lee WE, *The ion exchange phase in corrosion of nuclear waste glasses*, *J Nucl Mater* 358 (2006) 57-68.
- [Ojovan 2011] Ojovan MI, Lee WE, *Glassy wasteforms for nuclear waste immobilization*, *Metall Mater Trans A42* (2011) 837-851.
- [ONDRAF 2004] ONDRAF/NIRAS, *Multi-criteria analysis on the selection of a reference EBS design for vitrified high level waste*, NIRONDR 2004-03 (2004) 1-120.
- [ONDRAF 2013] ONDRAF/NIRAS, *ONDRAF/NIRAS Research, Development and Demonstration (RD&D) Plan for the geological disposal of high-level and/or long-lived radioactive waste including irradiated fuel if considered as waste*, NIRONDR-TR 2013-12 E (2013) 1-411.
- [Paul 1990] Paul A, *Chemistry of glasses 2nd edition*, Chapman and Hall, London (1990) 1-368
- [Petitjean 2002] Petitjean V, Fillet C, Boen R, Veyer C, Flament T, *Development of vitrification process and glass formulations for nuclear waste conditioning*, Waste Management '02, Tucson, AZ, USA (2002) 1-9.
- [Peuget 2006] Peuget S, Cachia JN, Jégou C, Deschanel X, Roudil D, Broudic V, Delaye JM, Bart JM, *Irradiation stability of R7T7-type borosilicate glass*, *J Nucl Mater* 354 (2006) 1-13.
- [Peuget 2007] Peuget S, Broudic V, Jégou C, Frugier P, Roudil D, Deschanel X, Rabiller H, Noel PY, *Effect of alpha radiation on the leaching behaviour of nuclear glass*, *J Nucl Mater* 362 (2007) 474-479.
- [Peuget 2014] Peuget S, Delaye JM, Jégou C, *Specific outcomes of the research on the radiation stability of the French nuclear glass towards alpha decay accumulation*, *J Nucl Mater* 444 (2014) 76-91.

- [Pierce 2008] Pierce EM, Rodriguez EA, Calligan LJ, Shaw WJ, McGrail BP, *An experimental study of the dissolution rates of simulated aluminoborosilicate waste glasses as a function of pH and temperature under dilute conditions*, Appl Geochem 223 (2008) 2559-2573.
- [Poinssot 2012] Poinssot C, Gin S, *Long-term behavior science: The cornerstone approach for reliably assessing the long-term performance of nuclear waste*, J Nucl Mater 420 (2012) 182-192
- [Putnis 2015] Putnis A, *Glass corrosion: Sharpened interface*, Nat Mater 14 (2015) 261-262.
- [Ribet 2004a] Ribet S, Gin S, *Role of neoformed phases on the mechanisms controlling the resumption of SON68 glass alteration in alkaline media*, J Nucl Mater 324 (2004) 152-164.
- [Ribet 2004b] Ribet I, Godon N, Gin S, Minet Y, Jollivet P, Frugier P, Vernaz E, Cavedon JM, Petitjean V, *The V_0 - V_r operational model for the long-term behavior of vitrified R7T7 waste packages*, Atalante 2004, June 21-25 2004, Nimes, France (2004) 1-8.
- [Ribet 2009] Ribet I, Bétrémieux S, Gin S, Angeli F, Jégou C, *Long-term behavior of vitrified waste packages*, Proceedings of Global 2009, September 6-11, Paris, France, Paper 9038 (2009) 1-8.
- [Rolland 2013] Rolland S, Tribet M, Jégou C, Broudic V, Magnin M, Peuket S, Wiss T, Janssen A, Blondel A, Toulhoat P, *^{99}Tc and ^{239}Pu doped glass leaching experiments: residual alteration rate and radionuclide behavior*, Int J Appl Glass Sci 4 (2013) 295-306.
- [Sales 1988] Sales BC, Boatner LA, *Lead-iron phosphate glass*, in: Lutze W, Ewing RC (eds) *Radioactive waste forms for the future*, North-Holland, Amsterdam (1988) 193-231.
- [Seetharam 2015] Seetharam S, Jacques D, *Potential degradation processes of the cementitious EBS components, their potential implications on safety functions and conceptual models for quantitative assessment*, OPERA-PU-SCK514 (2015) 1-90.
- [Sené 1999] Sené MR, Bailey M, Illerhaus B, Goebbels J, Haase O, Kulish A, Godon N, Choucan JL, *Characterisation of accessible surface area of HLW glass monoliths by high energy accelerator tomography and comparison with conventional techniques*, Contract No FI4W-CT96-0023 Final report EUR19119EN (1999) 1-61.
- [Smart 2004] Smart NR, Blackwood DJ, Marsh GP, Naish CC, O'Brien TM, Rance AP, Thomas MI, *The anaerobic corrosion of carbon and stainless steels in simulated cementitious repository environments: A summary review of Nirex research*, Report AEAT/ERRA-0313 (2004) 1-87.
- [Smith 2009] Smith P, Cornélis B, Capoeut M, Van Geet M, *The long-term safety strategy for the geological disposal of radioactive waste*, NIROND-TR-2009-12E (2009) 1-52.
- [Stefanovsky 1995] Stefanovsky SV, Ivanov IA, Gulín AN, *Aluminophosphate glasses with high sulfate content*, Mat Res Soc Symp Proc 353 (1995) 101-106.
- [Stefanovsky 2004] Stefanovsky SV, Yudinsev SV, Gieré R, Lumpkin GR, *Nuclear waste forms*, in: Gieré R, Stille P (eds) *Energy, Waste, and the Environment: A Geochemical Perspective*, Special Publications, 236, Geological Society, London (2004) 37-63.
- [Strachan 2001] Strachan DM, *Glass dissolution: Testing and modeling for long-term behaviour*, J Nucl Mater 298 (2001) 69-77.
- [Suyama 2012] Suyama T, Tachi Y, *Development of sorption database (JAEA-SDB): Update of sorption data including soil and cement systems*, JAEA-Data/Code 2011-022 (2012) 1-35.
- [Thoenen 2014] Thoenen T, Hummel W, Berner U, Curti E, *The PSI/Nagra Chemical Thermodynamic Database 12/07*, NAGRA Working Report NAB 14-49 (2014) 1-372.
- [Tits 2006] Tits J, Iijima K, Wieland E, Kamei G, *The uptake of radium by calcium silicate hydrates and hardened cement paste*, Radiochim Acta 94 (2006) 637-643.
- [TKSG 1997] Tweede Kamer der Staten-Generaal, *Opwerking van radioactief materiaal*, Kamerstuk 25 422, nr. 1, vergaderjaar 1996-1997 (1997) 1-14.
- [Utton 2011] Utton CA, Hand RJ, Hyatt NC, Swanton SW, *Glass durability in high pH environments: A review of the literature*, SERCO/TAS/003133/001 (2011) 1-62.

- [Utton 2012] Utton CA, Swanton SW, Schofield J, Hand RJ, Clacher A, Hyatt NC, *Chemical durability of vitrified wasteforms: effects of pH and solution composition*, *Min Mag* 76 (2012) 2919-2930.
- [Utton 2013] Utton CA, Hand RJ, Bingham PA, Hyatt NC, Swanton SW, Williams SJ, *Dissolution of vitrified wastes in a high-pH calcium-rich solution*, *J Nucl Mat* 435 (2013) 112-122.
- [van Humbeeck 2007] van Humbeeck H, de Bock C, Bastiaens W, *Demonstrating the construction and backfilling feasibility of the supercontainer design for HLW*, *Proceedings RepoSafe, International Conference on Radioactive Waste Disposal in Geological Formations, Braunschweig November 6 - 9 2007* (2007) 336-345.
- [Valcke 2006a] Valcke E, Smets S, Labat S, Lemmens K, van Iseghem P, Thomas P, Godon N, Jollivet P, Parisot G, Mestre JP, Jockwer N, Wieczorek K, Pozo C, *CORALUS: An integrated in situ corrosion test on a-active HLW glass*, *Mat Res Soc Symp Proc* 932 (2006) 67-78.
- [Valcke 2006b] Valcke E, Gysemans M, Moors H, van Iseghem P, Godon N, Jollivet P, *Leaching and migration of Np, Pu, and Am from a-doped SON68 HLW glass in contact with dense clay*, *Mat Res Soc Symp Proc* 932 (2006) 999-1006.
- [van Iseghem 2006] van Iseghem P, Lemmens K, Aertsens M, Gin S, Ribet I, Grambow B, Crovisier JL, Del Nero M, Curti E, Schwyn B, Luckscheiter B, McMenamin T, *Chemical durability of high-level waste glass in repository environment: main conclusions and remaining uncertainties from the GLASTAB and GLAMOR projects*, *Mat Res Soc Symp Proc* 932 (2006) 293-304.
- [van Iseghem 2007] van Iseghem P, Aertsens M, Gin S, Deneele D, Grambow B, McGrail P, Strachan D, Wicks G, *A critical evaluation of the dissolution mechanisms of high-level waste glasses in conditions of relevance for geological disposal (GLAMOR)*, *Contract No FIKW-CT-2001-00140, Final report EUR 23097* (2007) 1-160.
- [van Iseghem 2012] van Iseghem P, *Corrosion issues of radioactive waste packages in geological disposal systems*, in: Feron D (ed) *Nuclear corrosion science and engineering*, Woodhead Publishing (2012) 939-987.
- [Verhoef 2011a] Verhoef E, Neeft E, Grupa J, Poley A, *Outline of a disposal concept in clay OPERA-PG-COV008* (2011), 1-17.
- [Verhoef 2011b] Verhoef EV, Schröder T, *Research plan*, OPERA-PG-COV004 (2011) 1-24.
- [Verhoef, 2014a] Verhoef EV, Neeft EAC, Grupa JB, Poley AD, *Outline of a disposal concept in clay*, OPERA-PG-COV008_rev1 (2014) 1-18.
- [Verhoef 2014b] Verhoef EV, de Bruin AMG, Wiegers RB, Deissmann G, *Cementitious materials in OPERA disposal concept in Boom Clay*, OPERA-PG-COV020 (2014) 1-17.
- [Verhoef 2016] Verhoef EV, Neeft EAC, Deissmann G, Filby A, Wiegers RB, Kers DA, *Waste families in OPERA*, OPERA-PG-COV023 (2016) 1-39.
- [Vernaz 2001] Vernaz E, Gin S, Jégou C, Ribet I, *Present understanding of R7T7 glass alteration kinetics and their impact on long term behaviour modelling*, *J Nucl Mater* 298 (2001) 27-36.
- [Vernaz 2012] Vernaz E, Gin S, Veyer C, *Waste glass*, in: Konings RJM (ed) *Comprehensive Nuclear Materials, Volume 5: Material Performance and Corrosion/Waste Materials*, Elsevier (2012) 451-483.
- [Verney-Carron 2008] Verney-Carron A, Gin S, Libourel G, *A fractured roman glass block altered for 1800 years in seawater: analogy with nuclear waste glass in a deep geological repository*, *Geochim Cosmochim Acta* 72 (2008) 5372-5385.
- [Verney-Carron 2010] Verney-Carron A, Gin S, Libourel G, *Archaeological analogs and the future of nuclear waste glass*, *J Nucl Mater* 406 (2010) 365-370.
- [Vienna 2013] Vienna JD, Ryan JV, Gin S, Inagaki Y, *Current understanding and remaining challenges in modeling long-term degradation of borosilicate nuclear waste glasses*, *Int J Appl Glass Sci* 4 (2013) 283-294.
- [Wang 2009a] Wang L, *Near-field chemistry of a HLW/SF repository in Boom Clay - scoping calculations relevant to the supercontainer design*, *External Report SCK•CEN ER-17* (2009) 1-53.
- [Wang 2009b] Wang L, Martens E, Jacques D, de Cannière P, Berry J, Mallants D, *Review of sorption values for the cementitious near field of a near surface radioactive waste disposal facility*, *NIROND-TR 2008-23 E* (2009) 1-419.

- [Wang 2013a] Wang L, *Solubility of radionuclides in Supercontainer concrete*, External Report SCK•CEN ER-239 (2013) 1-43.
- [Wang 2013b] Wang L, Ochs M, Mallants D, Vielle-Petit L, Martens E, Jacques D, de Cannière P, Berry JA, Leterme B, *A new radionuclide sorption data base for benchmark cement accounting for geochemical evolution of cement*, in: Bart F, Cau-dit-Coumes C, Frizon F, Lorente S (eds) *Cement-based materials for nuclear waste storage*, Springer (2013) 103-112.
- [Weber 1997] Weber WJ, Ewing RC, Angell CA, Arnold GW, Cormack AN, Delaye JM, Griscom DL, Hobbs LW, Navrotsky A, Price DL, Stoneham AM, Weinberg MC, *Radiation effects in glasses used for immobilization of high-level waste and plutonium disposition*, *J Mater Res* 12 (1997) 1946-1978.
- [Weber 2009] Weber WJ, Navrotsky A, Stefanovsky S, Vance ER, Vernaz E, *Materials science of high-level nuclear waste immobilization*, *Mat Res Soc Bull* 34 (2009) 46-53.
- [Weber 2014] Weber WJ, *Radiation and thermal ageing of nuclear waste glass*, *Proc Mat Sci* 7 (2014) 237-246.
- [Wellmann 2005] Wellman DM, Icenhower JP, Weber WJ, *Elemental dissolution study of Pu-bearing borosilicate glasses*, *J Nucl Mater* 340 (2005) 149-162.
- [Wersin 2003] Wersin P, Johnson LH, Schwyn B, Berner U, Curti E, *Redox conditions in the near field of a repository for SF/HLW and ILW in Opalinus Clay*, NAGRA Technical Report NTB 02-13 (2003) 1-38.
- [Wersin 2004] Wersin P, Schwyn B, *Project Opalinus Clay: Integrated Approach for the development of geochemical databases used for safety assessment*, NAGRA Technical Report NTB 03-06 (2004) 1-71.
- [Wickham 2008] Wickham S, *Evolution of the near-field of the ONDRAF/NIRAS repository concept for category B and C wastes*, NIRONDR TR-2007-07 E (2008) 1-140.
- [Wieland 2001] Wieland E, *Experimental studies on the inventory of cement-derived colloids in the pore water of a cementitious backfill material*, NAGRA Technical Report NTB 01-02 (2001) 1-104.
- [Wieland 2002] Wieland E, Van Loon LR, *Cementitious near-field sorption data base for performance assessment of an ILW repository in Opalinus Clay*, NAGRA Technical Report NTB 02-20 (2002) 1-87.
- [Wieland 2014] Wieland E, *Sorption data base for the cementitious near field of L/ILW and ILW repositories for provisional safety analyses for SGT-E2*, NAGRA Technical Report NTB 14-08 (2014) 1-104.
- [WNA 2016a] World Nuclear Association, *Reactor Database - Borssele*, <http://www.world-nuclear.org/reactor/default.aspx/BORSSELE>, accessed on 01.03.2016.
- [WNA 2016b] World Nuclear Association, *Reactor Database - Dodewaard*, <http://www.world-nuclear.org/reactor/default.aspx/DODEWAARD>, accessed on 01.03.2016.
- [WNN 2011] http://www.world-nuclear-news.org/IT-Approval_for_MOX_use_at_Borssele-0607114.html, 06.07.2011, accessed on 01.03.2016.
- [Wolf 1996] Wolf JM, *Eurochemic (1956-1990) Thirty-five years of international co-operation in the field of nuclear engineering: The chemical processing of irradiated fuels and the management of radioactive wastes*, OECD-NEA, Paris (1996) 1-627.
- [Wolff-Boenisch 2004] Wolff-Boenisch D, Gislason SR, Oelkers EH, Putnis CV, *The dissolution rates of natural glasses as a function of their composition at pH 4 and 10.6, and temperatures from 25 to 74 °C*, *Geochim Cosmochim Acta* 68 (2004) 4843-4858.
- [Wronkiewicz 1993] Wronkiewicz DJ, *Effects of radionuclide decay on waste glass behavior - A critical review*, Argonne National Laboratory ANL-93/45 (1993) 1-64.
- [Wronkiewicz 1994] Wronkiewicz DJ, *Radionuclide decay effects on waste glass corrosion*, *Mat Res Soc Symp Proc* 333 (1994) 83-97.

Appendix 1

Table A-1 Activity per COGEMA canister filled with reprocessing wastes after 130 years decay time [Verhoef 2016]

Radionuclide	CSD-V Activity [Bq]	CSD-C Activity [Bq]	Radionuclide	CSD-V Activity [Bq]	CSD-C Activity [Bq]
Ac-226			Np-237	4.80E+10	7.80E+06
Ac-227	6.07E+02	< 1	Pa-231		
Ag-108m		1.63E+03	Pa-233		
Am-241	1.06E+14	5.33E+10	Pa-234		
Am-242m	1.56E+12	1.56E+08	Pb-202		
Am-243	2.57E+12	5.93E+08	Pb-210		
Ba-133			Pb-214		
Be-10			Pd-107	6.78E+09	6.74E+06
Bi-207			Pm-145		
Bi-214			Po-209		
C-14		1.38E+10	Pu-238	4.78E+11	1.20E+12
Ca-41		2.95E+06	Pu-239	1.44E+11	2.14E+11
Cd-113m			Pu-240	2.31E+11	3.68E+11
Cf-249		3.27E+03	Pu-241	7.35E+10	1.41E+11
Cf-251		< 1	Pu-242	1.01E+09	2.09E+09
Cf-252			Pu-244	4.91E+05	4.91E+01
Cl-36		6.31E-04	Ra-226	1.03E+02	1.03E-02
Cm-241			Re-186		
Cm-243	1.27E+11	1.27E+07	Sb-125		
Cm-244	2.21E+12	1.38E+10	Se-79	2.01E+10	5.50E+07
Cm-245	2.90E+09	1.09E+07	Si-32		
Cm-246	4.77E+10	4.77E+06	Sm-146		
Cm-247	2.63E+05	2.63E+01	Sm-151	5.47E+13	5.38E+11
Cm-248	1.62E+06	1.62E+02	Sn-121m		
Co-60			Sn-126	3.80E+10	8.83E+07
Cs-135	3.01E+10	1.04E+09	Sr-90	2.05E+14	2.76E+12
Cs-137	3.30E+14	3.25E+12	Tc-99	1.25E+12	9.17E+09
Eu-152		3.87E+06	Tc-99m		
Eu-152m			Th-229	1.17E+04	1.17E+00
H-3		9.96E+09	Th-230	1.68E+05	1.68E+01
Ho-166m			Th-231		
I-129		5.30E+07	Th-234		
K-40			Ti-44		
Kr-81			U-232	2.95E+09	2.95E+05
Kr-85		< 1	U-233	3.20E+06	3.20E+02
Mo-93		5.79E+09	U-234	4.77E+08	3.06E+06
Mo-99			U-235	2.88E+06	1.25E+06
Nb-93m			U-236	4.21E+07	1.21E+07
Nb-94		5.55E+10	U-238	5.53E+07	1.88E+07
Ni-59		3.59E+11	U-239		
Ni-63		1.76E+13	Zr-93	1.05E+11	8.91E+09

Table A-2 Inventory of radionuclides relevant for the long-term safety in vitrified HLW (CSD-V) originating from the reprocessing of spent nuclear fuel in the year 2130 [Hart 2014]

Radionuclide	Half-Life [years]	Activity [Bq]
Se-79	3.77E+05	2.92E+12
Sr-90	2.88E+01	1.76E+17
Zr-93	1.53E+06	6.59E+13
Tc-99	2.14E+05	7.83E+14
Pd-107	6.50E+06	4.24E+12
Sn-126	2.30E+05	2.37E+13
I-129	1.61E+07	1.62E+11
Cs-135	2.30E+06	1.88E+13
Cs-137	3.00E+01	2.82E+17
Pa-231	3.28E+04	1.01E+06
Np-237	2.14E+06	1.48E+13
U-234	2.46E+05	5.20E+10
U-235	7.04E+08	4.08E+08
U-236	2.37E+07	6.55E+09
U-238	4.47E+09	7.18E+09
Pu-238	8.77E+01	5.24E+13
Pu-239	2.41E+04	1.25E+13
Pu-240	6.56E+03	3.18E+14
Pu-241	1.43E+01	1.36E+13
Pu-242	3.74E+05	9.64E+10
Th-230	7.54E+04	3.19E+07
Th-232	1.41E+10	3.52E+01
Am-241	4.33E+02	5.84E+16
Am-243	7.36E+03	1.07E+15
Cm-244	1.80E+01	1.32E+15
Cm-245	8.50E+03	1.26E+13

Appendix 2

Table A-3 Predicted composition of cementitious pore waters in a repository in Opalinus Clay and reference Opalinus Clay pore water ([Berner 2003], [Wersin 2004]) - concentrations in mmol L⁻¹

	Initial stage water (Stage 1)	Reference water (Stage 2)	Opalinus Clay porewater
pH	13.44	12.55	7.24
E _H	-430 mV	-750 ... -230 mV	-167 mV
Na	101	169	169
K	303	5.7	5.65
Ca	0.84	20.1	10.5
Mg	<10 ⁻⁴	10 ⁻⁴	7.48
Al	0.01	0.005	<0.001
Si	0.05	0.016	0.178
CO ₃	0.204	0.01	2.7
SO ₄	0.75	0.10	24
Cl	-	160	160

Table A-4 Predicted composition of cementitious pore waters in an ILW repository in Opalinus Clay (after 10,000 years exchange with Opalinus Clay) [Berner 2014] and reference Opalinus Clay pore water used in the modelling study [Kosakowski 2013] - concentrations in mol kg⁻¹

	Concrete pore water (Stage 2)	Opalinus Clay pore water
pH	12.54	7.26
E _H	-498 mV	-168.5 mV
Na	4.228·10 ⁻²	1.646·10 ⁻¹
K	3.310·10 ⁻³	2.594·10 ⁻³
Ca	1.806·10 ⁻²	1.247·10 ⁻²
Mg	1.107·10 ⁻⁸	9.591·10 ⁻³
Al	6.912·10 ⁻⁶	1.750·10 ⁻⁸
Si	3.432·10 ⁻⁵	1.802·10 ⁻⁴
CO ₃	8.064·10 ⁻⁶	2.172·10 ⁻³
SO ₄	4.711·10 ⁻⁵	2.479·10 ⁻²
Cl	3.752·10 ⁻²	1.602·10 ⁻¹

Appendix 3

Table A-5 Database on nuclear waste glass dissolution rates under alkaline conditions

Glass type	Test method	Sample	Leachant	Duration [d]	Temperature [°C]	pH initial [-]	pH final [-]	Element	Dissolution rate [g m ⁻² d ⁻¹]	Reference	Comment
SON68	static	M	KOH		90	7		B	0.36	[Advocat 1991a]	initial rate
SON68	static	M	KOH		90	8		B	0.78	[Advocat 1991a]	initial rate
SON68	static	M	KOH		90	9		B	2.77	[Advocat 1991a]	initial rate
SON68	static	M	KOH	0.25	90	10		B	3.8	[Advocat 1991a]	initial rate
SON68	static	M	KH ₂ PO ₄	22	90	4.8		Si	0.08	[Advocat 1991a]	initial rate
SON68	static	M	KH ₂ PO ₄		90	5.5		Si	0.17	[Advocat 1991a]	initial rate
SON68	static	M	KOH		90	7		Si	0.36	[Advocat 1991a]	initial rate
SON68	static	M	KOH		90	8		Si	0.78	[Advocat 1991a]	initial rate
SON68	static	M	KOH		90	9		Si	2.77	[Advocat 1991a]	initial rate
SON68	static	M	KOH	0.25	90	10		Si	3.8	[Advocat 1991a]	initial rate
R7T7	static	M	mortar equil. water	7	90		12.3	Li	0.19	[Andriambololona 1992]	0 ... 7 d
R7T7	static	M	mortar equil. water	7	90		12.3	Li	0.19	[Andriambololona 1992]	0 ... 7 d
R7T7	static	M	mortar equil. water	7	90		12.3	Li	0.30	[Andriambololona 1992]	0 ... 7 d
R7T7	static	M	mortar equil. water	7	90		12.3	Li	0.10	[Andriambololona 1992]	0 ... 7 d
R7T7	static	M	KOH-NaOH-Ca(OH) ₂	7	90	12.5	12.8	Li	0.09	[Andriambololona 1992]	0 ... 7 d
R7T7	static	M	volvic water	7	90	7.2	8.5	Li	0.30	[Andriambololona 1992]	0 ... 7 d
R7T7	static	M	mortar equil. water	91	90		10.4	Li	0.62	[Andriambololona 1992]	56 ... 91 d
R7T7	static	M	mortar equil. water	91	90		9	Li	0.31	[Andriambololona 1992]	56 ... 91 d
R7T7	static	M	mortar equil. water	91	90		9.5	Li	0.20	[Andriambololona 1992]	56 ... 91 d
R7T7	static	M	mortar equil. water	91	90		10.7	Li	0.10	[Andriambololona 1992]	56 ... 91 d
R7T7	static	M	KOH-NaOH-Ca(OH) ₂	91	90	12.5	12.6	Li	0.72	[Andriambololona 1992]	56 ... 91 d
R7T7	static	M	volvic water	91	90	7.2	9.1	Li	0.02	[Andriambololona 1992]	56 ... 91 d
SON68	static	P	KOH		90	7		B	0.9	[Gin 2001]	initial rate
SON68	static	P	KOH		90	8		B	1.8	[Gin 2001]	initial rate
SON68	static	P	KOH		90	9.1		B	4.7	[Gin 2001]	initial rate
SON68	static	P	KOH		90	9.5		B	5	[Gin 2001]	initial rate
SON68	static	P	KOH		90	10		B	10.4	[Gin 2001]	initial rate
SON68	static	P	KOH		90	10.5		B	16.4	[Gin 2001]	initial rate
SON68	static	P	KOH		90	11		B	24.1	[Gin 2001]	initial rate
SON68	static	P	KOH		90	11.5		B	42	[Gin 2001]	initial rate
SON68	dynamic	P	KOH	9h	30	9	9	Si	0.01	[Ferrand 2008]	initial rate
SON68	dynamic	P	KOH	9h	30	11.5	11.5	Si	0.07	[Ferrand 2008]	initial rate
SON68	dynamic	P	KOH	9h	30	13	13	Si	0.17	[Ferrand 2008]	initial rate
SON68	dynamic	P	KOH	9h	30	14	14	Si	0.35	[Ferrand 2008]	initial rate
SON68	dynamic	P	KOH	9h	30	13	13	Si	0.17	[Ferrand 2012]	initial rate

Glass type	Test method	Sample	Leachant	Duration	Temperature	pH initial	pH final	Element	Dissolution rate	Reference	Comment
				[d]	[°C]	[-]	[-]		[g m ⁻² d ⁻¹]		
SON68	dynamic	P	KOH	9h	30	14	14	Si	0.35	[Ferrand 2012]	initial rate
SON68	dynamic	P	YCW	9h	30	13.5	13.5	Si	0.03	[Ferrand 2012]	initial rate
SON68	static	P	YCW + cement	556	30	13.5	13.3	ML	0.025 ... 0.082	[Ferrand 2012]	close to initial rate
SON68	static	P	YCW		30	13.5		B	0.0064	[Ferrand 2012]	initial rate
SON68	static	P	YCW		30	13.5		B	0.0049	[Ferrand 2012]	final rate
SON68	static	P	YCW	713	30	13.5		Li	0.006	[Ferrand 2013b]	similar to long-term
SON68	static	P	YCW + cement	713	30	13.5		Li	0.007	[Ferrand 2013b]	similar to long-term
SON68	static	M	YCW + cement	713	30	13.5		ML	0.005	[Ferrand 2013b, 2014]	similar to long-term
SON68	static	M	YCW + cement	713	30	13.5		ML	0.012	[Ferrand 2013b, 2014]	initial rate
SON68	static	M	YCW + cement	713	30	13.5		ML	0.04	[Ferrand 2013b, 2014]	initial rate
SON68	dynamic	P	YCW		30	13.5			0.061	[Ferrand 2013b, 2014]	maximum rate
SON68	static	M	YCW + cement	713	30	13.5	14	ML	0.25 ... 0.082	[Ferrand 2013a]	maximum rate
SON 68	dynamic	P	KOH		30	9	9	Si	0.013	[Ferrand 2013a]	forward/initial rate
SON 68	dynamic	P	KOH		30	11.5	11.5	Si	0.069	[Ferrand 2013a]	forward/initial rate
SON 68	dynamic	P	KOH		30		12.5	Si	0.13	[Ferrand 2013a]	forward/initial rate
SON 68	dynamic	P	KOH		30	13.1	13.1	Si	0.17	[Ferrand 2013a]	forward/initial rate
SON 68	dynamic	P	KOH		30		13.5	Si	0.23	[Ferrand 2013a]	forward/initial rate
SON 68	dynamic	P	KOH		30	14.3	14.3	Si	0.35	[Ferrand 2013a]	forward/initial rate
SON 68	dynamic	P	YCW		30	13.5	13.5	Si	0.042 ... 0.079	[Ferrand 2013a]	forward/initial rate
SON 68	dynamic	P	ECW		30	12.5	12.5	Si	>0.0037	[Ferrand 2013a]	forward/initial rate
SON 68	static	P	YCW	313	30	13.5	13.5	B	0.065	[Ferrand 2013a]	initial rate
SON 68	static	P	YCW	313	30	13.5	13.5	B	0.0085	[Ferrand 2013a]	long-term rate
SON 68	static	P	ECW	313	30	12.5	12.5	B	0.0048	[Ferrand 2013a]	initial rate
SON 68	static	P	ECW	313	30	12.5	12.5	B	0.0021	[Ferrand 2013a]	long-term rate
SON 68	static	P	OCW	313	30	11.3	11.3	B	0.0057	[Ferrand 2013a]	initial rate
SON 68	static	P	OCW	313	30	11.3	11.3	B	0.0014 ... 0.0006	[Ferrand 2013a]	long-term rate
SON 68	static	P	OCW	313	30	11.3	11.3	B	0.002	[Ferrand 2013a]	initial rate
SON 68	static	P	OCW	313	30	11.3	11.3	B	0.00005	[Ferrand 2013a]	long-term rate
SON 68	static	P	YCW	313	70	13.5	13.5	B	0.1	[Ferrand 2013a]	initial rate
SON 68	static	P	YCW	313	70	13.5	13.5	B	0.025	[Ferrand 2013a]	long-term rate
SON 68	static	P	YCW	313	70	13.5	13.5	B	0.059 ... 0.09	[Ferrand 2013a]	initial rate
SON 68	static	P	ECW	313	70	12.5	12.5	B	0.011	[Ferrand 2013a]	initial rate
SON 68	static	P	ECW	313	70	12.5	12.5	B	0.0052	[Ferrand 2013a]	long-term rate
SON 68	static	P	OCW	313	70	11.3	11.3	B	0.0041	[Ferrand 2013a]	initial rate

Glass type	Test method	Sample	Leachant	Duration	Temperature	pH initial	pH final	Element	Dissolution rate	Reference	Comment
				[d]	[°C]	[-]	[-]		[g m ⁻² d ⁻¹]		
SON 68	static	P	OCW	313	70	11.3	11.3	B	0.00018	[Ferrand 2013a]	long-term rate
SON 68	static	P	OCW	313	70	11.3	11.3	B	0.0056	[Ferrand 2013a]	initial rate
SON 68	static	P	OCW	313	70	11.3	11.3	B	0.0009	[Ferrand 2013a]	long-term rate
SON 68	static	M	YCW + cement	713	30		13.5	ML	0.025 ... 0.065	[Ferrand 2013a]	short term rate
SON 68	static	M	YCW + cement	713	30		13.5	ML	0.022 ... 0.80	[Ferrand 2013a]	short term rate
SON 68	static	M	YCW + cement	713	30		13.5	ML	0.0032 ... 0.0084	[Ferrand 2013a]	long-term rate
R7T7 / SON 68	static	P	DIW	12 a	90	8.9	8.9	B	1.30E-04	[Curti 2006]	>500 d
MW	static	P	DIW	12 a	90	9.1	9.1	B	9.60E-04	[Curti 2006]	>500 d
MW (simulant)	static	P	KOH	st	18	6.8		B	0.002	[Abraitis 2000a]	initial rate
MW (simulant)	static	P	KOH	st	18	7.8		B	0.001	[Abraitis 2000a]	initial rate
MW (simulant)	static	P	KOH	st	18	8.6		B	0.004	[Abraitis 2000a]	initial rate
MW (simulant)	static	P	KOH	st	18	9.9		B	0.012	[Abraitis 2000a]	initial rate
MW (simulant)	static	P	KOH	st	18	6.8		Si	0.001	[Abraitis 2000a]	initial rate
MW (simulant)	static	P	KOH	st	18	7.8		Si	0.001	[Abraitis 2000a]	initial rate
MW (simulant)	static	P	KOH	st	18	8.6		Si	0.003	[Abraitis 2000a]	initial rate
MW (simulant)	static	P	KOH	st	18	9.9		Si	0.009	[Abraitis 2000a]	initial rate
MW (simulant)	static	P	KOH	28	18	6.80		B	4.53E-05	[Abraitis 2000a]	3 ... 7 d
MW (simulant)	static	P	KOH	28	18	7.80		B	6.50E-05	[Abraitis 2000a]	3 ... 7 d
MW (simulant)	static	P	KOH	28	18	8.60		B	2.76E-04	[Abraitis 2000a]	3 ... 7 d
MW (simulant)	static	P	KOH	28	18	9.90		B	9.33E-04	[Abraitis 2000a]	3 ... 7 d
MW (simulant)	static	P	KOH	28	18	6.80		Si	1.92E-04	[Abraitis 2000a]	3 ... 7 d
MW (simulant)	static	P	KOH	28	18	7.80		Si	1.23E-04	[Abraitis 2000a]	3 ... 7 d
MW (simulant)	static	P	KOH	28	18	8.60		Si	3.62E-04	[Abraitis 2000a]	3 ... 7 d
MW (simulant)	static	P	KOH	28	18	9.90		Si	9.33E-04	[Abraitis 2000a]	3 ... 7 d
MW (simulant)	static	M	KOH	28	60	7.17		B	0.005	[Abraitis 2000a]	3 ... 7 d
MW (simulant)	static	M	KOH	28	60	8.18		B	0.026	[Abraitis 2000a]	3 ... 7 d
MW (simulant)	static	M	KOH	28	60	9.34		B	0.067	[Abraitis 2000a]	3 ... 7 d
MW (simulant)	static	M	KOH	28	60	11.02		B	0.174	[Abraitis 2000a]	3 ... 7 d
MW (simulant)	static	M	KOH	28	60	7.13		Si	0.020	[Abraitis 2000a]	3 ... 7 d
MW (simulant)	static	M	KOH	28	60	8.18		Si	0.025	[Abraitis 2000a]	3 ... 7 d
MW (simulant)	static	M	KOH	28	60	9.32		Si	0.084	[Abraitis 2000a]	3 ... 7 d
MW (simulant)	static	M	KOH	28	60	11.03		Si	0.256	[Abraitis 2000a]	3 ... 7 d
MW (simulant)	static	M	KOH	28	90	6.56		B	0.025	[Abraitis 2000a]	3 ... 7 d

Glass type	Test method	Sample	Leachant	Duration [d]	Temperature [°C]	pH initial [-]	pH final [-]	Element	Dissolution rate [g m ⁻² d ⁻¹]	Reference	Comment
MW (simulant)	static	M	KOH	28	90	7.53		B	0.045	[Abraitis 2000a]	3 ... 7 d
MW (simulant)	static	M	KOH	28	90	9.32		B	0.303	[Abraitis 2000a]	3 ... 7 d
MW (simulant)	static	M	KOH	28	90	6.58		Si	0.066	[Abraitis 2000a]	3 ... 7 d
MW (simulant)	static	M	KOH	28	90	7.53		Si	0.060	[Abraitis 2000a]	3 ... 7 d
MW (simulant)	static	M	KOH	28	90	9.34		Si	0.297	[Abraitis 2000a]	3 ... 7 d
MW (simulant)	SPFT	P	KOH/KCl	19	40	9.8	9.7	B	0.033 ... 0.170	[Abraitis 2000b]	initial / intermediate
MW (simulant)	SPFT	P	KOH/KCl + Al	12 ... 15	40		9.2	B	0.082 ... 0.223	[Abraitis 2000c]	initial / intermediate
MW (simulant)	SPFT	P	KOH/KCl + Si	12 ... 15	40		9.6	B	0.065 ... 0.104	[Abraitis 2000c]	initial / intermediate
MW (simulant)	SPFT	P	KOH/KCl + EDTA	12 ... 15	40		9.9	B	0.156 ... 0.235	[Abraitis 2000c]	initial / intermediate
MW (simulant)	static	P	NaOH	89	40	12	10.75	B	0.156	[Utton 2012]	initial rate
MW (simulant)	static	P	NaOH	89	40	12	10.75	Li	0.126	[Utton 2012]	initial rate
MW (simulant)	static	P	Ca(OH) ₂	89	40	12.5	11.7	B	0.029	[Utton 2012]	initial rate
MW (simulant)	static	P	Ca(OH) ₂	89	40	12.5	11.7	Li	0.038	[Utton 2012]	initial rate
MW (simulant)	static	P	DIW	89	40	7	9.8	B	0.024	[Utton 2012]	initial rate
MW (simulant)	static	P	DIW	89	40	7	9.8	Li	0.03	[Utton 2012]	initial rate
MW (simulant 25%WL)	static	P	DIW	28	50	6.1	9.8	B	1.29E-04	[Corkhill 2013]	initial rate, 0 ... 28 d
MW (simulant 25%WL)	static	P	DIW	168	50	6.1	9.8	B	1.88E-05	[Corkhill 2013]	residual, 28 ... 168 d
MW (simulant 25%WL)	static	P	DIW	28	50	6.1	9.8	Li	2.16E-04	[Corkhill 2013]	initial rate, 0 ... 28 d
MW (simulant 25%WL)	static	P	DIW	168	50	6.1	9.8	Li	1.68E-04	[Corkhill 2013]	residual, 28 ... 168 d
MW (simulant 25%WL)	static	P	DIW	28	50	6.1	9.8	Si	3.32E-05	[Corkhill 2013]	initial rate, 0 ... 28 d
MW (simulant 25%WL)	static	P	DIW	168	50	6.1	9.8	Si	4.21E-07	[Corkhill 2013]	residual, 28 ... 168 d
MW (simulant 25%WL)	static	P	Ca(OH) ₂	28	50	12.7	11.6	B	5.92E-05	[Corkhill 2013]	initial rate, 0 ... 28 d
MW (simulant 25%WL)	static	P	Ca(OH) ₂	84	50	12.7	10.5	B	2.91E-05	[Corkhill 2013]	intermediate, 28 ... 84 d
MW (simulant 25%WL)	static	P	Ca(OH) ₂	168	50	12.7	10.5	B	1.37E-05	[Corkhill 2013]	residual, 84 ... 168 d
MW (simulant 25%WL)	static	P	Ca(OH) ₂	28	50	12.7	11.6	Li	9.32E-05	[Corkhill 2013]	initial rate, 0 ... 28 d
MW (simulant 25%WL)	static	P	Ca(OH) ₂	84	50	12.7	10.5	Li	4.50E-05	[Corkhill 2013]	intermediate, 28 ... 84 d
MW (simulant 25%WL)	static	P	Ca(OH) ₂	168	50	12.7	10.5	Li	1.71E-05	[Corkhill 2013]	residual, 84 ... 168 d
MW (simulant 25%WL)	static	P	Ca(OH) ₂	28	50	12.7	11.6	Si	3.32E-07	[Corkhill 2013]	initial rate, 0 ... 28 d
MW (simulant 25%WL)	static	P	Ca(OH) ₂	84	50	12.7	10.5	Si	7.31E-06	[Corkhill 2013]	intermediate, 28 ... 84 d
MW (simulant 25%WL)	static	P	Ca(OH) ₂	168	50	12.7	10.5	Si	4.47E-06	[Corkhill 2013]	residual, 84 ... 168 d
MW (simulant 25%WL)	static	M	Ca(OH) ₂	70	50	12.7	12.5	B	1.68E-04	[Corkhill 2013]	initial, 0 ... 70 d
MW (simulant 25%WL)	static	M	Ca(OH) ₂	168	50	12.7	12.5	B	5.44E-05	[Corkhill 2013]	intermediate, 70 ... 168 d
MW (simulant 25%WL)	static	M	Ca(OH) ₂	70	50	12.7	12.5	Li	3.53E-04	[Corkhill 2013]	initial, 0 ... 70 d

Glass type	Test method	Sample	Leachant	Duration [d]	Temperature [°C]	pH initial [-]	pH final [-]	Element	Dissolution rate [g m ⁻² d ⁻¹]	Reference	Comment
MW (simulant 25%WL)	static	M	Ca(OH) ₂	168	50	12.7	12.5	Li	1.77E-04	[Corkhill 2013]	intermediate, 70 ... 168 d
MW (simulant 25%WL)	static	M	Ca(OH) ₂	70	50	12.7	12.5	Si	0.00E+00	[Corkhill 2013]	initial, 0 ... 70 d
MW (simulant 25%WL)	static	M	Ca(OH) ₂	168	50	12.7	12.5	Si	0.00E+00	[Corkhill 2013]	intermediate, 70 ... 168 d
MW-T blend (25%WL)	SPFT	P	THAM buffer		23	10	10	Si	0.027	[Cassingham 2015]	
MW-T blend (25%WL)	SPFT	P	THAM buffer		40	10	10	Si	0.321	[Cassingham 2015]	
MW-T blend (25%WL)	SPFT	P	THAM buffer		70	10	10	Si	4.148	[Cassingham 2015]	
MW-T blend (25%WL)	SPFT	P	LiOH + LiCl		23	12	12	Si	0.642	[Cassingham 2015]	
MW-T blend (25%WL)	SPFT	P	LiOH + LiCl		40	12	12	Si	4.403	[Cassingham 2015]	
MW-T blend (25%WL)	SPFT	P	LiOH + LiCl		70	12	12	Si	45.786	[Cassingham 2015]	
MW-T blend (25%WL)	SPFT	P	THAM buffer		23	10	10	B	0.027	[Cassingham 2015]	
MW-T blend (25%WL)	SPFT	P	THAM buffer		40	10	10	B	0.106	[Cassingham 2015]	
MW-T blend (25%WL)	SPFT	P	THAM buffer		70	10	10	B	2.548	[Cassingham 2015]	
MW-T blend (25%WL)	SPFT	P	LiOH + LiCl		23	12	12	B	0.489	[Cassingham 2015]	
MW-T blend (25%WL)	SPFT	P	LiOH + LiCl		40	12	12	B	2.160	[Cassingham 2015]	
MW-T blend (25%WL)	SPFT	P	LiOH + LiCl		70	12	12	B	12.059	[Cassingham 2015]	
MW-T blend (25%WL)	SPFT	P	THAM buffer		23	10	10	Na	0.010	[Cassingham 2015]	
MW-T blend (25%WL)	SPFT	P	THAM buffer		40	10	10	Na	0.225	[Cassingham 2015]	
MW-T blend (25%WL)	SPFT	P	THAM buffer		70	10	10	Na	4.827	[Cassingham 2015]	
MW-T blend (25%WL)	SPFT	P	LiOH + LiCl		23	12	12	Na	1.963	[Cassingham 2015]	
MW-T blend (25%WL)	SPFT	P	LiOH + LiCl		40	12	12	Na	6.827	[Cassingham 2015]	
MW-T blend (25%WL)	SPFT	P	LiOH + LiCl		70	12	12	Na	33.049	[Cassingham 2015]	
MW-T blend (30%WL)	SPFT	P	THAM buffer		23	10	10	Si	0.024	[Cassingham 2015]	
MW-T blend (30%WL)	SPFT	P	THAM buffer		40	10	10	Si	0.436	[Cassingham 2015]	
MW-T blend (30%WL)	SPFT	P	THAM buffer		70	10	10	Si	6.038	[Cassingham 2015]	
MW-T blend (30%WL)	SPFT	P	LiOH + LiCl		23	12	12	Si	0.778	[Cassingham 2015]	
MW-T blend (30%WL)	SPFT	P	LiOH + LiCl		40	12	12	Si	7.638	[Cassingham 2015]	
MW-T blend (30%WL)	SPFT	P	LiOH + LiCl		70	12	12	Si	61.292	[Cassingham 2015]	
MW-T blend (30%WL)	SPFT	P	THAM buffer		23	10	10	B	0.024	[Cassingham 2015]	
MW-T blend (30%WL)	SPFT	P	THAM buffer		40	10	10	B	0.189	[Cassingham 2015]	
MW-T blend (30%WL)	SPFT	P	THAM buffer		70	10	10	B	1.570	[Cassingham 2015]	
MW-T blend (30%WL)	SPFT	P	LiOH + LiCl		23	12	12	B	0.536	[Cassingham 2015]	
MW-T blend (30%WL)	SPFT	P	LiOH + LiCl		40	12	12	B	2.643	[Cassingham 2015]	
MW-T blend (30%WL)	SPFT	P	LiOH + LiCl		70	12	12	B	4.915	[Cassingham 2015]	

Glass type	Test method	Sample	Leachant	Duration [d]	Temperature [°C]	pH initial [-]	pH final [-]	Element	Dissolution rate [g m ⁻² d ⁻¹]	Reference	Comment
MW-T blend (30%WL)	SPFT	P	THAM buffer		23	10	10	Na	0.067	[Cassingham 2015]	
MW-T blend (30%WL)	SPFT	P	THAM buffer		40	10	10	Na	0.394	[Cassingham 2015]	
MW-T blend (30%WL)	SPFT	P	THAM buffer		70	10	10	Na	5.684	[Cassingham 2015]	
MW-T blend (30%WL)	SPFT	P	LiOH + LiCl		23	12	12	Na	0.899	[Cassingham 2015]	
MW-T blend (30%WL)	SPFT	P	LiOH + LiCl		40	12	12	Na	3.146	[Cassingham 2015]	
MW-T blend (30%WL)	SPFT	P	LiOH + LiCl		70	12	12	Na	18.763	[Cassingham 2015]	
CSD-B	static	P	KOH	h ... d	30	12.4	12.4	Si	0.290	[Depierre 2013]	initial rate
CSD-B	static	P	KOH	h ... d	50	11.7	11.7	Si	0.742	[Depierre 2013]	initial rate
CSD-B	static	P	Ca(OH) ₂	h ... d	30	12.4	12.4	Si	0.017	[Depierre 2013]	initial rate
CSD-B	static	P	Ca(OH) ₂	h ... d	50	11.7	11.7	Si	0.018	[Depierre 2013]	initial rate
CSD-B	static	P	Ca(OH) ₂	270	50	11.6	11.6	B	1.40E-04	[Depierre 2013]	long-term rate
ILW glass	static	M	KOH	8h ... 1 d	50	7	7	Si	0.016	[Mercado-Depierre 2013]	initial rate
ILW glass	static	M	KOH	8h ... 1 d	50	8	8	Si	0.033	[Mercado-Depierre 2013]	initial rate
ILW glass	static	M	KOH	8h ... 1 d	50	9	9	Si	0.095	[Mercado-Depierre 2013]	initial rate
ILW glass	static	M	KOH	8h ... 1 d	50	10	10	Si	0.278	[Mercado-Depierre 2013]	initial rate
ILW glass	static	M	KOH	8h ... 1 d	50	11.7	11.7	Si	0.588	[Mercado-Depierre 2013]	initial rate
ILW glass	static	M	Ca(OH) ₂	8h ... 1 d	50	7	7	Si	0.052	[Mercado-Depierre 2013]	initial rate
ILW glass	static	M	Ca(OH) ₂	8h ... 1 d	50	8	8	Si	0.155	[Mercado-Depierre 2013]	initial rate
ILW glass	static	M	Ca(OH) ₂	8h ... 1 d	50	9	9	Si	0.306	[Mercado-Depierre 2013]	initial rate
ILW glass	static	M	Ca(OH) ₂	8h ... 1 d	50	10	10	Si	0.497	[Mercado-Depierre 2013]	initial rate
ILW glass	static	M	Ca(OH) ₂	8h ... 1 d	50	10.5	10.5	Si	0.594	[Mercado-Depierre 2013]	initial rate
ILW glass	static	M	Ca(OH) ₂	8h ... 1 d	50	11	11	Si	0.399	[Mercado-Depierre 2013]	initial rate
ILW glass	static	M	Ca(OH) ₂	8h ... 1 d	50	11.7	11.7	Si	0.091	[Mercado-Depierre 2013]	initial rate
ILW glass	static	P	Ca(OH) ₂	647	50	11.6		Na	2.20E-05	[Mercado-Depierre 2013]	long-term rate
ILW glass	static	P	Ca(OH) ₂ + CaO	8	50	11.6		Li	0.082	[Mercado-Depierre 2013]	initial rate
ILW glass	static	P	Ca(OH) ₂ + CaO	344	50	11.6		Li	0.009	[Mercado-Depierre 2013]	long-term rate
ILW glass	static	P	KOH	8	50	11.6		Li	0.056	[Mercado-Depierre 2013]	initial rate
ILW glass	static	P	KOH	322	50	11.6		Li	3.50E-04	[Mercado-Depierre 2013]	long-term rate
ILW-glass (simulant)	static	P	Ca(OH) ₂	42	30	12.5	12.54	B	0.005	[Utton 2013]	initial rate
ILW-glass (simulant)	static	P	Ca(OH) ₂	42	50	12.5	12.37	B	0.043	[Utton 2013]	initial rate
ILW-glass (simulant)	static	P	Ca(OH) ₂	35	70	12.5	12.16	B	0.082	[Utton 2013]	initial rate
ILW-glass (simulant)	static	P	Ca(OH) ₂	28	90	12.5	12.18	B	0.240	[Utton 2013]	initial rate

SPFT: single-path flow through; P: powder, M: monolith; YCW: young cement water, ECW: evolved cement water, OCW: old cement water

Table A-6 Power law coefficients η for pH dependence of glass dissolution rates in the alkaline region

Glass type	T [°C]	pH range	η [-]	Element	Source
R7T7	90	7 ... 10	0.41	Si, B, Na	[Advocat 1991a]
R7T7	90	7 ... 11.5	0.39	Si, B, Na	[Advocat 1991b]
SON68	90	7 ... 11.5	0.39		[Gin 2001]
SON68		6 ... 10	0.40		[Frugier 2008]
SON68		9 ... 14	0.32		[Ferrand 2013]
Magnox MW	60	9 ... 12	0.40	Si, B, Li	[Abraitis 1998]
Magnox MW	18	7 ... 10	0.43	Si, B	[Abraitis 2000a]
Magnox blend MT25	23	8 ... 12	0.44	Si	[Cassingham 2015]
Magnox blend MT25	23	8 ... 12	0.35	B	[Cassingham 2015]
Magnox blend MT25	23	8 ... 12	0.56	Na	[Cassingham 2015]
Magnox blend MT25	40	8 ... 12	0.44	Si	[Cassingham 2015]
Magnox blend MT25	40	8 ... 12	0.45	B	[Cassingham 2015]
Magnox blend MT25	40	8 ... 12	0.46	Na	[Cassingham 2015]
Magnox blend MT25	70	8 ... 12	0.49	Si	[Cassingham 2015]
Magnox blend MT25	70	8 ... 12	0.33	B	[Cassingham 2015]
Magnox blend MT25	70	8 ... 12	0.58	Na	[Cassingham 2015]
Magnox blend MT30	23	8 ... 12	0.42	Si	[Cassingham 2015]
Magnox blend MT30	23	8 ... 12	0.52	B	[Cassingham 2015]
Magnox blend MT30	23	8 ... 12	0.51	Na	[Cassingham 2015]
Magnox blend MT30	40	8 ... 12	0.39	Si	[Cassingham 2015]
Magnox blend MT30	40	8 ... 12	0.58	B	[Cassingham 2015]
Magnox blend MT30	40	8 ... 12	0.53	Na	[Cassingham 2015]
Magnox blend MT30	70	8 ... 12	0.40	Si	[Cassingham 2015]
Magnox blend MT30	70	8 ... 12	0.36	B	[Cassingham 2015]
Magnox blend MT30	70	8 ... 12	0.42	Na	[Cassingham 2015]
Na-Ca-Al-borosilicate	25	7 ... 13	0.51	Si	[Knauss 1990]
Na-Ca-Al-borosilicate	50	7 ... 13	0.51	Si	[Knauss 1990]
Na-Ca-Al-borosilicate	70	7 ... 13	0.40	Si	[Knauss 1990]
Al-borosilicate LD6-5412	20 ... 90	6 ... 12	0.40	Si	[McGrail 1997]
Al-borosilicate LAWABP1	23 ... 90	5 ... 11	0.35		[McGrail 2001]
ILW-glass	50	7 ... 11.7	0.38	Si	[Mercado-Depierre 2013]
Al-borosilicates ¹⁾	23 ... 90	7 ... 12	0.34 ... 0.40	B	[Pierce 2008]
Al-borosilicates ¹⁾	23 ... 90	7 ... 12	0.33 ... 0.40	Na	[Pierce 2008]
Al-borosilicates ¹⁾	23 ... 90	7 ... 12	0.35 ... 0.40	Si	[Pierce 2008]
Al-borosilicates ¹⁾	23 ... 90	7 ... 12	0.31 ... 0.38	Al	[Pierce 2008]

¹⁾ LAWA44, LAWB45, LAWC22, SRL202

Appendix 4

Table A-7 Calculated and recommended radionuclide solubility limits in the cementitious near field (pH 12.55, E_H -230 mV, 25 °C) of an ILW repository [Berner 2003] - concentrations in mol L⁻¹ (NL: not limited)

Element	Calculated			Recommended		
	Lower limit	Maximum solubility	Upper limit	Lower limit	Maximum solubility	Upper limit
Cm	-	-	-	3E-10	2E-9	1E-8
Am	3E-10	2E-9	1E-8	-	-	-
Pu	1E-11	4E-11	2E-10	-	-	-
Np	3E-9	5E-9	1E-8	-	-	-
U	-	NL	-	-	1E-8	5E-7
Pa	-	-	-	-	~1E-8	-
Th	8E-10	3E-9	1E-8	-	-	-
Ra	-	1E-5	-	1E-6	-	2E-2
Cs	-	NL	-	-	-	-
I	-	NL	-	-	-	-
Tc	-	NL	-	-	-	-
Nb	-	NL	-	-	-	-
Se	-	NL (~0.1)	-	7E-6	1E-5	2E-5
Cl	-	NL	-	-	-	-
C _{inorg}	-	-	-	-	9.7E-6	2E-4
Ac	-	-	-	4E-9	2E-6	2E-5
Sn	1E-8	1E-7	2E-7	-	-	-
Pd	-	insignificantly low	-	8E-8	8E-7	8E-6
Zr	-	6E-6	-	6E-7	-	6E-5
Sr	-	3E-3	-	1E-3	-	6E-3
Ni	1E-8	3E-7	8E-6	-	-	-
Po	-	-	-	-	-	-
Pb	-	-	-	-	3E-3	2E-2
Hf	-	-	-	6E-7	6E-6	6E-5
Ho	-	-	-	4E-9	2E-6	2E-5
Eu	-	2E-6	2E-5	4E-9	-	-
Pm	-	-	-	4E-9	2E-6	2E-5
Sb	-	NL	-	-	-	-
Cd	-	-	-	-	4E-6	3E-5
Ag	-	-	-	-	insignificantly low	3E-6
Ru	-	-	-	-	-	high
Mo	-	-	-	-	3E-5	2E-3
Co	-	-	-	-	7E-7	8E-6

Table A-8: Calculated radionuclide solubilities in cementitious environments (recommended values, lower and upper guideline values) [Berner 2014] compared to earlier evaluations ([NAGRA 2002], [Berner 2003])

Concrete pore water, portlandite stage, pH 12.54				[NAGRA 2002], [Berner 2003]		
Element	Recommended value	Lower guideline value	Upper guideline value	Reference case	Lower limit	Upper limit
	[mol kg ⁻¹ H ₂ O]	[mol kg ⁻¹ H ₂ O]	[mol kg ⁻¹ H ₂ O]	[mol L ⁻¹]	[mol L ⁻¹]	[mol L ⁻¹]
Be	2.3 × 10 ⁻⁴	9.3 × 10 ⁻⁵	4.6 × 10 ⁻⁴	--	--	high
C _{inorg}	8.1 × 10 ⁻⁶			2 × 10 ⁻⁴	1 × 10 ⁻⁴	4 × 10 ⁻⁴
Cl	3.8 × 10 ⁻²			high	high	high
K	3.3 × 10 ⁻³			5.7 × 10 ⁻³	-	-
Ca	1.8 × 10 ⁻²			1.8 × 10 ⁻³	-	-
ISA a)	2.0 × 10 ⁻²					
ISA b)			2.9 × 10 ⁻²			
Co	5.4 × 10 ⁻⁷	3.8 × 10 ⁻¹¹	1.7 × 10 ⁻⁵	7 × 10 ⁻⁷	7 × 10 ⁻⁷	7 × 10 ⁻⁶
Ni	3.0 × 10 ⁻⁶	1.0 × 10 ⁻⁷	2.3 × 10 ⁻⁴	3 × 10 ⁻⁷	1 × 10 ⁻⁸	8 × 10 ⁻⁶
ISA a)	3.5 × 10 ⁻⁶					
ISA b)			4.7 × 10 ⁻⁶			
Se(-II)	2.1 × 10 ⁻⁶	7.2 × 10 ⁻¹¹	high	1 × 10 ⁻⁵	7 × 10 ⁻⁶	7 × 10 ⁻⁴
Sr	2.4 × 10 ⁻³	--	--	3 × 10 ⁻³	2 × 10 ⁻³	6 × 10 ⁻³
Zr	4.5 × 10 ⁻⁹	6.8 × 10 ⁻¹¹	1.3 × 10 ⁻⁴	6 × 10 ⁻⁶	6 × 10 ⁻⁷	6 × 10 ⁻⁵
ISA a)	4.9 × 10 ⁻⁷)					
Nb(V)	high	high	high	high	high	high
Mo(VI)	7.2 × 10 ⁻⁶	3.6 × 10 ⁻⁶	2.0 × 10 ⁻⁵	3 × 10 ⁻⁵	3 × 10 ⁻⁶	2 × 10 ⁻³
Tc(IV)	1.8 × 10 ⁻⁶	2.9 × 10 ⁻⁸	1.8 × 10 ⁻⁶	high	3 × 10 ⁻⁷	high
Pd	8.5 × 10 ⁻⁷	insignificant	2.5 × 10 ⁻⁵	8 × 10 ⁻⁷	--	--
Ag	1.8 × 10 ⁻⁶	2.9 × 10 ⁻¹⁴	1.7 × 10 ⁻⁴	insignificant	--	--
Sn(IV)	1.0 × 10 ⁻⁷	5.0 × 10 ⁻⁸	2.0 × 10 ⁻⁷	1 × 10 ⁻⁷	1 × 10 ⁻⁷	8 × 10 ⁻⁶
I	1.8 × 10 ⁻⁷	1.8 × 10 ⁻⁸	1.8 × 10 ⁻⁷	high	high	high
Cs	high	high	high	high	high	high
Sm	4.6 × 10 ⁻⁷	8.9 × 10 ⁻¹¹	4.6 × 10 ⁻⁷	2 × 10 ⁻⁶	2 × 10 ⁻⁷	2 × 10 ⁻⁵
ISA a)	2.9 × 10 ⁻⁴					
Eu	1.9 × 10 ⁻⁶	3.8 × 10 ⁻⁹	2.7 × 10 ⁻⁵	2 × 10 ⁻⁶	4 × 10 ⁻⁹	2 × 10 ⁻⁵
ISA a)	5.0 × 10 ⁻⁴	1.1 × 10 ⁻⁶				
ISA b)			2.2 × 10 ⁻³			
Ho	1.9 × 10 ⁻⁷	1.8 × 10 ⁻¹¹	1.9 × 10 ⁻⁷	2 × 10 ⁻⁶	4 × 10 ⁻⁹	2 × 10 ⁻⁵
ISA a)	1.2 × 10 ⁻⁴					
Pb	4.6 × 10 ⁻³	1.7 × 10 ⁻³	4.6 × 10 ⁻³	3 × 10 ⁻³	--	2 × 10 ⁻²
Po(IV)	6.4 × 10 ⁻⁸	1.6 × 10 ⁻¹⁰	6.4 × 10 ⁻⁸	high	high	high
Ra	9.7 × 10 ⁻⁷	2.1 × 10 ⁻⁷	1.7 × 10 ⁻⁵	1 × 10 ⁻⁵	1 × 10 ⁻⁶	2 × 10 ⁻⁵
Ac	(1.9 × 10 ⁻⁶)	(3.8 × 10 ⁻⁹)	(2.7 × 10 ⁻⁵)	2 × 10 ⁻⁶	4 × 10 ⁻⁹	2 × 10 ⁻⁵
ISA a)	5.0 × 10 ⁻⁴)					
Th	1.3 × 10 ⁻⁹	1.6 × 10 ⁻¹⁰	6.4 × 10 ⁻⁸	3 × 10 ⁻⁹	8 × 10 ⁻¹⁰	1 × 10 ⁻⁸
ISA a)	9.5 × 10 ⁻⁷		6.0 × 10 ⁻⁶			
ISA b)			3.0 × 10 ⁻⁵			

ISA a): calculations including 5 × 10⁻³ [mol kg⁻¹ H₂O] of (K⁺)ISA⁻
 ISA b): calculations with solid Ca(ISA)₂(cr) present.

Table A-8: Calculated radionuclide solubilities in cementitious environments (recommended values, lower and upper guideline values) [Berner 2014] compared to earlier evaluations ([NAGRA 2002], [Berner 2003]) (continued)

Concrete pore water, portlandite stage, pH 12.54				[NAGRA 2002], [Berner 2003]		
Element	Recommended value	Lower guideline value	Upper guideline value	Reference case	Lower limit	Upper limit
	[mol kg ⁻¹ H ₂ O]	[mol kg ⁻¹ H ₂ O]	[mol kg ⁻¹ H ₂ O]	[mol L ⁻¹]	[mol L ⁻¹]	[mol L ⁻¹]
Pa(V)	1.8 × 10 ⁻⁶	1.8 × 10 ⁻⁷	1.8 × 10 ⁻⁵	1 × 10 ⁻⁸	1 × 10 ⁻⁸	High
ISA a)	(2.3 × 10 ⁻⁶)					
U(VI)	7.0 × 10 ⁻⁷	1.7 × 10 ⁻⁸	1.4 × 10 ⁻⁴	1 × 10 ⁻⁸	1 × 10 ⁻⁸	5 × 10 ⁻⁷
ISA a)	8.4 × 10 ⁻⁷					
ISA b)			1.1 × 10 ⁻⁶			
Np(IV)	1.0 × 10 ⁻⁹	2.5 × 10 ⁻¹¹	4.0 × 10 ⁻⁸	5 × 10 ⁻⁹	3 × 10 ⁻⁹	1 × 10 ⁻⁸
ISA a)	3.5 × 10 ⁻⁹					
ISA b)			1.9 × 10 ⁻⁸			
Pu(IV)	2.3 × 10 ⁻¹²	2.3 × 10 ⁻¹³	8.2 × 10 ⁻⁸	4 × 10 ⁻¹¹	1 × 10 ⁻¹¹	1 × 10 ⁻¹⁰
ISA a)	(8.1 × 10 ⁻¹²)					
ISA b)			(4.4 × 10 ⁻¹¹)			
Am	5.4 × 10 ⁻¹⁰	2.2 × 10 ⁻¹²	1.1 × 10 ⁻⁸	2 × 10 ⁻⁹	3 × 10 ⁻¹⁰	1 × 10 ⁻⁸
ISA a)	8.9 × 10 ⁻⁸	4.4 × 10 ⁻⁹				
ISA b)			3.5 × 10 ⁻⁷			
Cm	1.1 × 10 ⁻⁹	1.5 × 10 ⁻¹⁰	8.6 × 10 ⁻⁹	2 × 10 ⁻⁹	3 × 10 ⁻¹⁰	1 × 10 ⁻⁸
(ISA a)	(1.8 × 10 ⁻⁷)					
(ISA b)			(7.1 × 10 ⁻⁷)			

ISA a): calculations including 5 × 10⁻³ [mol kg⁻¹ H₂O] of (K⁺)ISA⁻

ISA b): calculations with solid Ca(ISA)₂(cr) present.

OPERA

Meer informatie:

Postadres
Postbus 202
4380 AE Vlissingen

T 0113-616 666
F 0113-616 650
E info@covra.nl

www.covra.nl

